NASA CONTRACTOR REPORT

NASA CR-1660

DISTRIBUTED SYSTEM RESPONSE CHARACTERISTICS IN RANDOM PRESSURE FIELDS

by Richard L. Barnoski and John R. Maurer

Prepared by
MEASUREMENT ANALYSIS CORPORATION
Marina del Rey, Calif. 90291
for Goddard Space Flight Center

NATIONAL AERONAUTICS AND SPACE ADMINISTRATION • WASHINGTON, D. C. • SEPTEMBER 1970

Call

1. Report No.
NASA CR-1660

2. Government Accession No.

3. Recipient's Catalog No.

4. Title and Subtitle
Distributed System Response Characteristics in Random Pressure Fields

5. Report Date
~~September 1~~970

6. Performing Organization Code

7. Author(s)
Omit
Richard L. Barnoski & John R. Maurer

8. Performing Organization Report No.

9. Performing Organization Name and Address
M.L.
Measurement Analysis Corpo~~ration~~
~~A Digitek Company~~
~~4818 Lincoln~~ Blvd., ~~Marina del Rey~~,
California ~~90291~~

10. Work Unit No.

11. Contract or Grant No.
NAS5-11619 Omit

13. Type of Report and Period Covered
Contractor Report

12. Sponsoring Agency Name and Address
National Aeronautics and Space Administration
Washington, ~~D.C.~~ 20546

14. Sponsoring Agency Code

15. Supplementary Notes

16. Abstract
This report concerns the response characteristics of distributed structural systems to random excitation representative of three typical acoustic pressure fields. Emphasis is upon parametric results for response spectral density functions and the mean square response values at an arbitrary spatial location. The excitations considered are those representative of (1) a reverberant pressure field and (2) aerodynamic turbulence. A random progressive wave field is included mainly for illustrative purposes.

For each of the three pressure fields, joint and cross acceptance functions are determined for a structure of one dimension. Of particular interest are closed form response results for each of the system functions where filter approximations of the excitation acceptance functions are used. Contributions of modal cross terms are shown

17. Key Words (Selected by Author(s))
Structural random response
Random pressure fields

18. Distribution Statement
Unclassified - Unlimited

19. Security Classif. (of this report)	20. Security Classif. (of this page)	21. No. of Pages	22. Price*
U	U	200	$3.00

*For sale by the Clearinghouse for Federal Scientific and Technical Information, Springfield, Virginia 22151.

TABLE OF CONTENTS

1.0 INTRODUCTION

This report concerns an examination of the parameters that govern the response characteristics of linear, distributed structural systems to excitation which may be random both over the spatial extent of the system as well as in time. Such information is fundamental to response predictions and, subsequently, to rational structural design in a random environment. The system properties are those of finite continuous structures and the excitations principally of interest to the aerospace community. Specifically, the system is assumed governed by an equation of motion of the form

$$m\ddot{y}(\underset{\sim}{r}, t) + c\dot{y}(\underset{\sim}{r}, t) + D_{\underset{\sim}{r}}\, y(\underset{\sim}{r}, t) = f(\underset{\sim}{r}, t) \tag{1.1}$$

where r denotes a spatial vector, $D_{\underset{\sim}{r}}$ a spatial differential operator, and $f(\underset{\sim}{r}, t)$ an applied excitation. The coefficients m and c are assumed constant. Three excitations, each an acoustic pressure field, are considered. Their properties are assumed to be those characteristic of

- a random progressive wave field
- a reverberant field
- aerodynamic turbulence

Our concern focuses upon the parameters that govern the system response spectral density $S_y(\underset{\sim}{r}, \omega)$ and the system mean square response $\sigma_y^2(\underset{\sim}{r})$.

Now the basic theory and mathematical procedures to solve the above equation for both the response spectral density and response in mean square are not new+. This class of problems has been considered in one form or another by many investigators associated with structural

+The reader is referred to the references at the end of the report. Although this list is by no means exhaustive, it provides an ample introduction to the subject.

vibrations and acoustics and, not surprisingly, about as many forms of solutions have been advanced. The notation, method of formulation, completeness of background theory, degree of approximation, and display of results vary sufficiently so that it is not always a simple matter to use such results either to understand or to solve practical problems. With such variations, the underlying theory so necessary to problem solving tends to be masked in a profusion of symbols and jargon. This report represents an attempt to consolidate some of this theory, and in so doing, perhaps to clarify it as well.

Most important, the results presented here provide an indication of the expected response behavior of distributed structural systems in realistic random pressure fields. The theme throughout is to provide results in the form of functional expressions and/or parametric plots for, in this way, the shown information is applicable to a wide variety of system problems. For one-dimensional systems, the results can be applied directly. For systems with more than a single dimension, the results can be adapted to compatible forms of series solutions.

Although the virtually traditional results for joint acceptance functions and the mean square response are included, in addition, we consider cross acceptance terms and detailed evaluations of the response spectral densities and responses in mean square for three typical system functions. For the reverberant and turbulence fields, conventional filter theory is used to approximate the structural coupling of such pressure fields, and closed form results thus established for the mean square response. These "approximate" analytical expressions then are compared with results from numerical integration computations. Exact integrations are carried out and evaluated for the progressive wave field.

2.0 BASIC THEORY

This section concerns mainly derivations of the spectral density function for the response at any point on a continuous system to distributed as well as discretized random excitation. Before we concentrate upon such derivations, let us first examine, by way of review, several formulations of the system response to an arbitrary deterministic excitation. To reinforce the physical meaning of the parameters and terms used here, much of the theory is applied to solve illustrative problems for simple systems in Appendix A.

2.1 DETERMINISTIC EXCITATION

Let us assume the vibration behavior of the system is governed by linear theory, there is no interaction between the system and excitation, and all shown functional expressions are mathematically tractable. The damping is termed proportional [6].

2.1.1 Modal Theory

The time history at the position $\underset{\sim}{r}$ of the system deflection $y(\underset{\sim}{r}, t)$ may be expressed as the series

$$y(\underset{\sim}{r}, t) = \sum_{j=1}^{\infty} \phi_j(\underset{\sim}{r}) q_j(t) \tag{2.1}$$

where $\phi_j(r)$ is the undamped jth normal mode and $q_j(t)$ is the deflection in the jth normal (or principal) coordinate. Since the mode shapes are orthogonal functions in the spatial variable $\underset{\sim}{r}$,

$$\int_R m(\underset{\sim}{r}) \phi_j(\underset{\sim}{r}) \phi_k(\underset{\sim}{r}) d\underset{\sim}{r} = \begin{cases} 0, & \text{for } j \neq k \\ m_j, & \text{for } j = k \end{cases} \tag{2.2}$$

where

$$m_j = \int_R m(\underset{\sim}{r})\ \phi_j^2(\underset{\sim}{r})d\underset{\sim}{r} \tag{2.3}$$

The quantity m_j is called the generalized mass.

The undamped normal modes are obtained from solutions to the undamped homogeneous form of Equation (1.1)

$$m\ddot{y}(\underset{\sim}{r}, t) + D_{\underset{\sim}{r}}y(\underset{\sim}{r}, t) = 0 \tag{2.4}$$

This equation conventionally is solved for $\phi_j(r)$ by a separation-of-variables technique subject to the boundary conditions of the system. The generalized deflections are determined from solutions to the second-order differential equation

$$m_j\ddot{q}_j(t) + c_j\dot{q}_j(t) + \bar{k}_jq_j(t) = f_j(t) \tag{2.5}$$

where

$$c_j = c\int_R \phi_j^2\ (\underset{\sim}{r})\ d\underset{\sim}{r}$$

$$f_j(t) = \int_R \phi_j(\underset{\sim}{r})\ f(\underset{\sim}{r}, t)\ d\underset{\sim}{r} \tag{2.6}$$

Frequently, Equation (2.6) is written as

$$\ddot{q}_j(t) + 2\zeta_j\omega_jq_j(t) + \omega_j^2q_j(t) = \frac{1}{m_j}\ f_j(t) \tag{2.7}$$

where

$$\omega_j^2 = \frac{\bar{k}_j}{m_j}$$

$$2\zeta_j \omega_j = \frac{c_j}{m_j} \tag{2.8}$$

By the convolution integral

$$q_j(t) = \int_0^t h_j(\alpha) f_j(t-\alpha)\, d\alpha \tag{2.9}$$

where $h_j(\alpha)$ is the response of the jth single degree-of-freedom system to a jth unit impulse forcing function and α is but the variable of integration. Consistent with the "generalized" terminology, c_j is termed the generalized damping, $\bar{k}_j$ the generalized stiffness, $f_j(t)$ the generalized force, ω_j the jth modal frequency of the system, and ζ_j the damping factor in the jth mode. Since the form of Equation (2.5) is that of a single degree-of-freedom system (or a mechanical oscillator, if you like), the modal series solution may be considered as a transformation which converts the physical system into an equivalent set of modal oscillators, infinite in number, and where the output of each oscillator is weighted by its corresponding mode shape. The response of the physical system at $\underset{\sim}{r}$ thus can be represented by a summation of outputs from each of the modal oscillators, each such output weighted by $\phi_j(\underset{\sim}{r})$ evaluated at $\underset{\sim}{r}$.

2.1.2 Impulse Response Formuation

This method reflects an extension to multidimensional systems of analysis procedures frequently used in network analysis; it sometimes is termed a Green's function approach. Central to the formulation is the space-time unit inpulse response ($h(\underset{\sim}{r}, \underset{\sim}{s}, t)$); this function describes the response time history of the system at $\underset{\sim}{r}$ to a unit impulse excitation applied at $\underset{\sim}{s}$. By convolution in time and superposition over space [14],

$$y(\underset{\sim}{r}, t) = \int_R \int_0^t h(\underset{\sim}{r}, \underset{\sim}{s}, \eta)\, f(\underset{\sim}{s}, t - \eta) d\eta\, d\underset{\sim}{s} \tag{2.10}$$

and, alternatively,

$$y(\underset{\sim}{r}, t) = \int_R \int_{-\infty}^{\infty} h(\underset{\sim}{r}, \underset{\sim}{s}, \eta)\, f(\underset{\sim}{s}, t - \eta) d\eta\, d\underset{\sim}{s} \tag{2.10a}$$

since $h(\underset{\sim}{r}, \underset{\sim}{s}, t) = 0$ for $t \leq 0$. The system function $H(\underset{\sim}{r}, \underset{\sim}{s}, \omega)$ and $h(\underset{\sim}{r}, \underset{\sim}{s}, t)$ are related as the Fourier Transform pair

$$h(\underset{\sim}{r}, \underset{\sim}{s}, t) \longleftrightarrow H(\underset{\sim}{r}, \underset{\sim}{s}, \omega) \tag{2.11}$$

where

$$H(\underset{\sim}{r}, \underset{\sim}{s}, \omega) = \int_{-\infty}^{\infty} h(\underset{\sim}{r}, \underset{\sim}{s}, t)\, e^{-i\omega t} dt \tag{2.12}$$

Note that $H(\underset{\sim}{r}, \underset{\sim}{s}, \omega)$ is amenable to experimental measurements and, in contrast to the series representation of modal theory, appears somewhat simpler in in this functional form.

2.1.3 Transform Solutions

The transforms considered are linear transform pairs of the form

$$f(t) \longleftrightarrow F(\eta) \tag{2.13}$$

where

$$F(\eta) = \int_{a_1}^{a_2} K(t,\eta)\, f(t)\, dt$$

$$f(t) = \int_{b_1}^{b_2} H(t,\eta)\, F(\eta)\, d\eta \tag{2.14}$$

Here we concentrate upon the Fourier transform pair *

$$F(\omega) = \int_{-\infty}^{\infty} f(t)\, e^{-i\omega t}\, dt$$

$$f(t) = \frac{1}{2\pi} \int_{-\infty}^{\infty} F(\omega) e^{i\omega t}\, d\omega \tag{2.15}$$

and make token mention in Appendix A of the Laplace transform pair

$$F(s) = \int_0^{\infty} f(t) e^{-st} dt, \quad f(t) = \frac{1}{2\pi i} \int_{b-i\infty}^{b+i\infty} F(s) e^{st} ds \tag{2.16}$$

*This pair seemingly is popular with circuit analysts and mathematicians. Since placement of the 2π term and sign of the exponent is a matter of choice, various equivalent forms are used throughout the literature.

For our purposes, we potentially can use any one of the three transform pairs

$$
\begin{aligned}
y(\underset{\sim}{r}, t) &\longleftrightarrow Y(\underset{\sim}{r}, \omega) \\
y(\underset{\sim}{r}, t) &\longleftrightarrow Y(\underset{\sim}{k}, t) \qquad (2.17) \\
y(\underset{\sim}{r}, t) &\longleftrightarrow Y(\underset{\sim}{k}, \omega)
\end{aligned}
$$

Note the last pair defines the double transformation

$$
\begin{aligned}
Y(\underset{\sim}{k}, \omega) &= \int_{-\infty}^{\infty}\int_{-\infty}^{\infty} y(\underset{\sim}{r}, t) e^{-i(\underset{\sim}{k}\underset{\sim}{r} + \omega t)} d\underset{\sim}{r}\, dt \\
& \qquad\qquad\qquad\qquad\qquad\qquad\qquad (2.18) \\
y(\underset{\sim}{r}, t) &= \frac{1}{(2\pi)^2} \int_{-\infty}^{\infty}\int_{-\infty}^{\infty} Y(\underset{\sim}{k}, \omega) e^{i(\underset{\sim}{k}\underset{\sim}{r} + \omega t)} d\underset{\sim}{k}\, d\omega
\end{aligned}
$$

where $Y(\underset{\sim}{k}, \omega)$ describes a wave number-frequency response function. Such a formulation lends itself to interpreting a distributed structural system as a filter with selectivity characteristics dependent upon both spatial wave-number and frequency. The multiplicity of integration defined by Equation (2.18) depends upon the dimensions associated with the spatial variable $\underset{\sim}{r}$; for example, a two-dimensional structure, such as a plate, requires a three-fold integration to compute $Y(\underset{\sim}{k}, \omega)$ whereas a one-dimensional structure such as a beam, requires but a two-fold integration.

By the Fourier transform of the equation of motion

$$Y(\underset{\sim}{k},\omega) = H(\underset{\sim}{k},\omega)\ F(\underset{\sim}{k},\omega) \tag{2.19}$$

where the system function $H(\underset{\sim}{k},\omega)$ is of the form

$$H(\underset{\sim}{k},\omega) = \frac{1}{D_{\underset{\sim}{k}} - \omega^2 m + ic\omega} \tag{2.20}$$

and the wave number-frequency description of the applied excitation is given by

$$F(\underset{\sim}{k},\omega) = \int_{-\infty}^{\infty}\int_{-\infty}^{\infty} f(\underset{\sim}{r},t)e^{-i(\underset{\sim}{k}\underset{\sim}{r}+\omega t)}d\underset{\sim}{r}\ dt \tag{2.21}$$

Conceptually, Equation (2.19) constitutes a solution for the system response to an arbitrary deterministic loading in the wave number-frequency domain. For a space-time description of this response, $Y(\underset{\sim}{k},\omega)$ is converted to $y(\underset{\sim}{r},t)$ by the inversion integral of Equation (2.18). Although very compact in form, be forewarned that the evaluation of such integrals frequently represents a nontrivial and/or tedious mathematical task for practical problems. This comes about, in part, due to the finite transforms that are encountered when dealing with finite structures.

2.2 RANDOM EXCITATION

Let us make several preliminary remarks at the outset. Correlation functions (or, equivalently, their spectral densities) are representative of second statistical moments. For Gaussian processes, only the first two moments are necessary to describe the statistical properties of the process; for Gaussian processes with zero mean, only the second moment is required. We also recall that the resultant output of a linear operation on a Gaussian process is itself Gaussian.

If the input $f(\underset{\sim}{r}, t)$ is termed random or stochastic, this function may be random either over the spatial extent of the structure or/and in time; that is, both $\underset{\sim}{r}$ and t may be random variables. Since a linear system acts as a linear operator on the input process, the response process $y(\underset{\sim}{r}, t)$ is random; its properties are governed by the system characteristics of the structure and the stochastic nature of the excitation. Thus, to characterize the output process, considerations of correlation functions, spectral density functions and mean square response values naturally arise.

2.2.1 Distributed Random Loadings

Let us examine the various forms we may choose to characterize an input loading. Consider $f(\underset{\sim}{r}, t)$ when the excitation is said to be nonhomogeneous and nonstationary. The correlation function is of the form

$$R_f(\underset{\sim}{r}, \underset{\sim}{r}', t_1, t_2) = E\left[f(\underset{\sim}{r}_1 t_1)\, f(\underset{\sim}{r}_1' t_2)\right] \tag{2.22}$$

where $E[\quad]$ is the expectation of $[\quad]$. This expression implies ensemble averaging over all combinations of spatial locations and time; such represents a most formidable task, at best. We know from the Wiener-Khintchin relation that a correlation function and its associated spectral density are related as a Fourier Transform pair. So, in a very general sense,

$$R_f(\underset{\sim}{r}, \underset{\sim}{r}', t_1, t_2) \longleftrightarrow S_f(\underset{\sim}{k}, \underset{\sim}{k}', \omega_1, \omega_2) \tag{2.23}$$

The quantity $S_f(\underset{\sim}{k}, \underset{\sim}{k}', \omega_1, \omega_2)$ is called a generalized power spectral density or multi-dimensional spectra of the input excitation. It is noted here as a two-sided cross spectral density functionally dependent upon the wave numbers $\underset{\sim}{k}$ and $\underset{\sim}{k}'$, and the frequencies ω_1 and ω_2. For a one-dimensional structure in the spatial variable x,

$$S_f(k, k', \omega_1, \omega_2) = \frac{1}{(2\pi)^4} \int_0^{\ell} \cdots \int_{-\infty}^{\infty} R_f(x, x', t_1, t_2)\, e^{i(kx - k'x' + \omega_1 t_1 - \omega_2 t_2)} dx\, dx'\, dt_1\, dt_2$$

$$R_f(x, x', t_1, t_2) = \int_{-\infty}^{\infty} \cdots \int_{-\infty}^{\infty} S_f(k, k', \omega_1, \omega_2)\, e^{-i(kx - k'x' + \omega_1 t_1 - \omega_2 t_2)} dk\, dk'\, d\omega_1\, d\omega_2 \tag{2.24}$$

where the spatial integrations are taken over the extent of the structure (in this case, the length). If a two-dimensional structure were assumed, the integrations implicit in Equation (2.23) would be six-fold; four for the spatial coordinates, and two for the time variable.

Now any consistent set of variables can be selected to establish a F. T. pair. Since all such sets provide basically the same information, it should be clear that no set inherently is more "correct" than any other although, admittedly, some forms may prove mathematically more convenient than others. For example,

$$R_f(\underset{\sim}{r}, \underset{\sim}{r}', t_1, t_2) \longleftrightarrow S_f(\underset{\sim}{r}, \underset{\sim}{r}', \omega_1, t_2) \tag{2.25}$$

yields $S_f(\underset{\sim}{r}, \underset{\sim}{r}', \omega_1, t_2)$ as a time varying cross spectral density function while

$$R_f(\underset{\sim}{r}, \underset{\sim}{r}', t_1, t_2) \longleftrightarrow R_f(\underset{\sim}{k}, \underset{\sim}{k}', t_1, t_2) \tag{2.26}$$

defines $R_f(\underset{\sim}{k}, \underset{\sim}{k}', t_1, t_2)$ as a nonstationary wave number-time correlation function. Practically, the format used is dictated by costs and comprises associated with instrumentation, experimental tests, data processing, and mathematical form of the prediction model. Simply, there is no "best" format for all problems. It is appropriate to mention here that fast transform techniques permit the rapid computation of spectral quantities directly from measured data. Correlation functions, likewise, can be determined from the raw data although, due to fast transform procedures, it frequently is more efficient to compute such functions by taking the Fourier transforms of their respective spectral densities.

If we assume the process $f(\underset{\sim}{r}, t)$ is stationary, then the statistical properties in time become dependent only upon the time difference $\tau = t_2 - t_1$ so that the generalized spectral density function of the input $f(\underset{\sim}{r}, t)$ is

$$S_f(\underset{\sim}{k}, \underset{\sim}{k}', \omega) \longleftrightarrow R_f(\underset{\sim}{r}, \underset{\sim}{r}', \tau) \tag{2.27}$$

where

$$R_f(\underset{\sim}{r}, \underset{\sim}{r}', \tau) = E\left[f(\underset{\sim}{r}, t)\, f\,(\underset{\sim}{r}', t + \tau)\right] \tag{2.28}$$

Now if the process is ergodic as well, we can replace this ensemble average by

$$R_f(\underset{\sim}{r}, \underset{\sim}{r}', \tau) = \lim_{T\to\infty} \frac{1}{2T} \int_{-T}^{T} f(\underset{\sim}{r}, t)\, f\,(\underset{\sim}{r}', t+\tau)\, dt \tag{2.29}$$

and for the spatial location $\underset{\sim}{r}_o$,

$$R_f(\underset{\sim}{r}_o, \tau) = \lim_{T\to\infty} \frac{1}{2T} \int_{-T}^{T} f(\underset{\sim}{r}_o, t)\, f\,(\underset{\sim}{r}_o, t+\tau)\, dt \tag{2.30}$$

where $R_f(\underset{\sim}{r}_o, \tau)$ is simply the autocorrelation function of a stationary forcing function evaluated at $\underset{\sim}{r}_o$.

If the process $f(\underset{\sim}{r}, t)$ is assumed homogeneous, then the statistical characteristics over the space of the structure become dependent only upon the spatial difference $\underset{\sim}{u} = \underset{\sim}{r}' - \underset{\sim}{r}$ and the generalized spectral density becomes of the form

$$S_f(\underset{\sim}{k}, \omega_1, \omega_2) \longleftrightarrow R_f(\underset{\sim}{u}, t_1, t_2) \tag{2.31}$$

where

$$R_f(\underset{\sim}{u}, t_1, t_2) = E\left[f(r, t_1)\, f\,(r + \underset{\sim}{u}, t_2)\right] \tag{2.32}$$

If the process is assumed isotropic, then $\underset{\sim}{u} \to |r' - r| = u$ and

$$R_f(u, t_1, t_2) = \lim_{R\to A} \frac{1}{R} \int_{R} f(r, t_1)\, f\,(r + u, t_2)\, d(r) \tag{2.33}$$

Further, if $R_f(u, t_1, t_2)$ is assumed ergodic, then

$$R_f(u, t_1, t_2) \rightarrow R_f(u, \tau) = \lim_{\substack{T \to \infty \\ R \to A}} \frac{1}{2TR} \int_{-T}^{T} \int_{R} f(r, t) \, f \, (r+u, t+\tau) dr \, dt \tag{2.34}$$

and the generalized spectra is

$$S_f(k, \omega) \longleftrightarrow R_f(u, \tau) \tag{2.35}$$

Thus, ergodicity allows time averaging of a single record to define the statistical nature of the time characteristics of the process whereas isotropicity allows a single set of spatial averages to account for the spatial characteristics. For reasons principally related to costs for more exacting measurements as well as experimental and data reduction programs, it is almost traditional (at this point in time) to assume the input excitation as both homogeneous and stationary. Recent advances [1] concerning nonstationary properties should prove of value, however.

By way of a simple illustration, consider now various functional representations of a pressure field obtained by a speaker (energized by bandwidth limited white noise) directed at normal incidence to a flat rigid surface. Assuming no near field effects, the excitation which impinges on the surface is a stationary, isotropic plane pressure wave at normal incidence. The space-time correlation function for this random pressure wave may be depicted as shown in Figure 2.1(a). Other equivalent descriptors are represented by Figures 2.1(b), 2.1(c) and 2.1(d);

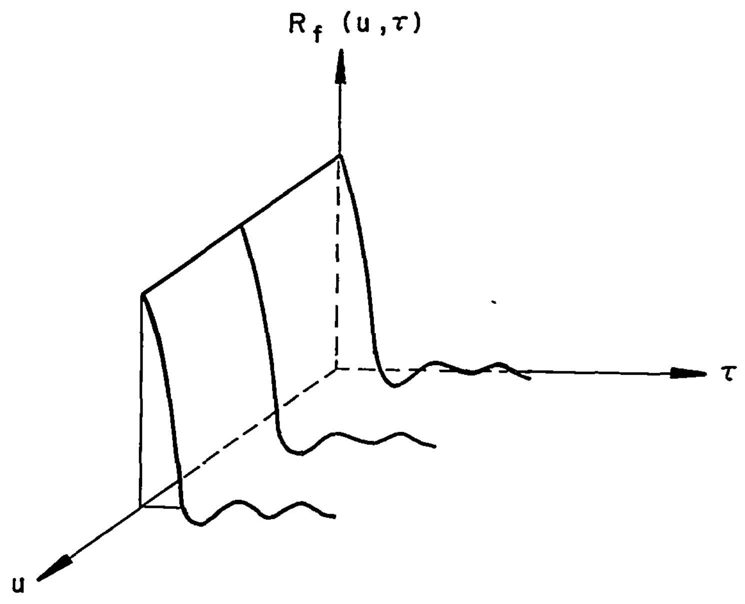

(a) Space - Time Correlation Function

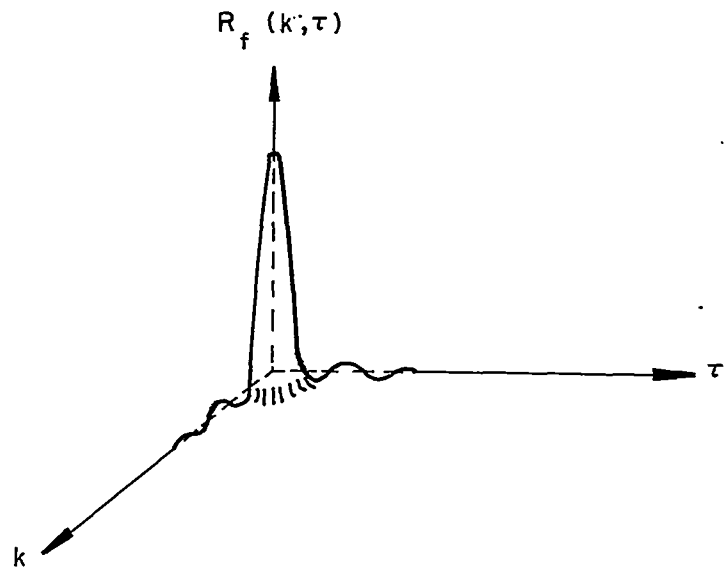

(b) Wave Number - Time Correlation Function

FIGURE 2.1 RANDOM PRESSURE WAVE AT NORMAL INCIDENCE

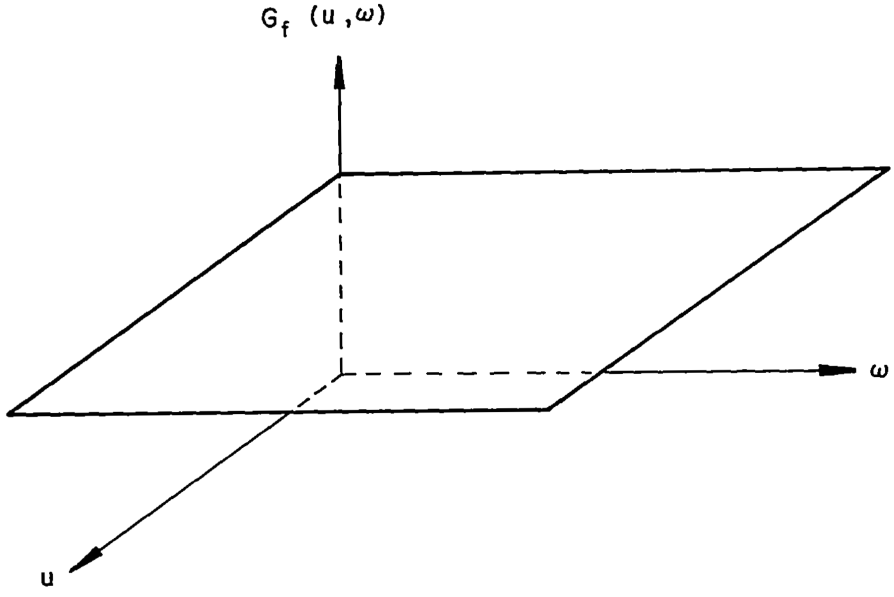

(c) Cross Spectral Density

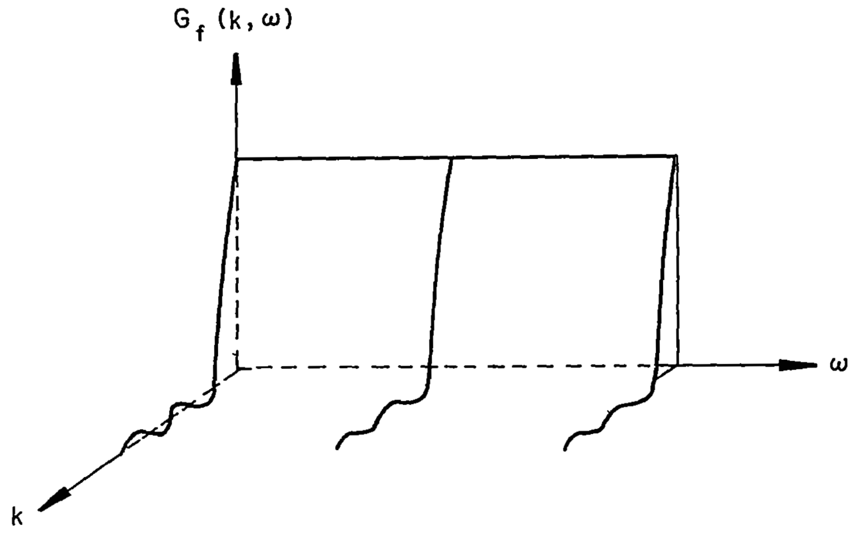

(d) Generalized Power Spectra

FIGURE 2.1 RANDOM PRESSURE WAVE AT NORMAL INCIDENCE these, in turn, are related to the space-time correlation function by the Fourier transformations

$$R_f(u,\tau) \longleftrightarrow R_f(k,\tau)$$
$$R_f(u,\tau) \longleftrightarrow G_f(u,\omega) \tag{2.36}$$
$$R_f(u,\tau) \longleftrightarrow G_f(k,\omega)$$

We recognize the notation $G_f(u,\omega)$ denotes a one-sided spectral density in ω; it is related to $S_f(u,\omega)$ by folding the ω-axis of this two-sided function so that

$$\begin{aligned} G_f(u,\omega) &= 2\,S_f(u,\omega), \quad \text{for } \omega \geq 0 \\ &= 0, \quad\quad\quad\quad\;\; \text{for } \omega < 0 \end{aligned} \tag{2.37}$$

2.2.2 Mean Square Response Formulations

Let us direct our attention now to the development of expressions which, when evaluated, lead to the mean square response of the system. The mean square response at any location $\underset{\sim}{r}$ of a linear distributed structure to stationary random excitation is given by

$$E\left[y^2(\underset{\sim}{r},t)\right] = \sigma_y^2(\underset{\sim}{r}) = \int_{-\infty}^{\infty} S_y(\underset{\sim}{r},\omega)d\omega \tag{2.38}$$

where $S_y(\underset{\sim}{r},\omega)$ is the ordinary spectral density of the response $y(\underset{\sim}{r},t)$.

Since

$$R_y(\underset{\sim}{r},\tau) \longleftrightarrow S_y(\underset{\sim}{r},\omega) \tag{2.39}$$

it follows that

$$\sigma_y^2(\underset{\sim}{r}) = R_y(\underset{\sim}{r}, 0) \tag{2.40}$$

Since the key to computing $\sigma_y^2(\underset{\sim}{r})$ is the spectral density $S_y(\underset{\sim}{r},\omega)$, let us consider a formulation of this spectral function.

Our approach is to establish a space-time correlation function of $y(\underset{\sim}{r}, t)$, take advantage of certain functional relationships associated with a linear system, then take the Fourier transform according to the Wiener-Khintchin relations. Consistent with this approach, the space-time correlation function for $y(\underset{\sim}{r}, t)$ assumed ergodic is

$$R_y(\underset{\sim}{r}, \tau) = \lim_{T\to\infty} \frac{1}{2T} \int_{-T}^{T} y(\underset{\sim}{r}, t)y(\underset{\sim}{r}, t+\tau)dt \tag{2.41}$$

For a modal representation such as that of Equation (2.1) with the response $q_j(t)$ written in terms of the convolution integral

$$q_j(t) = h_j(t)*f_j(t)= \int_{-\infty}^{\infty} h_j(\eta)\ f_j\ (t-\eta)d\eta, \tag{2.42}$$

it follows that

$$R_y(\underset{\sim}{r}, \tau) = \sum_{j=1}^{\infty} \sum_{k=1}^{\infty} \phi_j(\underset{\sim}{r})\phi_k(\underset{\sim}{r}) \int_{-\infty}^{\infty}\int_{-\infty}^{\infty} h_j(\alpha)\ h_k(\eta)\ R_{jk}(\tau + \alpha - \eta)d\alpha\, d\eta \tag{2.43}$$

where

$$R_{jk}(\tau+\alpha-\eta) = \lim_{T\to\infty} \frac{1}{2T} \int_{-T}^{T} f_j(t-\alpha) f_k(t+\tau-\eta)dt \tag{2.44}$$

We note the form of Equation (2.43) is that of a double convolution in τ; thus, it can be expressed more compactly by

$$R_y(\underset{\sim}{r}, \tau) = \sum_{j=1}^{\infty}\sum_{k=1}^{\infty} \phi_j(\underset{\sim}{r})\phi_k(\underset{\sim}{r})\, h_j(-\tau) * h_k(\tau) * R_{jk}(\tau) \tag{2.45}$$

where

$$R_{jk}(\tau) = \lim_{T\to\infty} \frac{1}{2T} \int_{-T}^{T} f_j(t)\, f_k(t+\tau)dt \tag{2.46}$$

For a linear system,

$$h_j(\tau) \longleftrightarrow \frac{1}{m_j\, \omega_j^2}\, \overline{H}_j(\omega) \tag{2.47}$$

where the modal magnification factor $\overline{H}_j(\omega)$ is defined as

$$\overline{H}_j(\omega) = \frac{1}{1 - \left(\frac{\omega}{\omega_j}\right)^2 + i2\zeta_j \left(\frac{\omega}{\omega_j}\right)} \tag{2.48}$$

In expanded form, the Wiener-Khintchin relations defined previously as Equation (2.39) are

$$S_y(\underset{\sim}{r},\omega) = \frac{1}{2\pi}\int_{-\infty}^{\infty} R_y(\underset{\sim}{r},\tau)e^{-i\omega\tau}d\tau$$

$$R_y(\underset{\sim}{r},\tau) = \int_{-\infty}^{\infty} S_y(\underset{\sim}{r},\omega)e^{i\omega\tau}d\omega \tag{2.49}$$

By the time convolution theorem [9, pg. 26], the F. T. of the convolution of two functions, say $f_1(t)$ and $f_2(t)$, equals the product of the F. T. of these two functions. By applying this theorem to a double convolution in τ, the F. T. of Equation (2.45) produces

$$S_y(\underset{\sim}{r},\omega) = \sum_{j=1}^{\infty}\sum_{k=1}^{\infty} \phi_j(\underset{\sim}{r})\phi_k(\underset{\sim}{r})\, H_j^*(\omega)\, H_k(\omega)\, S_{jk}(\omega) \tag{2.50}$$

where

$$H_j(\omega) = \frac{1}{m_j\,\omega_j^2}\quad \bar{H}_j(\omega)$$

$$S_{jk}(\omega) = \iint_R \phi_j(\underset{\sim}{r})\phi_k(\underset{\sim}{r}')\, S_f(\underset{\sim}{r},\underset{\sim}{r}',\omega)\, d\underset{\sim}{r}\, d\underset{\sim}{r}' \tag{2.51}$$

The quantity $S_f(\underset{\sim}{r},\underset{\sim}{r}',\omega)$ is the cross spectral density function of the distributed random loading.

It often is convenient to normalize the modal cross spectral density by dividing by the surface area of the region R and defining the cross spectral density function

$$\hat{C}_f(\underset{\sim}{r}, \underset{\sim}{r}', \omega) = \frac{S_f(\underset{\sim}{r}, \underset{\sim}{r}', \omega)}{S_o(\underset{\sim}{r}_o, \omega)} \tag{2.52}$$

so that

$$S_{jk}(\omega) = A^2 S_o(r_o, \omega) J_{jk}(\omega) \tag{2.53}$$

where

$$J_{jk}(\omega) = \frac{1}{A^2} \iint_R \phi_j(\underset{\sim}{r}) \phi_k(\underset{\sim}{r}') \hat{C}_f(\underset{\sim}{r}, \underset{\sim}{r}', \omega) \, d\underset{\sim}{r} \, d\underset{\sim}{r}' \tag{2.54}$$

The density function $\hat{C}_f(\underset{\sim}{r}, \underset{\sim}{r}', \omega)$ is termed a normalized cross-spectral density function or a narrowband cross spectral coefficient. The cross acceptance function $J_{jk}(\omega)$ provides a measure of how well the random excitation couples with the structure because of the spatial characteristics of both the loading and the structure.

Now Equations (2.38), (2.50), and (2.53) collectively emphasize a distributed linear structure acts as a filter with selectivity characteristics both in space and in frequency (time). Accordingly, the output response of such a filter is dependent upon the nature of the input loading and both the spatial and frequency characteristics of the filter. A system thus may be excited into "resonance" either in space or in frequency, or coincidentally in both space and frequency. Simultaneous resonance in both space and frequency is termed "coincidence". To predict the system output response to a random distributed loading, in addition to the system representation, we require a statistically meaningful description of the manner in which the loading is distributed in space and is applied in time; namely, the cross spectral density $C_f(\underset{\sim}{x}, \underset{\sim}{x}', \omega)$. For a deterministic loading[+], we need an explicit representation of how the loading is distributed over the structure and how it is applied in time; namely, $f(\underset{\sim}{r}, t)$.

Consider the form of the spectral density $S_y(\underset{\sim}{r}, \omega)$ for a continuous structure with discretized, stationary random loadings. The desired result is that of Equation (2.50) with $S_{jk}(\omega)$ altered to account for a set of 'n' pointwise inputs. If we represent such a loading by

$$f(\underset{\sim}{r}, t) = \sum_r f(\underset{\sim}{r}, t)\, \delta(\underset{\sim}{r} - \underset{\sim}{r}_r), \quad r = 1, 2, 3 \cdots n \qquad (2.55)$$

then the modal cross-correlation function defined by

$$R_{jk}(\tau) = \lim_{T \to \infty} \frac{1}{2T} \int_{-T}^{T} f_j(t)\, f_k(t+\tau)\, dt \qquad (2.56)$$

[+]This can be seen easily by an examination of the properties associated with the generalized force $f_j(t)$ and the solution for the normal coordinate $q_j(t)$.

reduces to

$$R_{jk}(\tau) = \sum_{r=1}^{n} \sum_{s=1}^{n} \phi_j(\underset{\sim}{r}_r)\phi_k(\underset{\sim}{r}_s)\, R_f(\underset{\sim}{r}_r, \underset{\sim}{r}_s, \tau) \tag{2.57}$$

where

$$R_f(\underset{\sim}{r}_r, \underset{\sim}{r}_s, \tau) = \lim_{T\to\infty} \frac{1}{2T} \int_{-T}^{T} f(\underset{\sim}{r}_r, t)\, f\,(\underset{\sim}{r}_s, t+\tau)\, dt \tag{2.58}$$

By the Fourier transform

$$R_{jk}(\tau) \longleftrightarrow S_{jk}(\omega) \tag{2.59}$$

the modal cross-spectral density becomes

$$S_{jk}(\omega) = \sum_{r=1}^{n} \sum_{s=1}^{n} \phi_j(\underset{\sim}{r}_r)\, \phi_k(\underset{\sim}{r}_s)\, S_f(\underset{\sim}{r}_r, \underset{\sim}{r}_s, \omega) \tag{2.60}$$

since

$$R_f(\underset{\sim}{r}_r, \underset{\sim}{r}_s, \tau) \longleftrightarrow S_f(\underset{\sim}{r}_r, \underset{\sim}{r}_s, \omega) \tag{2.61}$$

2.2.3 Properties of Special Interest

In the previous section, formulations of $S_y(\underline{x},\omega)$ and $\sigma_y^2(\underline{x})$ are presented for distributed linear systems and nonhomogeneous, stationary loadings. Theoretically, we can argue this class of problems now has been reduced to two operations, both mathematical in nature, that of

- developing the required integrand function
- carrying out the stated integrations

As we shall see later in this report, even with the simplest of structures and not overly-complicated representations of random pressure fields, the evaluation of the integral expressions simply is not a casual exercise in mathematics. Although a precise evaluation is desirable from a theoretical point of view and practically advantageous as well, assumptions frequently are made to provide "quick order-of-magnitude estimates" of response levels. Such assumptions are physically plausible and essentially reduce the complexity of the integral expressions so that the required mathematical operations can be carried out with ease. Let us mention some of these approximations and special situations as well.

To remove from consideration the off-diagonal terms in the summation for $\sigma_y^2(\underline{x})$, we assume a lightly damped structural system where

- the modal frequencies are sufficiently separated so that

$$\left| H_j(\omega) \right|^2 >> \mathrm{Re} \left| H_j^*(\omega)\, H_k(\omega) \right|$$

- the mode shapes and force field are such that

$$J_j(\omega) >> J_{jk}(\omega)$$

- the force field is such that its frequency characteristics are nearly constant over ω

For such conditions, the off-diagonal or $j \neq k$ terms become negligibly small so that

$$S_y(\underset{\sim}{r}, \omega) = \sum_{j=1}^{\infty} \phi_j(\underset{\sim}{r}) \left| H_j(\omega) \right|^2 S_j(\omega) \tag{2.62}$$

where

$$S_j(\omega) = \iint_R \phi_j(\underset{\sim}{r}) \phi_j(\underset{\sim}{r}') \, S_f(\underset{\sim}{r}, \underset{\sim}{r}', \omega) \, d\underset{\sim}{r} \, d\underset{\sim}{r}' \tag{2.63}$$

The mean square response then reduces to the form

$$\sigma_y^2 (r) = \sum_{j=1}^{\infty} \phi_j^2 (r) \int_{-\infty}^{\infty} \left| H_j(\omega) \right|^2 S_j(\omega) \, d\omega \tag{2.64}$$

Consider the above form of $\sigma_y^2 (\underset{\sim}{r})$ for two extremes of spatial correlation for a random loading with white noise time characteristics; that where the loading is correlated uniformly over the structure as well as that where the loading is uncorrelated perfectly in space. For an isotropic loading correlated as a constant over the extent of the structure, such as for a random pressure wave at normal incidence, the cross-spectral density reduces as

$$S_f(r, r', \omega) \longrightarrow S_o \tag{2.65}$$

and

$$S_j(\omega) = S_o \left[\int_R \phi_j(r) \, dr \right]^2 \tag{2.66}$$

The mean square response is given by

$$\sigma_y^2(\underset{\sim}{r}) \simeq S_o \sum_{j=1}^{\infty} \phi_j^2(\underset{\sim}{r}) \left[\int_R \phi_j(\underset{\sim}{r}) d\underset{\sim}{r} \right]^2 \int_{-\infty}^{\infty} \left| H_j(\omega) \right|^2 d\omega \tag{2.67}$$

where

$$\int_{-\infty}^{\infty} \left| H_j(\omega) \right|^2 d\omega = \frac{\pi Q_j}{m_j^2 \omega_j^3} \tag{2.68}$$

so that

$$\sigma_y^2(\underset{\sim}{r}) = \pi S_o \sum_{j=1}^{\infty} \frac{\left[\int_R \phi_j(\underset{\sim}{r}) d\underset{\sim}{r} \right]^2}{m_j^2} \cdot \frac{\phi_j^2(\underset{\sim}{r}) Q_j}{\omega_j^3} \tag{2.69}$$

Now for a completely uncorrelated loading over the extent of the structure, such as that for raindrops on a roof,

$$S_f(\underset{\sim}{r}, \underset{\sim}{r}', \omega) \longrightarrow \hat{S}_o \, \delta(\underset{\sim}{r} - \underset{\sim}{r}') \tag{2.70}$$

and

$$S_j(\omega) = \hat{S}_o \int_R \phi_j^2(\underset{\sim}{r}) d\underset{\sim}{r} \tag{2.71}$$

so that for a structure with uniform mass distribution

$$\sigma_y^2(\underset{\sim}{r}) \simeq \frac{\pi \hat{S}_o}{m} \sum_{j=1}^{\infty} \frac{\phi_j^2(\underset{\sim}{r}) Q_j}{m_j \omega_j^3} \tag{2.72}$$

because

$$\int_R \phi_j^2(\underset{\sim}{r})\, d\underset{\sim}{r} = \frac{m_j}{m} \tag{2.73}$$

Pictorial representations of such loadings are shown by the sketches of Figures 2.1 and 2.2

In test specification and vibration prediction work, it frequently is required to estimate an "average" response level for a structural zone. This may be accomplished by

$$\langle \sigma_y^2 \rangle = \frac{1}{A} \int_R \sigma_y^2(\underset{\sim}{r})\, d\underset{\sim}{r} \tag{2.74}$$

which, due to orthogonality properties of the normal modes, reduces to

$$\langle \sigma_y^2 \rangle = \sum_{j=1}^{\infty} \frac{\int_R \phi_j^2(\underset{\sim}{r})\, d\underset{\sim}{r}}{A} \int_{-\infty}^{\infty} \left| H_j(\omega) \right|^2 S_j(\omega)\, d\omega \tag{2.75}$$

For uniform structures with simple harmonic mode shapes

$$\phi_j(\underset{\sim}{r}) = \sin k_j x \quad , \quad \text{where } k_j = \frac{j\pi}{\ell} \tag{2.76}$$

the generalized mass and integral of the mode shape are

$$m_j = \frac{m\ell}{2} \tag{2.77}$$

$$\int_0^{\ell} \phi_j(x)\, dx = \begin{cases} 0, & j = 2, 4, 6, \ldots \\ \dfrac{2\ell}{j\pi}, & j = 1, 3, 5, \ldots \end{cases}$$

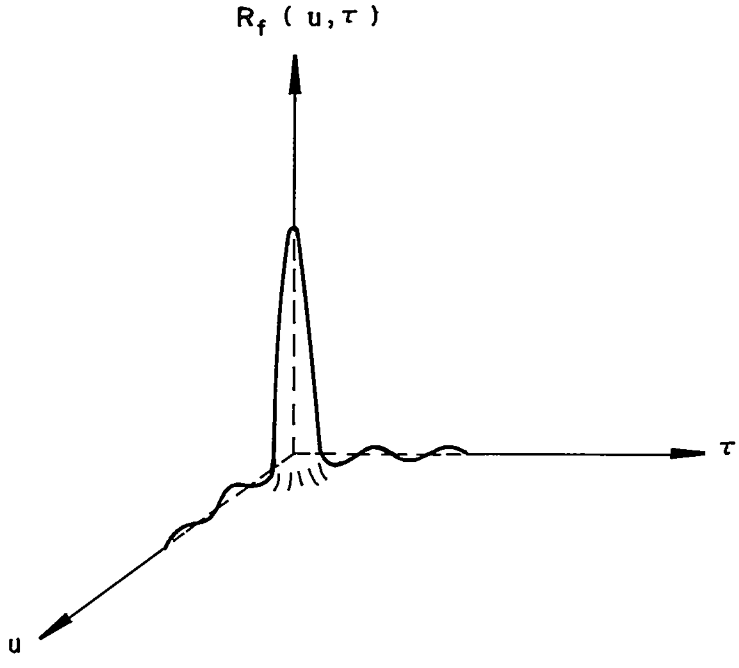

(a) Space – Time Correlation Function

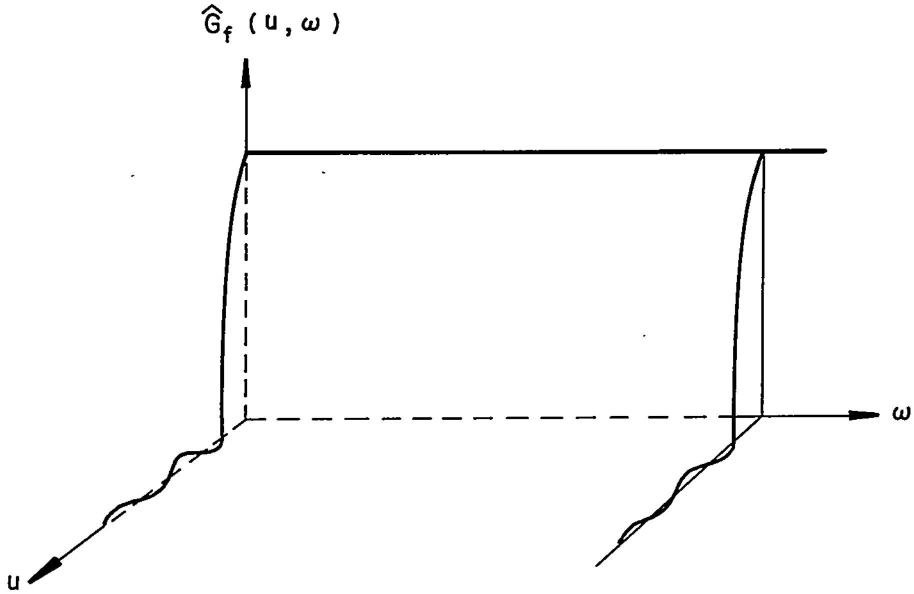

(b) Cross Spectral Density

FIGURE 2.2 SPATIALLY UNCORRELATED WHITE NOISE RANDOM LOADING

Then for the spatially correlated white noise loading,

$$<\sigma_y^2> \simeq \frac{8S_o}{\pi m^2} \sum_{j=1,3}^{\infty} \frac{Q_j}{j^2 \omega_j^3} \tag{2.78}$$

and, for the spatially uncorrelated case,

$$<\sigma_y^2> = \frac{\pi \hat{S}_o}{\ell m^2} \sum_{j=1}^{\infty} \frac{Q_j}{\omega_j^3} \tag{2.79}$$

In a more general sense, let us go back and assess the relative magnitude of the off-diagonal terms of $S_y(\underset{\sim}{r},\omega)$ for each of the two previous loadings. For the spatially correlated case,

$$S_{jk}(\omega) = S_o \int_R \phi_j(\underset{\sim}{r})\, d\underset{\sim}{r} \bullet \int_R \phi_k(\underset{\sim}{r}')\, d\underset{\sim}{r}' \tag{2.80}$$

and

$$\begin{aligned} \sigma_y^2(\underset{\sim}{r}) &= S_o \sum_{j}^{(j=k)} \phi_j^2(\underset{\sim}{r}) \left[\int_R \phi_j(\underset{\sim}{r}) d\underset{\sim}{r}\right]^2 \int_{-\infty}^{\infty} \left|H_j(\omega)\right|^2 d\omega \\ &+ S_o \sum_j \sum_k^{(j \neq k)} \phi_j(\underset{\sim}{r})\, \phi_k(\underset{\sim}{r}) \bullet \int_R \phi_j(\underset{\sim}{r})\, d\underset{\sim}{r} \bullet \int_R \phi_k(\underset{\sim}{r}) d\underset{\sim}{r} \int_{-\infty}^{\infty} H_j^*(\omega)\, H_k(\omega)\, d\omega \end{aligned} \tag{2.81}$$

By residue theory with $a_j = \omega_j(1-\zeta_j^2)^{1/2}$ and $b_j = \zeta_j \omega_j$,

$$\int_{-\infty}^{\infty} H_j^*(\omega)\, H_k(\omega) d\omega = \frac{4\pi}{m_j m_k} \left[\frac{b_j + b_k}{\left[(a_j^2 - a_k^2) - (b_j + b_k)^2\right]^2 + 4a_j^2 (b_j + b_k)^2}\right] \tag{2.82}$$

and a relative measure of the importance of the $j \neq k$ terms is offered by the ratio (where $m_j = m_k$)

$$\frac{2\int_{-\infty}^{\infty} H_j^*(\omega)\, H_k(\omega)\, d\omega}{\int_{-\infty}^{\infty} \left| H_j(\omega) \right|^2 d\omega} = \frac{16\, b_j(b_j+b_k)\,(a_j^2+b_j^2)}{\left[(a_j^2-a_k^2)-(b_j+b_k)^2\right]^2 + 4a_j^2(b_j+b_k)^2} \tag{2.83}$$

Figure 2.3 shows the behavior of this expression by a family of curves in modal damping with $\zeta_j = \zeta_k$

For the spatially uncorrelated loading, the cross-modal spectral density is given by

$$S_{jk}(\omega) = \hat{S}_o \int_R \phi_j(\underline{r})\, \phi_k(\underline{r})\, d\underline{r} \tag{2.84}$$

and, due to modal orthogonality,

$$S_{jk}(\omega) = \begin{cases} 0, & \text{for } j \neq k \\ \hat{S}_o \int_R \phi_j^2(\underline{r})\, d\underline{r}, & \text{for } j = k \end{cases} \tag{2.85}$$

so that the expression for $\sigma_y^2(\underline{r})$ reduces to Equation (2.72) which is void of $j \neq k$ terms.

As our last special topic, consider the situation where the spectral characteristics of the input are those of bandwidth limited noise in contrast to those of pure white noise. For this condition, the mean square response is written as

$$\sigma_y^2(\underline{r}) = \int_{-\omega_c}^{\omega_c} S_y(\underline{r}, \omega)\, d\omega \tag{2.86}$$

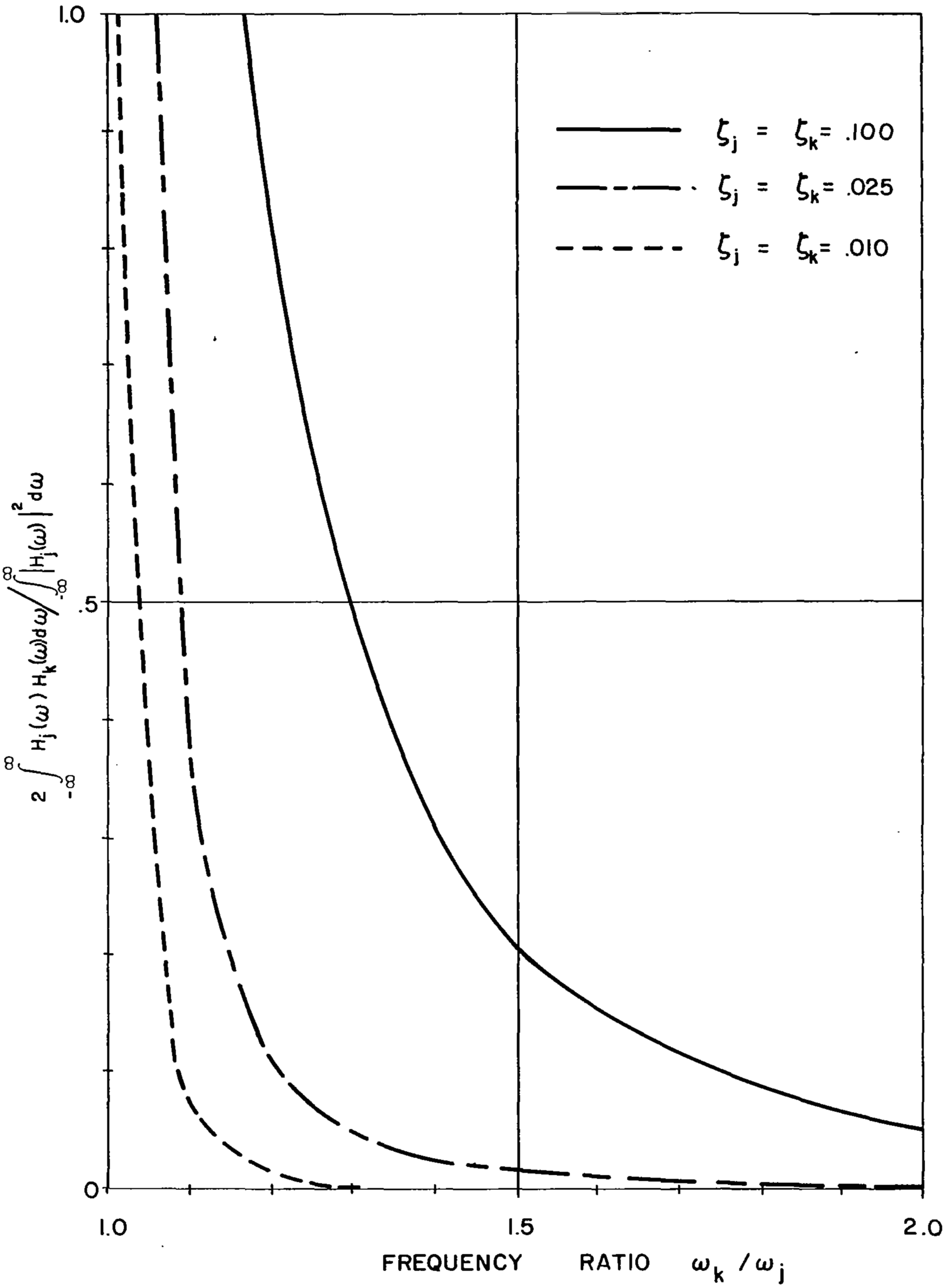

FIGURE 2.3. RELATIVE EFFECT OF OFF-DIAGONAL MODAL TERMS

where ω_c is the cutoff frequency of the input noise. For a constant spectrum over the bandwidth of the input, our previous work is altered only in that

$$\int_{-\infty}^{\infty} H_j^*(\omega)\, H_k(\omega) d\omega \longrightarrow \int_{-\omega_c}^{\omega_c} H_j^*(\omega)\, H_k(\omega)\, d\omega \tag{2.87}$$

and, for the j = k terms,

$$\int_{-\omega_c}^{\omega_c} \left| H_j(\omega) \right|^2 d\omega = \frac{\pi Q_j}{m_j^2 \; \omega_j^3} \quad I_j \tag{2.88}$$

where

$$I_j = \frac{4\zeta_j}{\pi} \int_0^a \left| H_j(\omega) \right|^2 d\omega \tag{2.89}$$

with $a = \omega_c/\omega_j$. Upon integration, the quantity I_j reduces to

$$I_j = \frac{1}{\pi} \tan^{-1} \frac{2a\zeta_j}{1-a^2} + \frac{\zeta_j}{2\pi(1-\zeta_j^2)^{1/2}} \quad \ell n \frac{1 + a^2 + 2a\,(1-\zeta_j^2)^{1/2}}{1 + a^2 - 2a\,(1-\zeta_j^2)^{1/2}} \tag{2.90}$$

The behavior of this function is shown by Figure 2.4 as a family of curves in the modal damping factor ζ_j. Note the curves depict the system function $\left|H_j(\omega)\right|$ as a highly selective bandpass filter in ω for small values of ζ_j; it admits frequency components centered about and approximately equal to ω_j and rejects the components where $\omega_c/\omega_j \gg 1$.

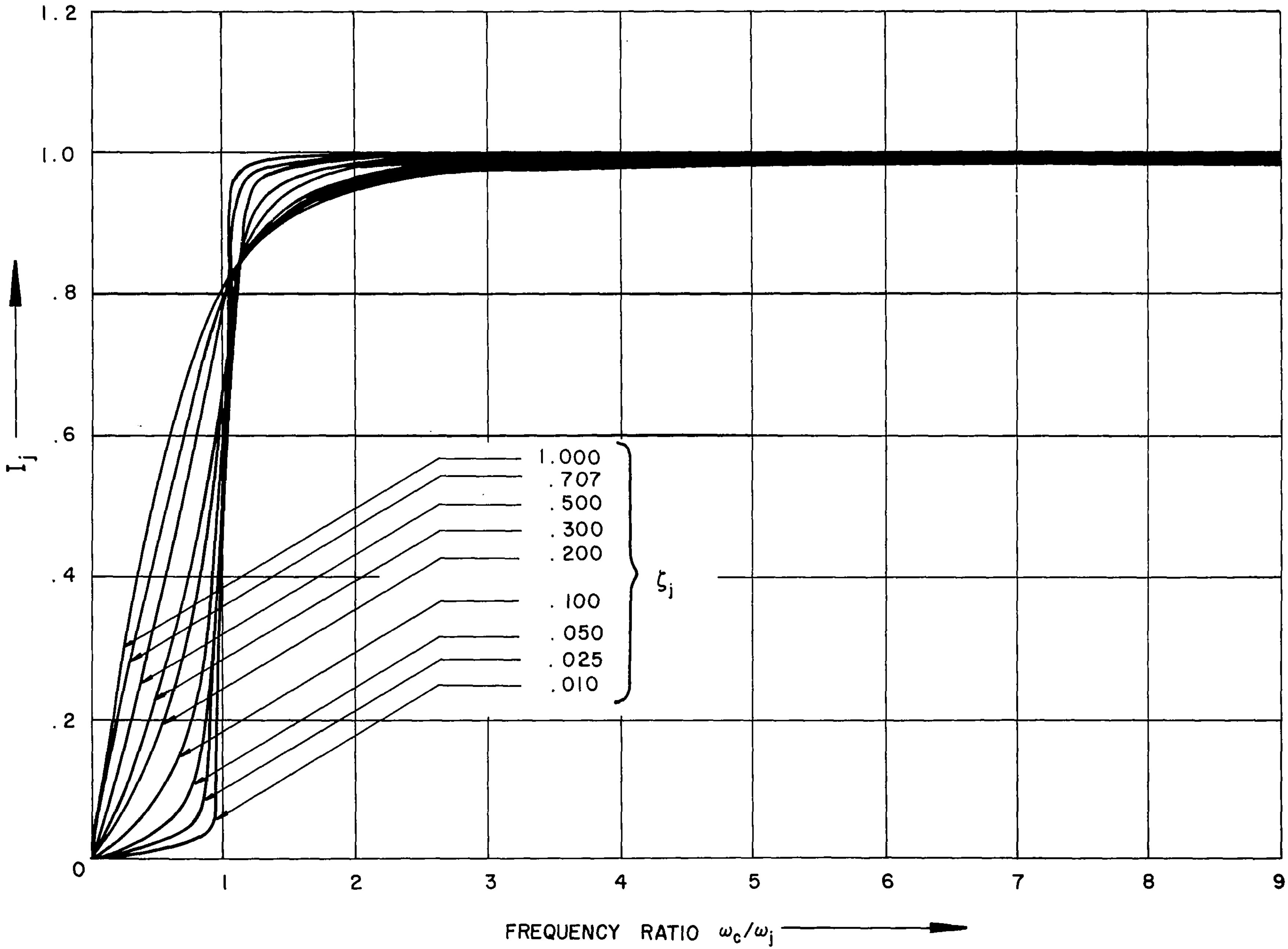

FIGURE 2.4 VALUE OF THE INTEGRAL I_j

2.2.4 Cross-Correlation and Related Spectral Density Function

Let us consider now the correlation function and the associated spectral density between the input excitation $f(\underline{r}, t)$ at $\underline{r} = \underline{r}_o$ and the response $y(\underline{r}', t)$. The desired cross-correlation function is defined by

$$R_{fy}(\underline{r}_o, \underline{r}', \tau) = \lim_{T\to\infty} \frac{1}{2T} \int_{-T}^{T} f(\underline{r}_o, t) y(\underline{r}', t+\tau) dt \tag{2.91}$$

Upon substituting the modal solution for $y(\underline{r}', t + \tau)$ and rearranging the order of integration,

$$R_{fy}(\underline{r}_o, \underline{r}', \tau) = \sum_{j=1}^{\infty} \phi_j(\underline{r}') \int_R \phi_j(\underline{r}'') \left[h_j(\tau) * R_f(\underline{r}_o, \underline{r}'', \tau)\right] d\underline{r}'' \tag{2.92}$$

where

$$R_f(\underline{r}_o, \underline{r}'', \tau) = \lim_{T\to\infty} \frac{1}{2T} \int_{-T}^{T} f(\underline{r}_o, t) f(\underline{r}'', t+\tau) dt \tag{2.93}$$

Since

$$R_{fy}(\underline{r}_o, \underline{r}', \tau) \longleftrightarrow S_{fy}(\underline{r}_o, \underline{r}', \omega), \tag{2.94}$$

the cross-spectral density becomes

$$S_{fy}(\underline{r}_o, \underline{r}', \omega) = \sum_{j=1}^{\infty} \phi_j(\underline{r}') H_j(\omega) \int_R \phi_j(\underline{r}'') S_f(\underline{r}_o, \underline{r}'', \omega) d\underline{r}'' \tag{2.95}$$

If the input loading is discretized according to Equation (2.55), then

$$\int \phi_j(\underset{\sim}{r}'') S_f(\underset{\sim}{r}_o, \underset{\sim}{r}'', \omega) d\underset{\sim}{r}'' = \sum_{s=1}^{n} \phi_j(\underset{\sim}{r}_s) S_f(\underset{\sim}{r}_o, \underset{\sim}{r}_s, \omega) \tag{2.96}$$

since

$$R_f(\underset{\sim}{r}_o, \underset{\sim}{r}'', \tau) = \sum_{s=1}^{n} \lim_{T\to\infty} \frac{1}{2T} \int_{-T}^{T} f(\underset{\sim}{r}_o, t) f(\underset{\sim}{r}'', t+\tau) dt \; \delta(\underset{\sim}{r}'' - \underset{\sim}{r}_s) \tag{2.97}$$

Therefore,

$$S_{fy}(\underset{\sim}{r}_o, \underset{\sim}{r}', \omega) = \sum_{j=1}^{\infty} \phi_j(\underset{\sim}{r}') H_j(\omega) \sum_{s=1}^{\infty} \phi_j(\underset{\sim}{r}_s) S_f(\underset{\sim}{r}_o, \underset{\sim}{r}_s, \omega) \tag{2.98}$$

and for a single point loading at $\underset{\sim}{r} = \underset{\sim}{r}_o$,

$$S_{fy}(\underset{\sim}{r}_o, \underset{\sim}{r}', \omega) = S_f(\underset{\sim}{r}_o, \omega) \, \delta(\underset{\sim}{r}_o) \sum_{j=1}^{\infty} \phi_j(\underset{\sim}{r}_o) \phi_j(\underset{\sim}{r}') H_j(\omega) \tag{2.99}$$

where $S_f(\underset{\sim}{r}_o, \omega)$ is the ordinary spectral density of the input excitation at $\underset{\sim}{r}_o$.

It is useful in some applications to know the cross-correlation function or the cross-spectral density of the response measured at two different locations, say $y(\underset{\sim}{r}_o, t)$ and $y(\underset{\sim}{r}, t)$. Such a cross-correlation function for a stationary process is noted by

$$R_y(\underset{\sim}{r}_o, \underset{\sim}{r}, \tau) = \lim_{T\to\infty} \frac{1}{2T} \int_{-T}^{T} y(\underset{\sim}{r}_o, t) y(\underset{\sim}{r}, t+\tau) dt \tag{2.100}$$

By using modal theory and paralleling the development for $S_y(\underset{\sim}{r},\omega)$ used earlier in the text,

$$R_y(\underset{\sim}{r}_o, \underset{\sim}{r}, \tau) = \sum_{j=1}^{\infty}\sum_{k=1}^{\infty} \phi_j(\underset{\sim}{r}_o)\phi_k(\underset{\sim}{r})\, h_j(-\tau)*h_k(\tau)*R_{jk}(\tau) \tag{2.101}$$

Thus,

$$R_y(\underset{\sim}{r}_o, \underset{\sim}{r}, \tau) \longleftrightarrow S_y(r_o, \underset{\sim}{r}, \omega) \tag{2.102}$$

and

$$S_y(\underset{\sim}{r}_o, \underset{\sim}{r}, \omega) = \sum_{j=1}^{\infty}\sum_{k=1}^{\infty} \phi_j(\underset{\sim}{r}_o)\phi_k(\underset{\sim}{r})\, H_j^*(\omega)\, H_k(\omega)\, S_{jk}(\omega) \tag{2.103}$$

where both $H_j(\omega)$ and $S_{jk}(\omega)$ are those previously defined.

2.2.5 Alternate Formulations

In the previous sections, we have developed formulations using modal theory and Fourier transforms. Direct use of the system function provides alternate and frequently quoted formulations. For completeness, let us make token mention of such results. By substitution of the response $y(\underset{\sim}{r}, t)$ defined by the convolution integral into Equation (2.41), the Fourier transform of the resultant expression provides

$$S_y(r,\omega) = \int_S\int_{S'} H^*(\underset{\sim}{r}, \underset{\sim}{s},\omega)\, H(\underset{\sim}{r}, \underset{\sim}{s}',\omega) S_f(\underset{\sim}{s}, \underset{\sim}{s}',\omega)\, d\underset{\sim}{s}\, d\underset{\sim}{s}' \tag{2.104}$$

similarly,

$$S_y(\underset{\sim}{r}_o, \underset{\sim}{r}, \omega) = \int_S\int_{S'} H^*(\underset{\sim}{r}_o, \underset{\sim}{s},\omega)\, H(\underset{\sim}{r}, \underset{\sim}{s}',\omega)\, S_f(\underset{\sim}{s}, \underset{\sim}{s}',\omega) d\underset{\sim}{s}\, d\underset{\sim}{s}' \tag{2.105}$$

For 'n' discretized loadings,

$$S_y(\underset{\sim}{r},\omega) = \sum_j^n \sum_k^n H^*(\underset{\sim}{r}, \underset{\sim}{s}_j, \omega)\, H(\underset{\sim}{r}, \underset{\sim}{s}_k, \omega)\, S_f(\underset{\sim}{s}_j, \underset{\sim}{s}_k, \omega) \tag{2.106}$$

$$S_y(\underset{\sim}{r}_o, \underset{\sim}{r},\omega) = \sum_j^n \sum_k^n H^*(\underset{\sim}{r}_o, \underset{\sim}{s}_j, \omega)\, H(\underset{\sim}{r}, \underset{\sim}{s}_k, \omega)\, S_f(\underset{\sim}{s}_j, \underset{\sim}{s}_k, \omega)$$

where both summations extend over the range 1 . . . 'n'. Since the structural characteristics are defined as continuous functions over both space and frequency instead of by an infinite modal series, these expressions appear more compact than the equivalent modal formulations. Such is intuitively satisfying. Practically, the development of such system functions is not without measurement and computational difficulties; moreover, the resultant double integration, as with that for $J_{jk}(\omega)$, will prove somewhat taxing to carry out for practical excitation fields.

3.0 RESPONSE TO SELECTED PRESSURE FIELDS

Since the intent here is exploratory in nature, our concern focuses upon the forms of the expressions which govern the response of a structure to each of three pressure fields adjudged of interest to the aerospace community. Such forms are fundamental to any rational effort in design and in response prediction for a structural system immersed in a random environment. Largely to simplify the mathematics, we choose a structure of one dimension with harmonic mode shapes. Let the pressure fields be characterized by the normalized cross-spectral density functions

$$\bullet\ C_f(x, x', \omega) = \cos\left[K_o(x-x')\cos\theta\right]$$

$$\bullet\ C_f(x, x', \omega) = \frac{\sin K(x-x')}{K(x-x')} \tag{3.1}$$

$$\bullet\ C_f(x, x', \omega) = e^{-\alpha\bar{K}|x-x'|}\cos\bar{K}(x-x')$$

where the wave numbers K_o, K and $\bar{K}$ are

$$K_o = \frac{\omega_o}{c}, \quad K = \frac{\omega}{c}, \quad \bar{K} = \frac{\omega}{U_c} \tag{3.2}$$

These normalized cross-spectral densities imply homogeneous, stationary random loadings and correspond physically to

- a random progressive wave field
- a reverberant pressure field
- aerodynamic turbulence

Let us now apply the theory developed in the previous section.

To paraphrase some of our earlier remarks, we seek $S_y(x,\omega)$ and $\sigma_y^2(x)$ for each of the three pressure fields. The mean square response is given by the integral

$$\sigma_y^2(x) = \int_{-\infty}^{\infty} S_y(x,\omega)\, d\omega \tag{3.3}$$

We choose to represent the response spectral density in its two-sided form

$$S_y(x,\omega) = \sum_{j=1}^{\infty} \sum_{k=1}^{\infty} \phi_j(x)\phi_k(x)\, H_j^*(\omega)\, H_k(\omega)\, S_{jk}(\omega) \tag{3.4}$$

and the modal cross-spectral density by

$$S_{jk}(\omega) = \ell^2\, S(x_o, \omega)\;\; J_{jk}(\omega) \tag{3.5}$$

where

$$J_{jk}(\omega) = \frac{1}{\ell^2} \int_0^{\ell} \int_0^{\ell} \phi_j(x)\, \phi_k(x')\, C_f(x, x', \omega)\, dx\, dx' \tag{3.6}$$

We further assume harmonic mode shapes of the form

$$\phi_j(x) = \sin k_j x \tag{3.7}$$

where the structural wavenumber k_j is given by

$$k_j = \frac{j\pi}{\ell}, \qquad j = 1, 2, 3. \;. \;. \;. \tag{3.8}$$

and the associated modal frequency ω_j by

$$\omega_j^2 = \frac{E\,I}{m\,\ell^4}\,(k_j\,\ell)^4 \tag{3.9}$$

The computation of the mean square response, therefore, reduces to two tasks for each pressure field:

- evaluating the spatial integral associated with $J_{jk}(\omega)$
- performing the spectral integration associated with $\sigma_y^2(x)$

3.1 JOINT AND CROSS ACCEPTANCE CONSIDERATIONS

For homogeneous pressure fields,

$$C_f(x, x', \omega) \longrightarrow C_f(x - x', \omega) \tag{3.10}$$

so that for our problem

$$J_{jk}(\omega) = \frac{1}{\ell^2} \int_0^\ell \int_0^\ell C_f(x-x', \omega) \sin k_j x \ \sin k_k x' \, dx \, dx' \tag{3.11}$$

This double integral can be expressed in terms of a single integral function by means of the relationship [13]

$$\iint_R f(x, x') \, dx \, dx' = \iint_{R'} f(u, v) \ | J | \ du \, dv \tag{3.12}$$

where the Jacobian is given by

$$| J | = \begin{vmatrix} \dfrac{\partial x}{\partial u} & \dfrac{\partial x'}{\partial u} \\ \dfrac{\partial x}{\partial v} & \dfrac{\partial x'}{\partial v} \end{vmatrix} \tag{3.13}$$

with the coordinate transformation

$$\begin{aligned} u &= x - x' \\ v &= x + x' \end{aligned} \tag{3.14}$$

These relationships serve to map the area of integration R in the x-x' plane into the area R' in the u-v plane as shown by Figure 3.1.

$$\iint_R F(x,x')\,dx\,dx' = \iint_{R'} F(u,v)\,|J|\,du\,dv$$

$$u = x - x'$$

$$v = x + x'$$

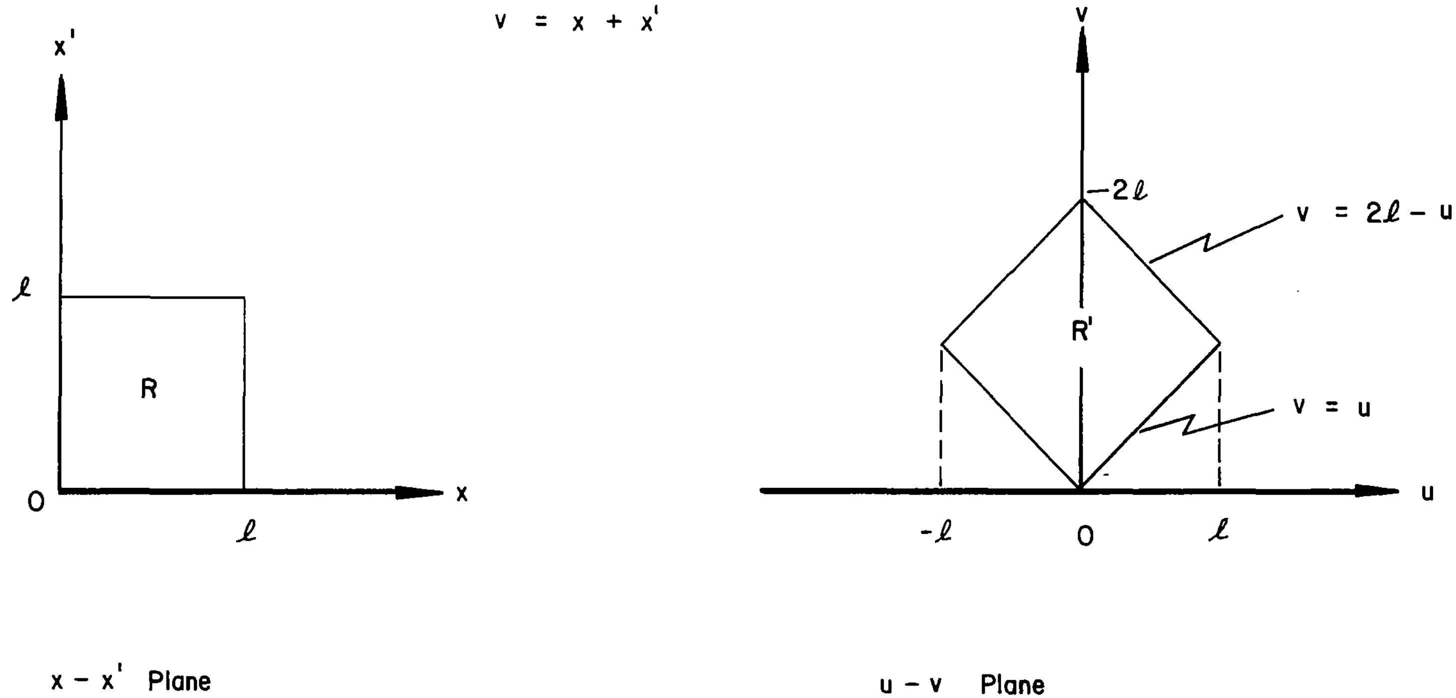

FIGURE 3.1 TRANSFORMATION OF THE INTEGRATION SPACE

Thus, we can write Equation (3.11) in the form

$$J_{jk}(\omega) = \frac{1}{2\ell^2} \int_{-\ell}^{\ell} \int_{u}^{2\ell-|u|} C_f(u,\omega) \sin \frac{1}{2} k_j(u+v) \sin \frac{1}{2} k_k(v-u) \, dv \, du \tag{3.15}$$

and for $C_f(u,\omega)$ a symmetric function in u,

$$J_{jk}(\omega) = \frac{1}{2\ell^2} \int_{0}^{\ell} C_f(u,\omega) K_{jk}(u) \, du \tag{3.16}$$

where

$$\begin{aligned} K_{jk}(u) = \frac{1}{2} \int_{u}^{2\ell-u} \Big[& \cos \frac{1}{2}(av+bu) - \cos \frac{1}{2}(bv+au) \\ & + \cos \frac{1}{2}(-av+bu) - \cos \frac{1}{2}(bv-au) \Big] \, dv \end{aligned} \tag{3.17}$$

with

$$\begin{aligned} a &= k_k - k_j \\ b &= k_k + k_j \end{aligned} \tag{3.18}$$

Upon integration of Equation (3.17),

$$\begin{aligned} K_{jk}(u) = \; & A_{jk} \left[\cos k_j u + \cos k_k u\right] \\ & + B_{jk} \left[\sin k_j u + \sin k_k u\right] \\ & + C_{jk} \left[\sin k_j u - \sin k_k u\right] \end{aligned} \tag{3.19}$$

where the coefficients are given by

$$A_{jk} = \begin{cases} 0, & \text{for } j \neq k \\ \ell, & \text{for } j = k \end{cases}$$

$$B_{jk} = \frac{\ell}{(j+k)\pi}\left[1 + (-1)^{j+k}\right] \tag{3.20}$$

$$C_{jk} = \frac{\ell}{(j-k)\pi}\left[1 + (-1)^{j+k}\right]$$

The cross acceptance terms then take on value according to whether the sum j + k is either an odd number or an even number. For j + k odd, $A_{jk} = B_{jk} = C_{jk} = 0$ so that $K_{jk}(u) = 0$ and $J_{jk}(\omega) = 0$. Such behavior can be anticipated inasmuch as we note the mode shapes are even and odd harmonic functions referenced to the mid-span of the structure. Likewise, the pressure fields are characterized as symmetrical real functions in $x-x'$. Now products involving even and odd functions are odd, the resultant integration of an odd function over the space of the structure is zero; those products involving either both odd or both even functions are even, the resultant integration of an even function over the space of the structure produces a value. The sum j + k odd implies an integration of an odd function so that $J_{jk}(\omega)$ is zero, as expected.

For j + k even, the coefficients for the cross acceptance become

$$A_{jk} = 0$$

$$B_{jk} = \frac{2\ell}{(j+k)\pi} \tag{3.21}$$

$$C_{jk} = \frac{2\ell}{(j-k)\pi}$$

so that

$$K_{jk}(u) = \frac{4\ell}{(k^2-j^2)\pi} \left[k \sin \frac{j\pi u}{\ell} - j \sin \frac{k\pi u}{\ell} \right]. \tag{3.22}$$

Alternatively, for the joint acceptance, we find

$$J_j(\omega) = \frac{1}{2\ell^2} \int_0^{\ell} C_f(u,\omega)\, K_j(u)\, du \tag{3.23}$$

where

$$K_j(u) = 2(\ell-u) \cos \frac{j\pi u}{\ell} + \frac{2\ell}{j\pi} \sin \frac{j\pi u}{\ell} \tag{3.24}$$

3.1.1 Progressive Wave Field

Our description of the inputs is limited to quoting the appropriate normalized cross-spectral density function for each of the pressure fields. It is instructive to digress here and consider a more complete calculation leading to $C_f(x, x', \omega)$. We naturally select that which is mathematically the simplest, a plane progressive wave.+

Figure 3.2 depicts a plane wave of frequency f_o and wave length λ_o which impinges upon a surface at the incidence angle θ. The wave speed c is noted as

$$c = \lambda_o f_o \tag{3.25}$$

+ If the input is of fixed frequency, we need not use the formulation developed for random excitation. Indeed, it may be simpler to use any of the techniques mentioned in Section 2.1 for computing the response, squaring this result, then averaging over time to obtain the response in mean square.

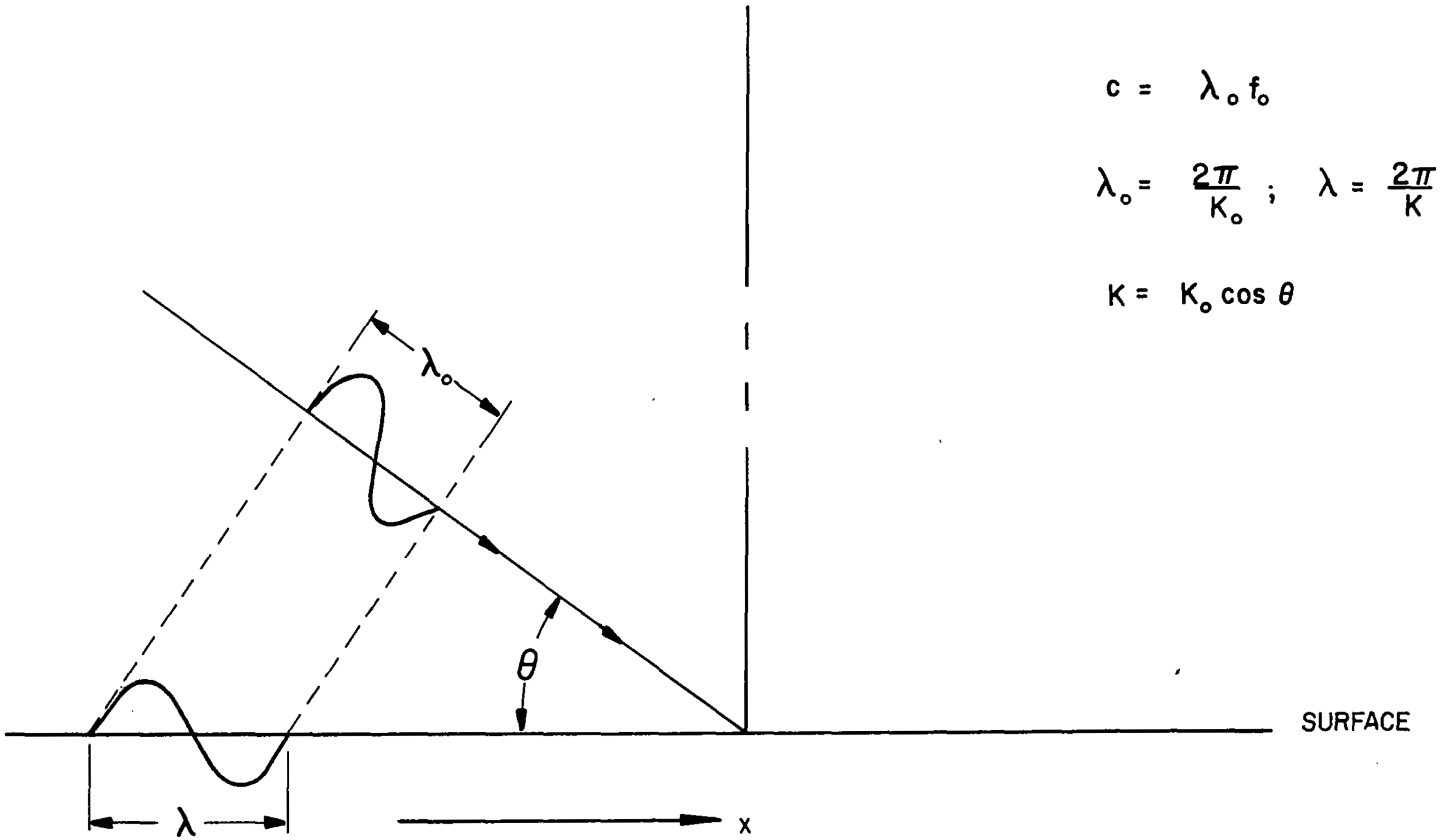

FIGURE 3.2 PLANE PRESSURE WAVE AT DISCRETE FREQUENCY AND FIXED INCIDENCE ANGLE

and

$$\lambda = \frac{\lambda_o}{\cos\theta} \tag{3.26}$$

where λ is the wave trace referenced to the surface. For a harmonic wave which propagates in the positive x direction,

$$f(x,t) = P \sin(\omega' t - Kx) \tag{3.27}$$

where $\omega' = 2\pi f'$ and P is the pressure amplitude at x. The spatial cross-correlation function for this wave is given by

$$R_f(x,x',\tau) = PP' \lim_{T\to\infty} \frac{1}{2T} \int_{-T}^{T} \sin\left[\omega' t - Kx\right] \sin\left[\omega'(t+\tau) - Kx'\right] dt \tag{3.28}$$

and becomes in the limit

$$R_f(x,x',\tau) = \frac{PP'}{2} \cos\left[K(x-x') - \omega'\tau\right] \tag{3.29}$$

The cross-spectral density then is determined by the transformation

$$R_f(x,x',\tau) \longleftrightarrow S_f(x,x',\omega) \tag{3.30}$$

so that

$$S_f(x,x',\omega) = \frac{PP'}{4\pi} \int_{-\infty}^{\infty} \cos\left[\omega'\tau - K(x-x')\right] e^{-i\omega\tau} d\tau \tag{3.31}$$

which resolves to the complex expression

$$S_f(x,x',\omega) = \frac{PP'}{4} \Big\{ \cos K(x'-x) \left[\delta(\omega-\omega') + \delta(\omega+\omega')\right] + i \sin K(x'-x) \left[\delta(\omega+\omega') - \delta(\omega-\omega')\right]\Big\} \tag{3.32}$$

Now if we normalize $S_f(x, x', \omega)$ according to the ratio given as Equation (2.52),

$$\hat{C}_f(x, x', \omega) = C_f(x, x', \omega) - i\, Q_f(x, x', \omega) \tag{3.33}$$

where $C_f(x, x', \omega)$ is the co-spectra of $\hat{C}_f(x, x', \omega)$ and $Q_f(x, x', \omega)$ the associated quad-spectra. Due to homogeneity of the excitation field,

$$S_f(x', x, \omega) = S_f^*(x, x', \omega) \tag{3.34}$$

so that the cross-acceptance function reduces to

$$J_{jk}(\omega) = \frac{1}{\ell^2} \int_0^\ell \int_0^\ell \phi_j(x)\phi_k(x') 2\, \mathrm{Re}\left[\hat{C}_f(x, x', \omega)\right] dx\, dx' \tag{3.35}$$

as the quad-spectra contribution resolves to zero over the double integration. With

$$S(x_o, \omega) = S_f(x_o, \omega) = \frac{P_o^2}{2}$$

$$\frac{PP'}{P_o^2} = 1 \tag{3.36}$$

the cross acceptance becomes

$$J_{jk}(\omega) = \frac{1}{\ell^2} \int_0^\ell \int_0^\ell \phi_j(x)\, \phi_k(x')\, C_f(x, x', \omega)\, dx\, dx' \tag{3.37}$$

where

$$C_f(x, x', \omega) = \cos K(x - x') \left[\delta(\omega - \omega') + \delta(\omega + \omega')\right] \tag{3.38}$$

which, except for the delta functions, is the form quoted at the beginning of this section for a random progressive wave field.

Consider now the evaluation of $J_{jk}(\omega)$. The values for the cross acceptance are given by the integral

$$J_{jk}(\omega) = \frac{1}{2\ell^2} \int_0^{\ell} K_{jk}(u) \cos \frac{\omega u}{c} \, du \tag{3.39}$$

which, in terms of the variable β, produces for $j \neq k$

$$\begin{aligned} J_{jk}(\beta) &= \frac{2}{\pi^2} \frac{jk\left[1-(-1)^j \cos \pi\beta\right]}{\left[j^2-\beta^2\right]\left[k^2-\beta^2\right]}, \quad j+k \text{ even} \\ J_{jk}(\beta) &= 0, \quad j+k \text{ odd} \end{aligned} \tag{3.40}$$

where

$$\beta = \frac{K\ell}{\pi} = \frac{\ell}{c\pi}\omega \tag{3.41}$$

For the joint acceptance

$$J_j(\omega) = \frac{1}{2\ell^2} \int_0^{\ell} K_j(u) \cos \frac{\omega u}{c} \, du \tag{3.42}$$

and, upon integration,

$$J_j(\beta) = \frac{2}{\pi^2} \frac{j^2\left[1-(-1)^j \cos \pi\beta\right]}{\left[j^2-\beta^2\right]^2} \tag{3.43}$$

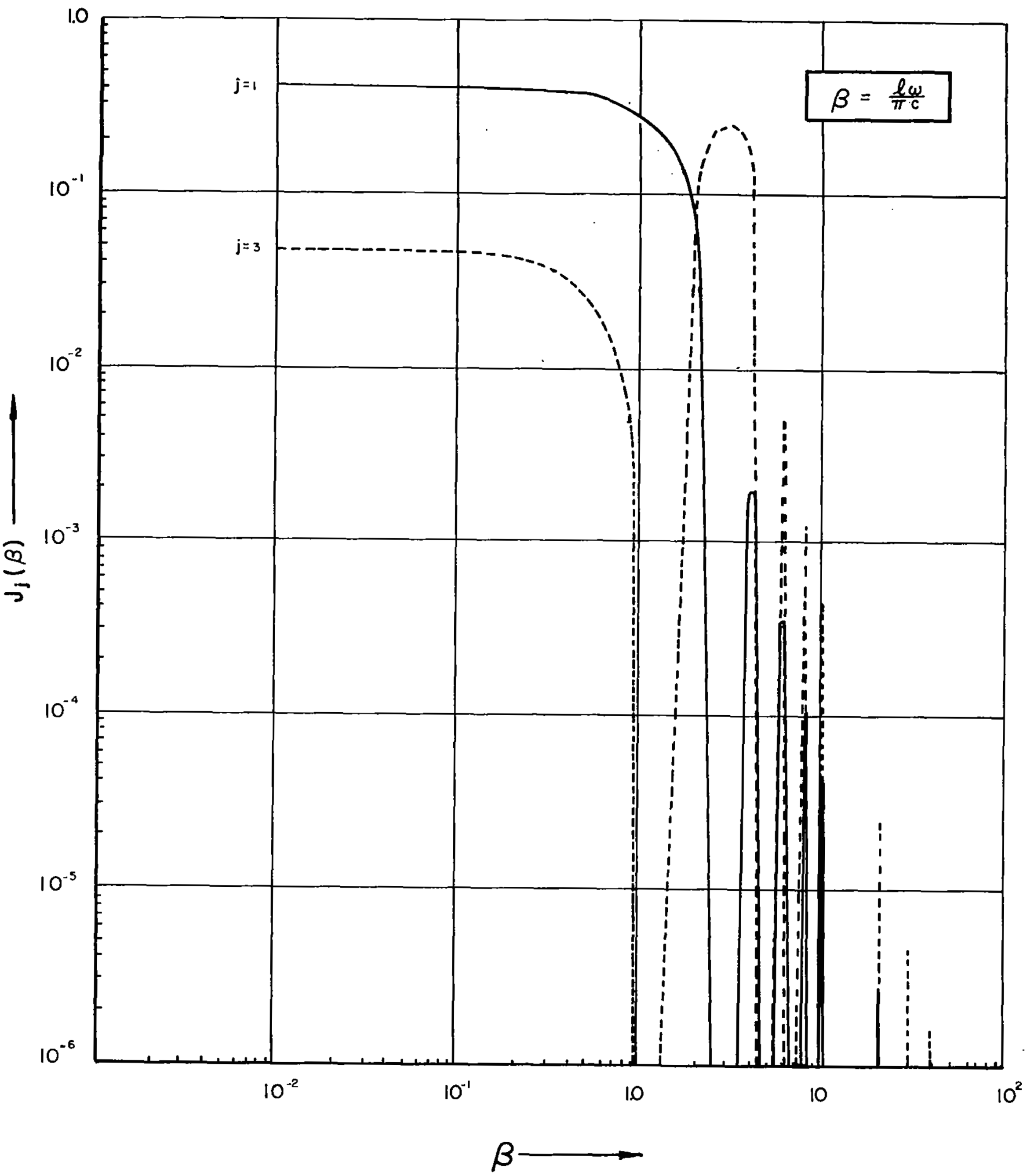

FIGURE 3.3 JOINT ACCEPTANCE FUNCTIONS FOR A RANDOM PROGRESSIVE WAVE (ODD TERMS ONLY)

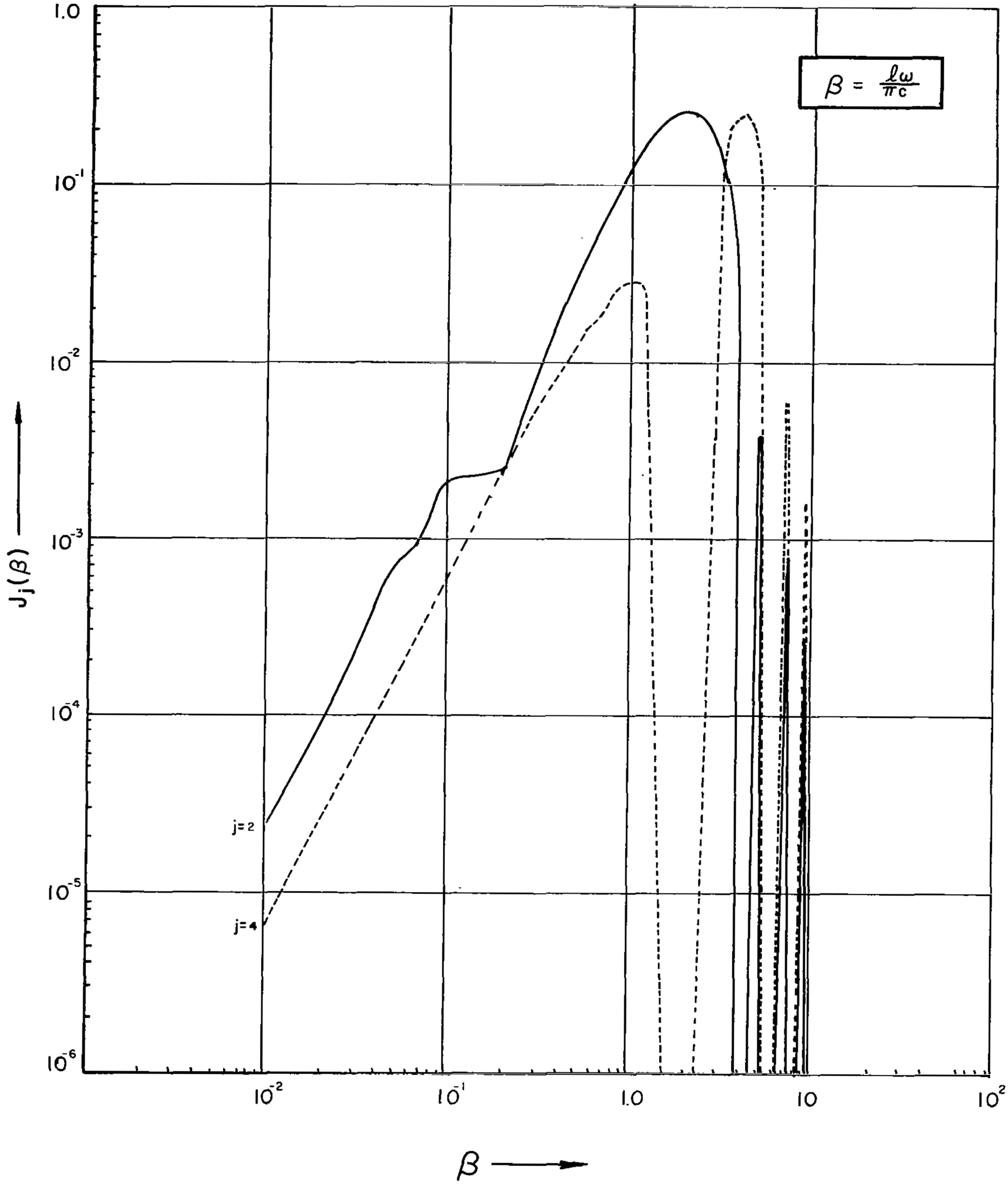

FIGURE 3.4 JOINT ACCEPTANCE FUNCTIONS FOR A RANDOM PROGRESSIVE WAVE (EVEN TERMS ONLY)

When a wave number of the trace of the progressive wave corresponds to a modal wave number,

$$K = k_j = \frac{j\pi}{\ell} \qquad (3.44)$$

For this condition of spatial resonance, the joint acceptance resolves to the constant $J_j(\beta) = 1/4$.

Plots of the joint acceptance for the first two odd-numbered modes are shown as Figure 3.3, and for the first two even-numbered modes as Figure 3.4. Of note is the pronounced selectivity of each function, in particular the peaks which correspond to the values of spatial resonance. The odd-numbered modes display low-pass characteristics for $\beta \le 1$ whereas the even-numbered modes act more nearly like band-pass filters over this same range and reject the excitation components below, say, $\beta \le 0.1$.

3.1.2 Reverberant Pressure Field

For this field with $K = \frac{\omega}{c}$,

$$J_{jk}(K) = \frac{1}{2\ell^2} \int_0^{\ell} K_{jk}(u) \frac{\sin Ku}{Ku} \, du \qquad (3.45)$$

which, in terms of β, yields $J_{jk}(\beta) = 0$ for $j \neq k$ and $j + k$ odd, while for $j \neq k$ and $j + k$ even,

$$J_{jk}(\beta) = \frac{1}{(k^2-j^2)\pi^2\beta} \left\{ k \left[\text{Cin } \pi(\beta+j) - \text{Cin } \pi(\beta-j) \right] - j \left[\text{Cin } \pi(\beta+k) - \text{Cin } \pi(\beta-k) \right] \right\} \qquad (3.46)$$

where

$$\beta = \frac{\ell}{c\pi} \omega$$

$$\mathrm{Cin}\,(z) = \int_0^z \frac{1-\cos x}{x}\,dx \tag{3.47}$$

For the joint acceptance,

$$J_j(K) = \frac{1}{2\ell^2}\int_0^{\ell} K_j(u)\,\frac{\sin Ku}{Ku}\,du \tag{3.48}$$

which becomes

$$\begin{aligned} J_j(\beta) &= \frac{1}{2j\pi^2\beta}\left[\mathrm{Cin}\,\pi\,(\beta+j) - \mathrm{Cin}\,\pi\,(\beta-j)\right] \\ &+ \frac{1}{2\pi\beta}\left[\mathrm{Si}\,\pi\,(\beta+j) + \mathrm{Si}\,\pi\,(\beta-j)\right] \\ &+ \frac{1}{\pi^2(j^2-\beta^2)}\left[1 - (-1)^j\cos\pi\beta\right] \end{aligned} \tag{3.49}$$

where

$$\mathrm{Si}(z) = \int_0^z \frac{\sin x}{x}\,dx \tag{3.50}$$

Polynomial expressions and/or tabular listings for the functions Cin(z) and Si(z) are found in standard tables of integrals [18].

Plots of $J_j(\beta)$ and $J_{jk}(\beta)$ are shown as Figures 3.5 through 3.8. The main diagonal expressions for the odd-numbered modes are shown as Figure 3.5; for the even-numbered modes as Figure 3.7.

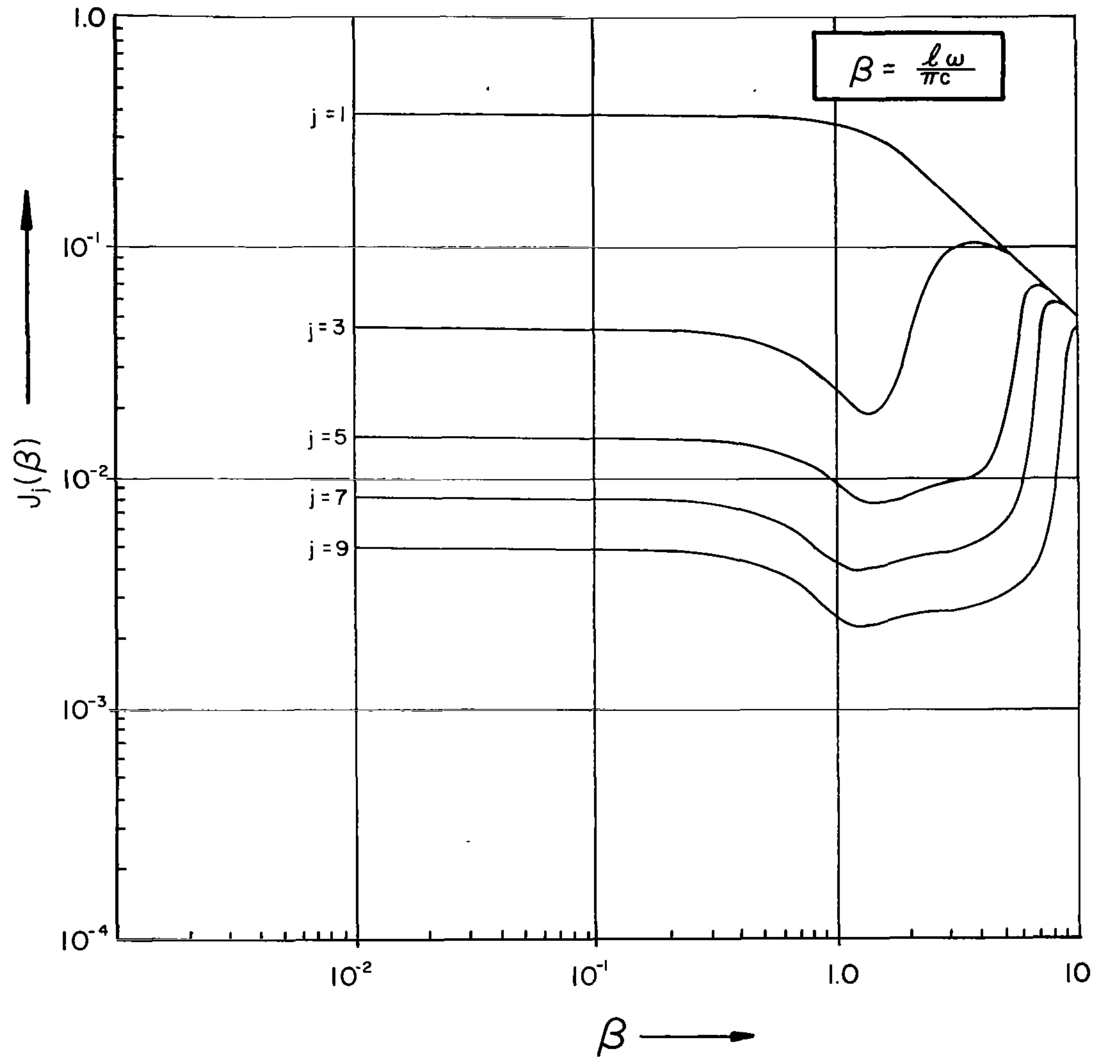

FIGURE 3.5 JOINT ACCEPTANCE FUNCTIONS FOR A REVERBERANT FIELD (ODD TERMS ONLY)

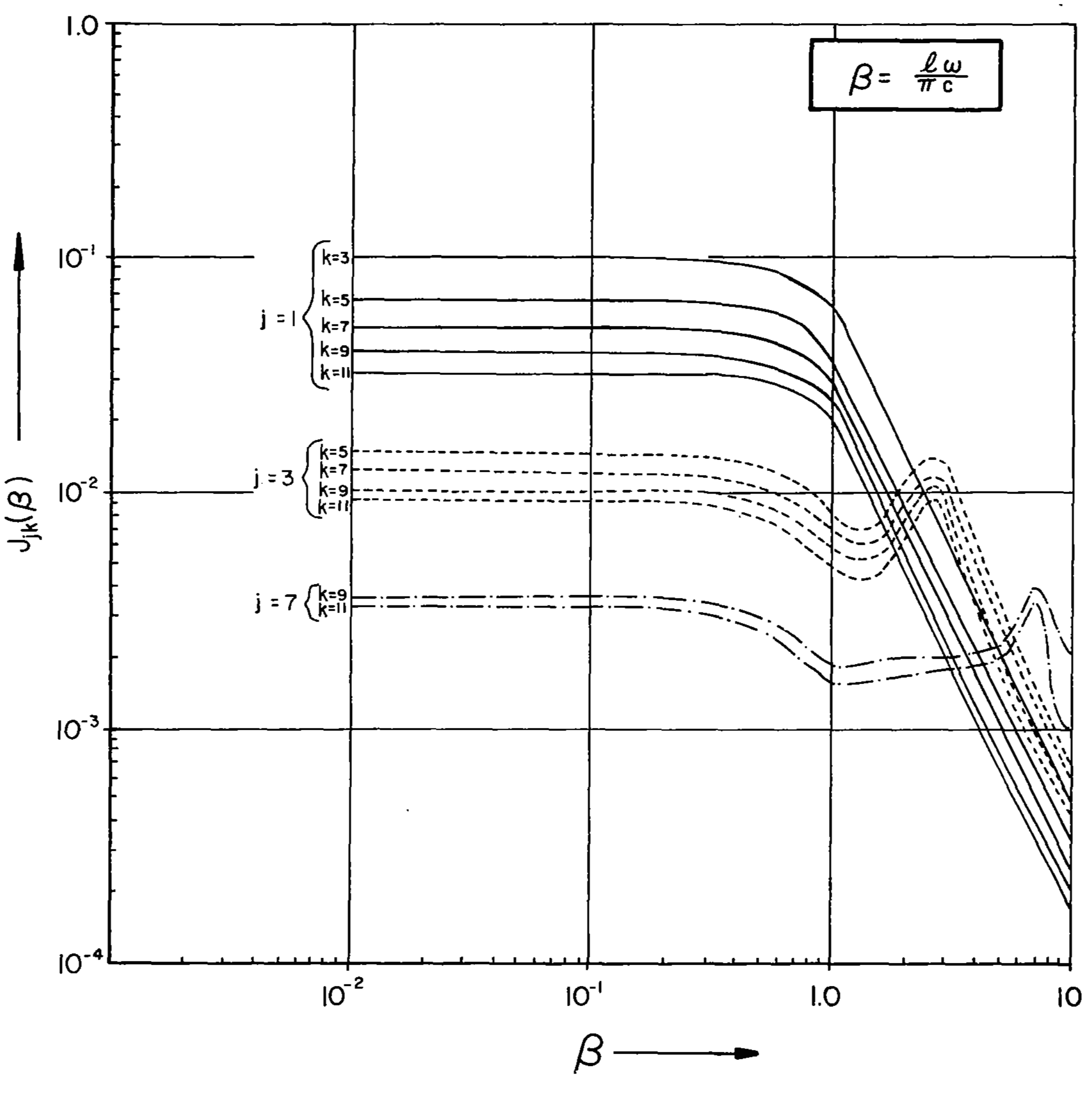

FIGURE 3.6 CROSS ACCEPTANCE FUNCTIONS FOR A REVERBERANT FIELD (ODD TERMS ONLY)

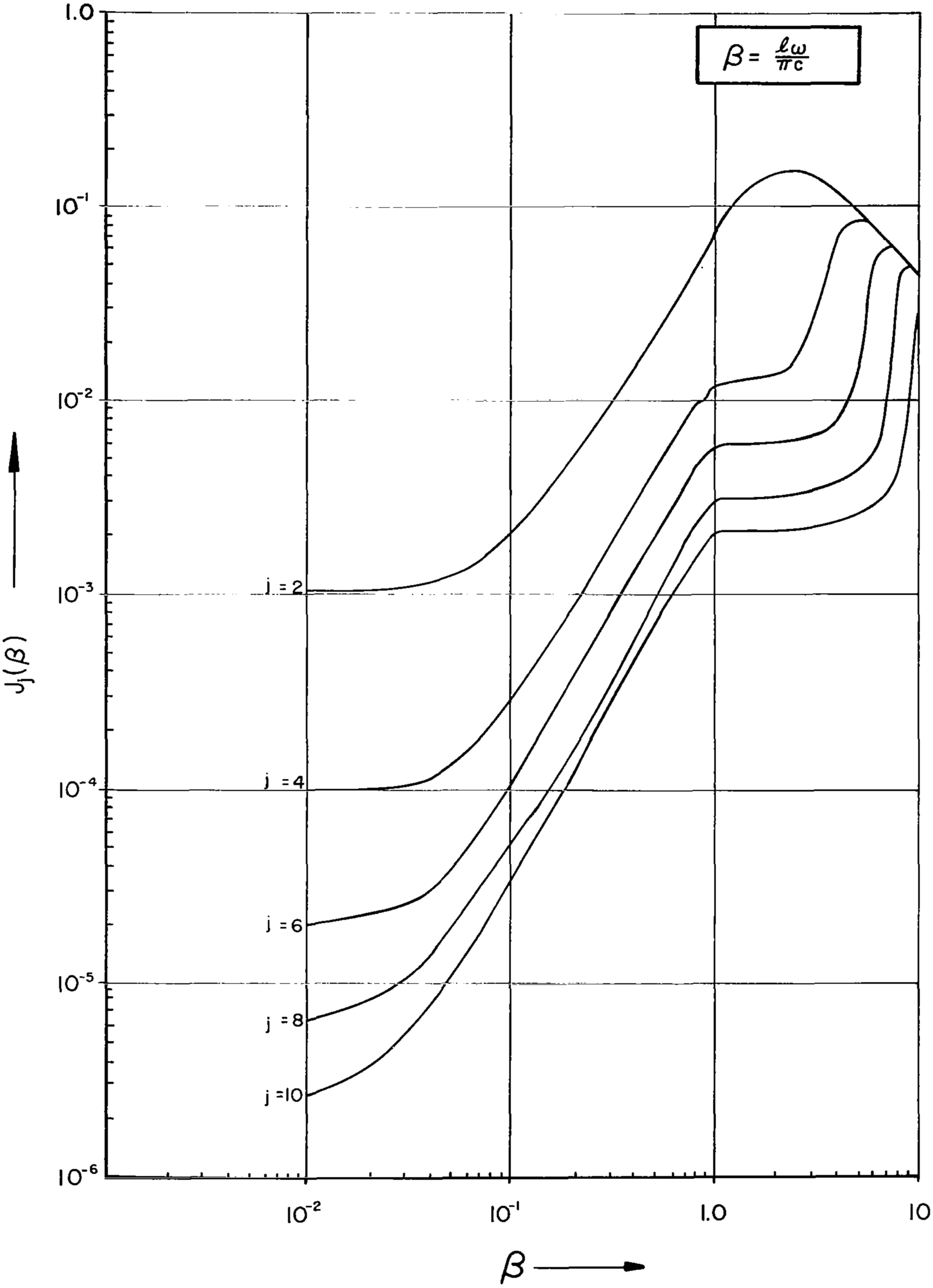

FIGURE 3.7 JOINT ACCEPTANCE FUNCTIONS FOR A REVERBERANT FIELD (EVEN TERMS ONLY)

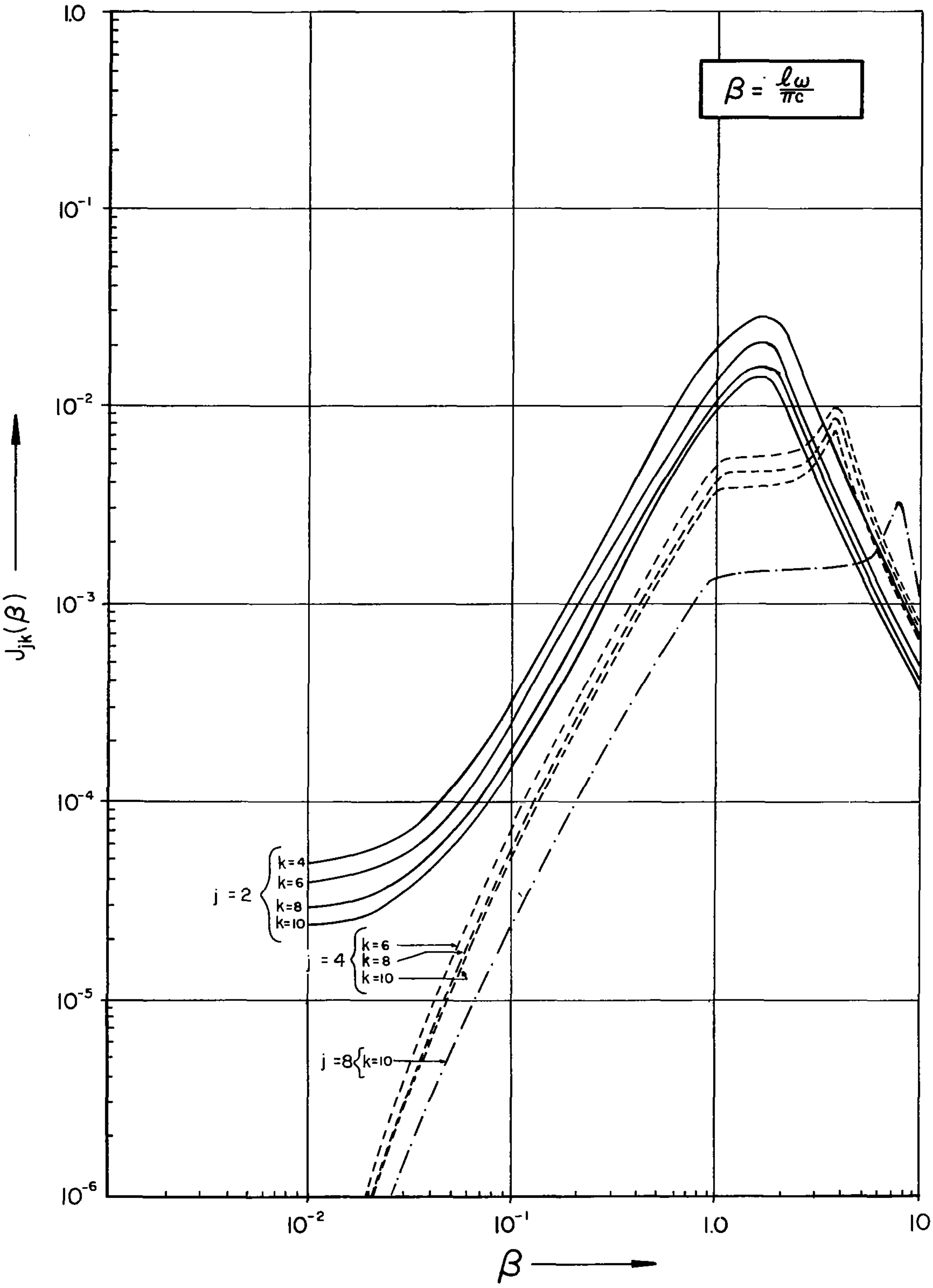

FIGURE 3.8 CROSS ACCEPTANCE FUNCTIONS FOR A REVERBERANT FIELD (EVEN TERMS ONLY)

The off-diagonal terms for the odd-numbered modes are displayed as Figure 3.6; for the even-numbered modes as Figure 3.8.

As is expected, a system with harmonic modes discriminates between individual as well as combinational sums of even and odd-numbered modes. For a reverberant field, the joint acceptance plot for $j = 1$ bounds the other joint and cross-acceptance values; it has nearly a constant value over $.01 \leq \beta \leq 1$ and decays with a constant (logarithmic) slope beyond $\beta > 1$. For all modes except for $j = 1$, both the joint and cross acceptance appear relatively selective (near the various resonant frequencies) beyond the first resonance value. For lower values of β, say $\beta \leq .2$, the even-numbered modes are suppressed whereas the odd-numbered modes are characterized by constant valued functions with magnitudes dependent upon the mode number.

3.1.3 Aerodynamic Turbulence

For this excitation with $\bar{K} = \dfrac{\omega}{U_c}$,

$$J_{jk}(\bar{K}) = \frac{1}{2\ell^2} \int_0^\ell K_{jk}(u)\, e^{-\alpha\bar{K}|u|} \cos \bar{K}u \, du \tag{3.51}$$

which, in terms of β, yields for $j \neq k$

$$\begin{aligned} J_{jk}(\beta) = {} & A_{jk}\left[1 - (-1)^j e^{-\pi\alpha\beta} \cos \pi\beta\right] \\ & + B_{jk}\left[(-1)^j e^{-\pi\alpha\beta} \sin \pi\beta\right] \end{aligned} \tag{3.52}$$

where the coefficients are given by

$$A_{jk} = \frac{(j^2+k^2)^2}{2\pi^2 j^3 k^3 D_j D_k} \left[\left[(\alpha^2-1)\,\beta_1{}^2+1\right]^2 - 4\left[\alpha\,\beta_1{}^2\right]^2 - \left[\frac{k^2-j^2}{k^2+j^2}\right]^2 \right]$$

$$B_{jk} = \frac{2(j^2+k^2)^2}{\pi^2 j^3 k^3 D_j D_k}\,\alpha\,\beta_1{}^2 \left[(\alpha^2-1)\,\beta_1{}^2+1\right]$$

$$D_j = \left[(\alpha^2+1)\,\beta_j^2+1\right]^2 - 4\,\beta_j^2 \tag{3.53}$$

$$\beta_j = \frac{\beta}{j}$$

$$\beta_1 = \left[\frac{2}{j^2+k^2}\right]^{1/2} \beta$$

$$\beta = \frac{K\ell}{\pi} = \frac{\ell}{\pi U_c}\,\omega$$

Similarly, the joint acceptance is expressed by the integral

$$J_j(\overline{K}) = \frac{1}{2\ell^2} \int_0^{\ell} K_j(u)\, e^{-\alpha \overline{K}|u|} \cos Ku \, du \tag{3.54}$$

which resolves to

$$J_j(\beta) = A_j \left[1 - (-1)^j e^{-\pi\alpha\beta} \cos \pi\beta \right] + B_j(-1)^j e^{-\pi\alpha\beta} \sin \pi\beta + C_j \qquad (3.55)$$

where

$$A_j = \frac{2}{(j\pi)^2 D_j^2} \left[\left[(\alpha^2 - 1)\, \beta_j^2 + 1 \right]^2 - 4 \left[\alpha\, \beta_j^2 \right]^2 \right]$$

$$B_j = \frac{8}{(j\pi)^2 D_j^2} \; \alpha \beta_j^2 \left[\left[\alpha^2 - 1 \right] \beta_j^2 + 1 \right] \qquad (3.56)$$

$$C_j = \frac{1}{j\pi D_j} \; \alpha \beta_j \left[\left[\alpha^2 + 1 \right] \beta_j^2 + 1 \right]$$

The remaining terms are those stated previously. The exponential coefficient corresponds to that used elsewhere [17] , it is written as

$$\alpha = 0.1 + \frac{0.265}{\pi\beta} \left[\frac{\ell}{\delta_b} \right] \qquad (3.57)$$

where δ_b is the depth of the boundary layer.

Plots of $J_j(\beta)$ and $J_{jk}(\beta)$ are shown by Figures 3.9 through 3.15. Figures 3.9 through 3.11 show the joint and cross acceptance functions for $\ell/\delta_b = 1$ while Figures 3.13 through 3.15 display these same functions for $\ell/\delta_b = 30$. For the modes considered, note that the off-diagonal or cross acceptance plots have negative values

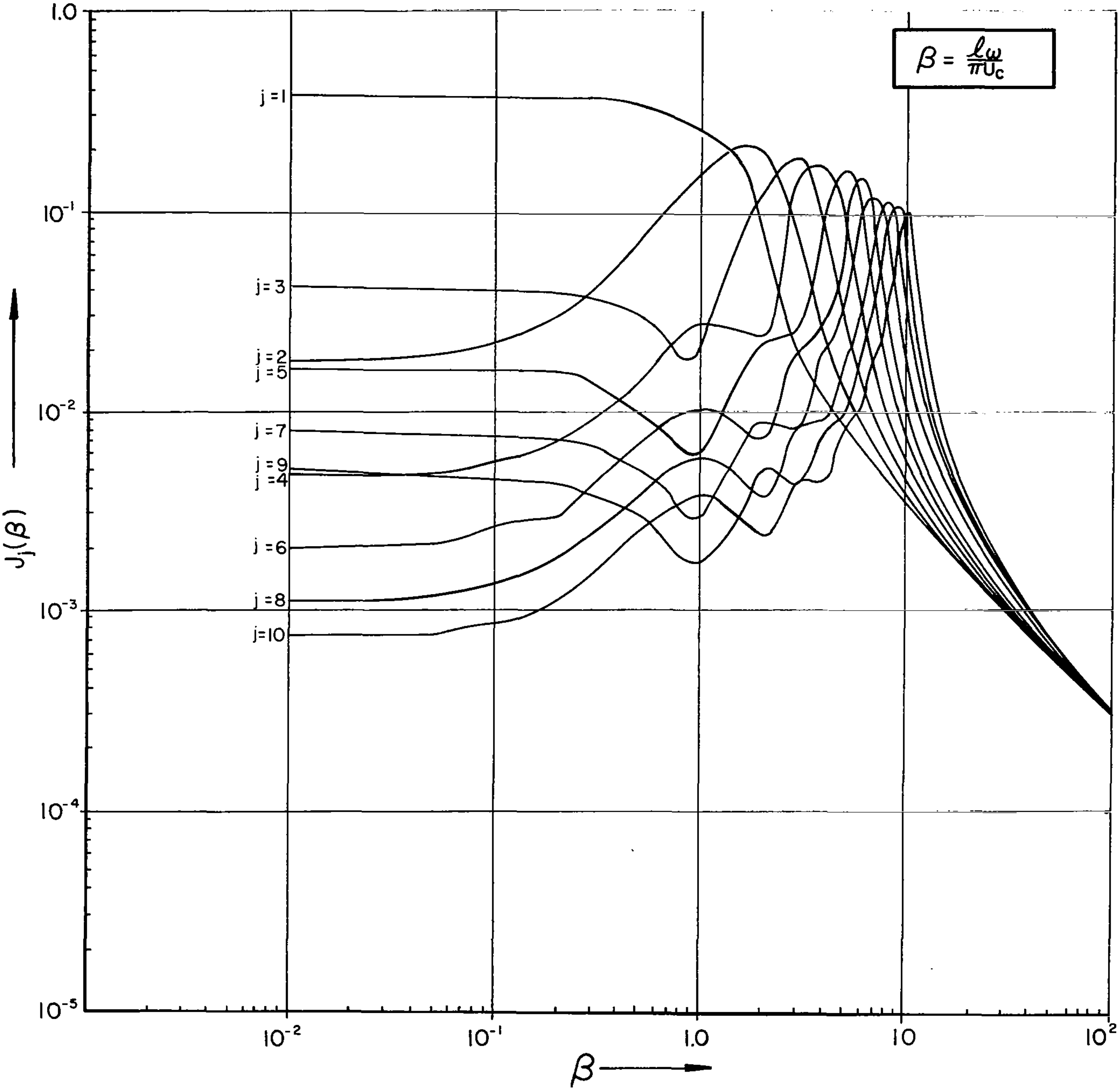

FIGURE 3.9 JOINT ACCEPTANCE FUNCTIONS FOR AERODYNAMIC TURBULENCE, $\ell/\delta_b = 1$

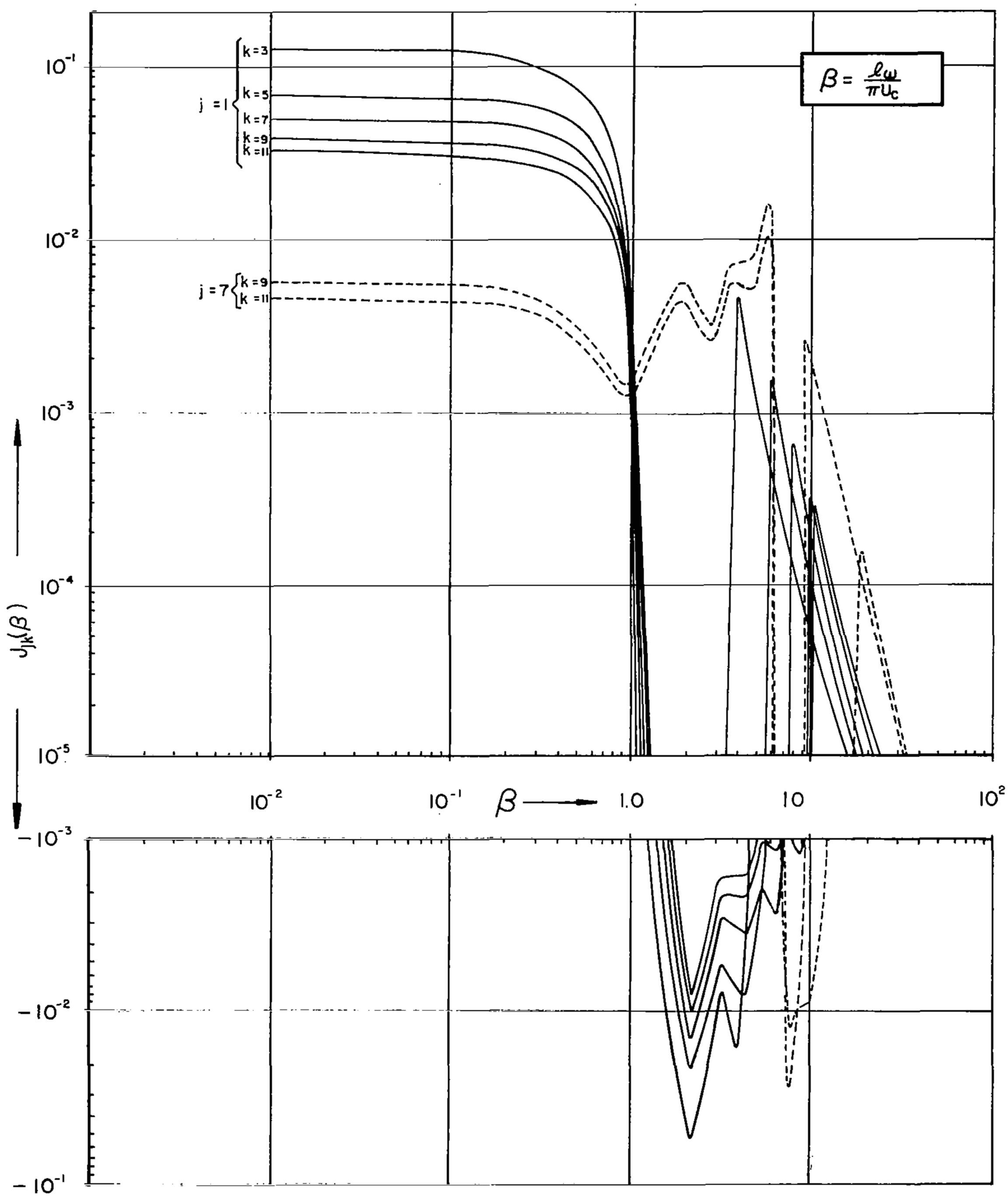

FIGURE 3.10 CROSS ACCEPTANCE FUNCTIONS FOR AERODYNAMIC TURBULENCE, ℓ/δ_b = 1 (ODD TERMS ONLY)

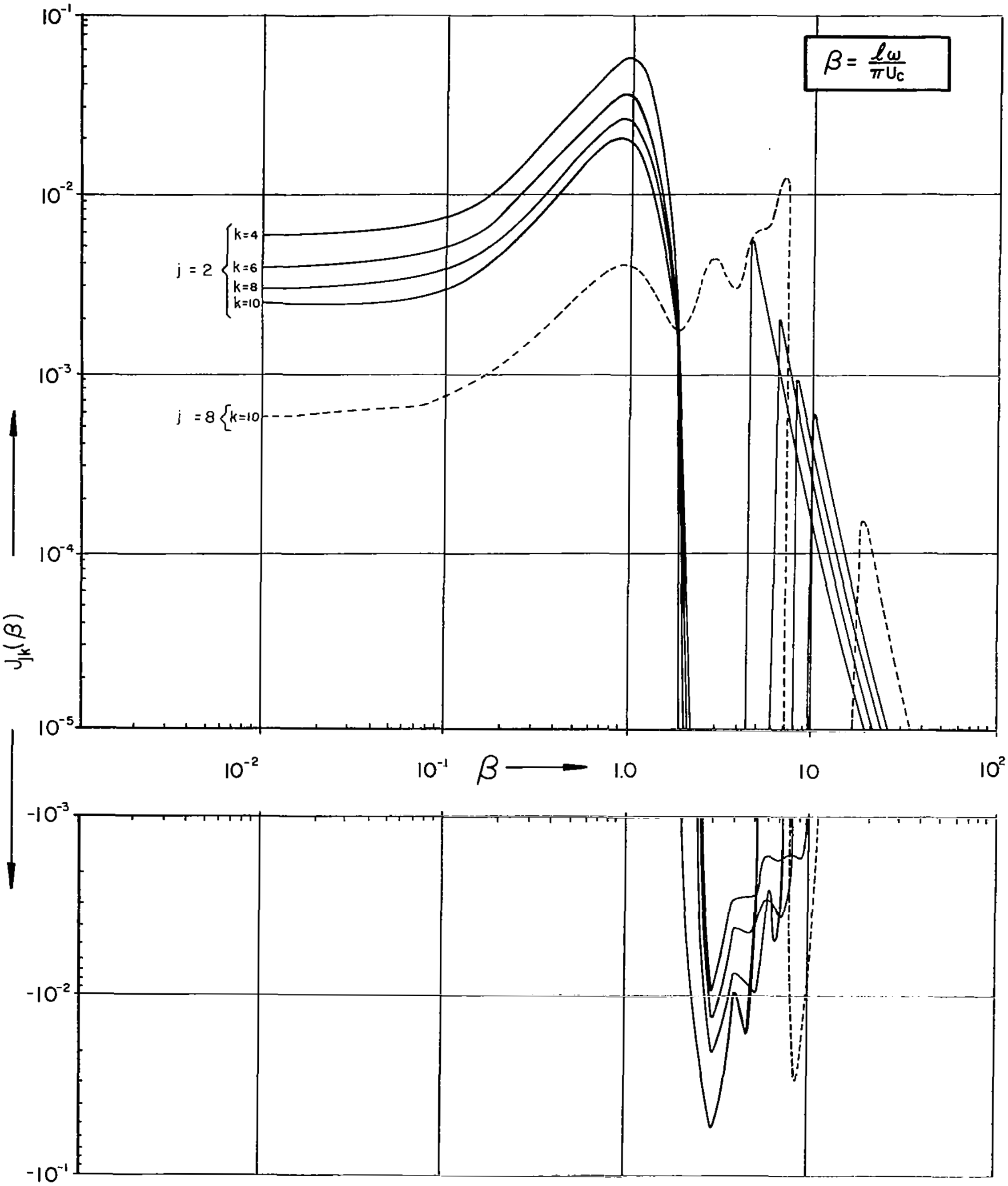

FIGURE 3.11 CROSS ACCEPTANCE FUNCTIONS FOR AERODYNAMIC TURBULENCE, ℓ/δ_b = 1 (EVEN TERMS ONLY)

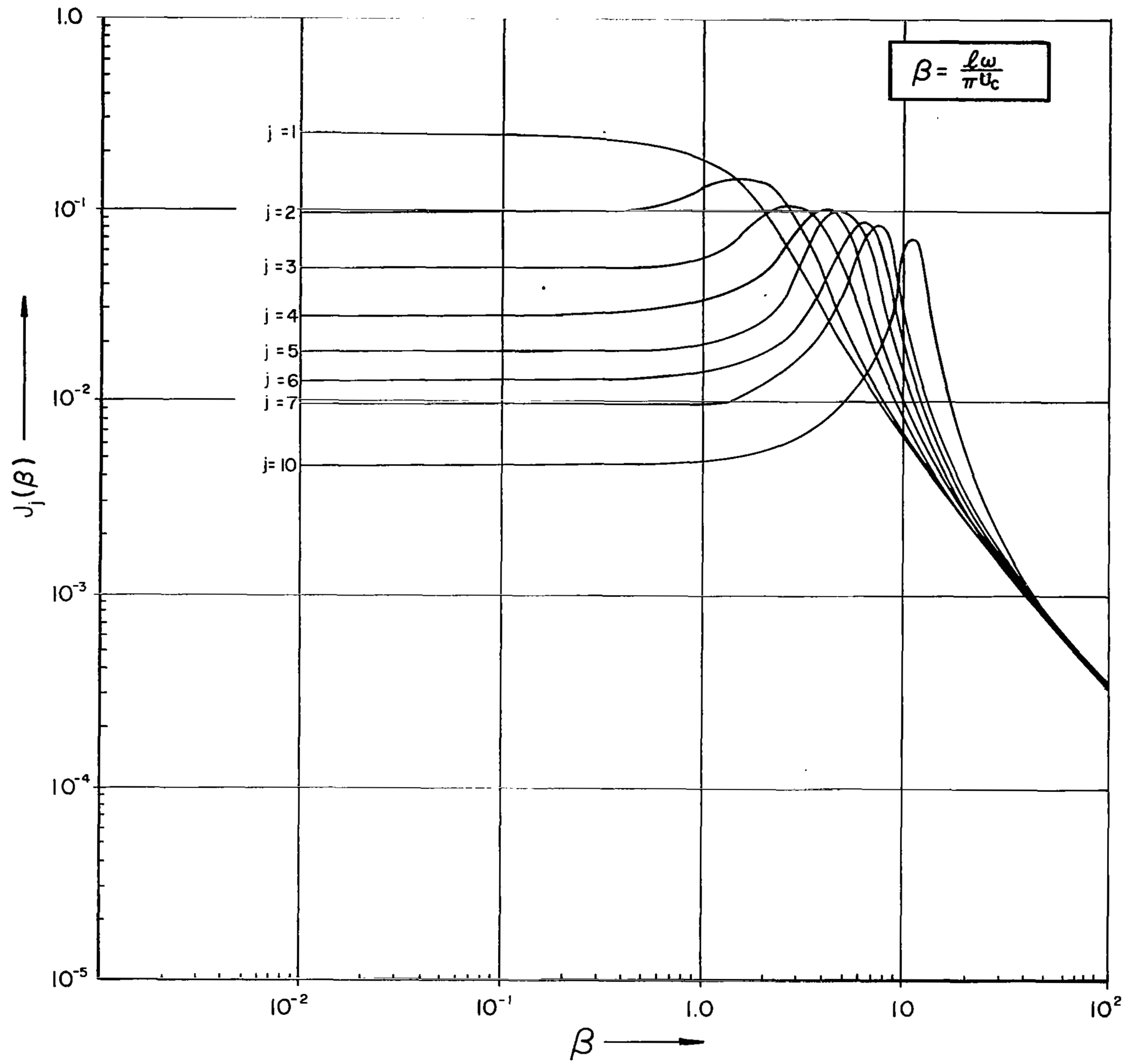

FIGURE 3.12 JOINT ACCEPTANCE FUNCTIONS FOR AERODYNAMIC TURBULENCE, ℓ/δ_b = 10

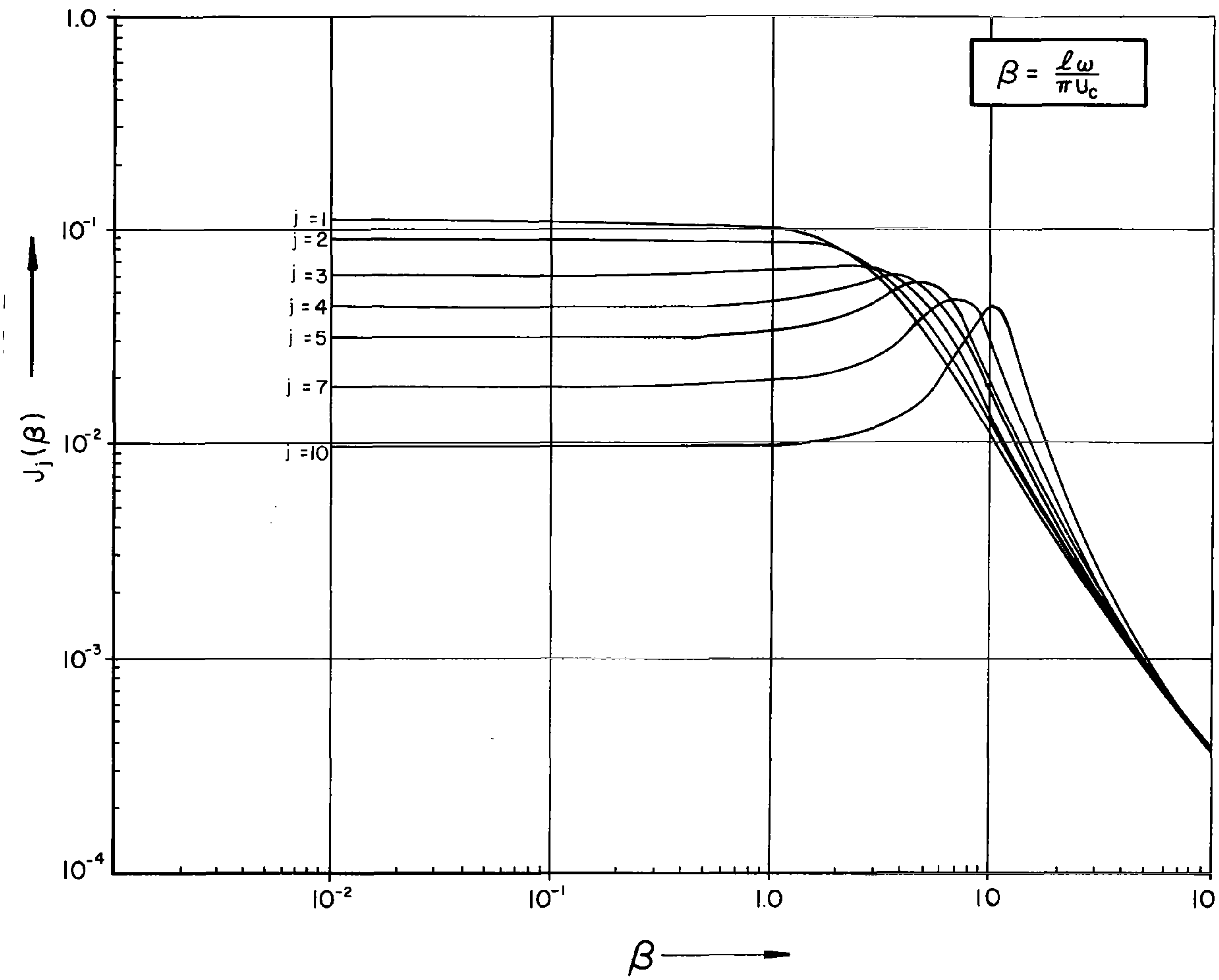

FIGURE 3.13 JOINT ACCEPTANCE FUNCTIONS FOR AERODYNAMIC TURBULENCE, ℓ/δ_b = 30

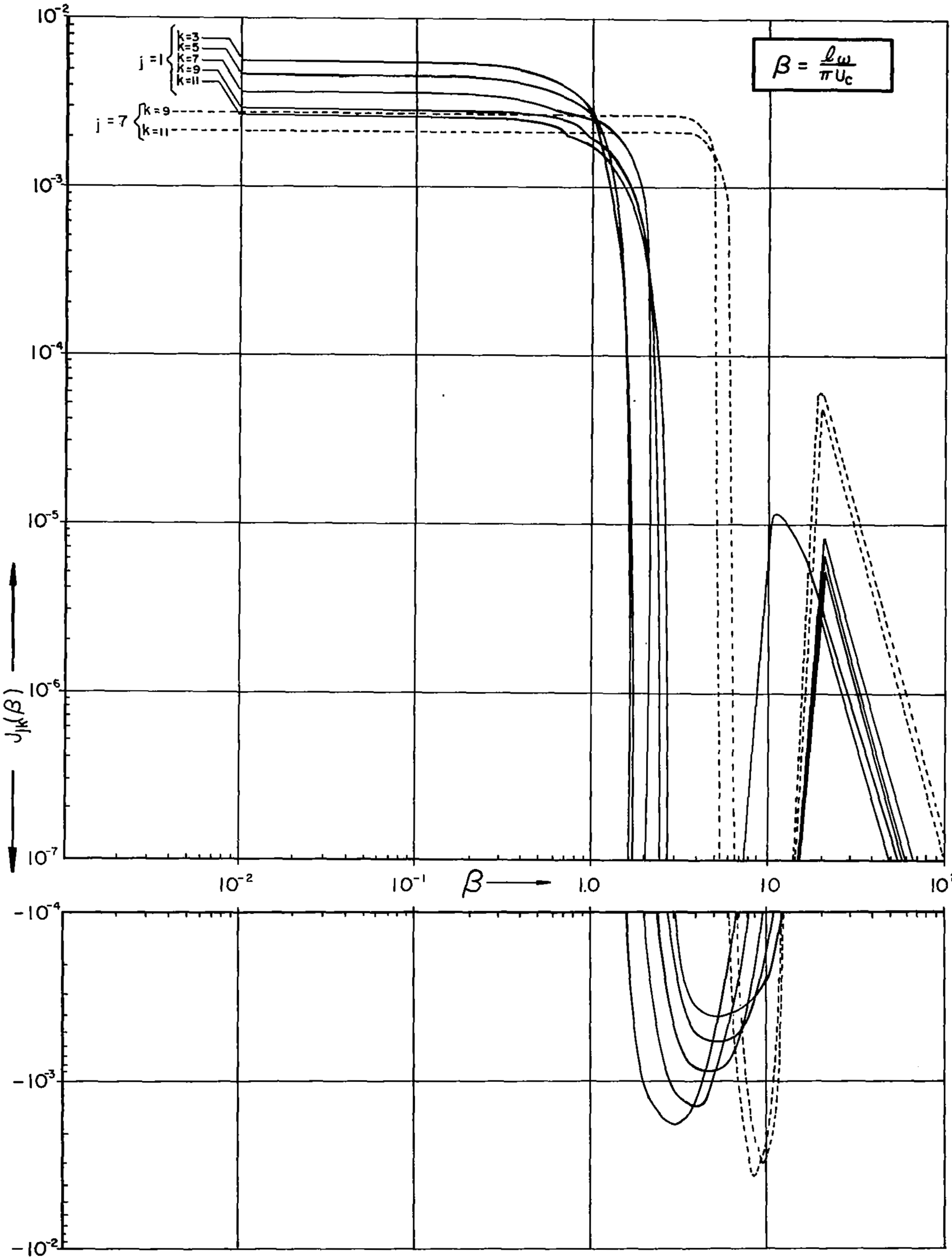

FIGURE 3.14 CROSS ACCEPTANCE FUNCTIONS FOR AERODYNAMIC TURBULENCE, ℓ/δ_b = 30 (ODD TERMS ONLY)

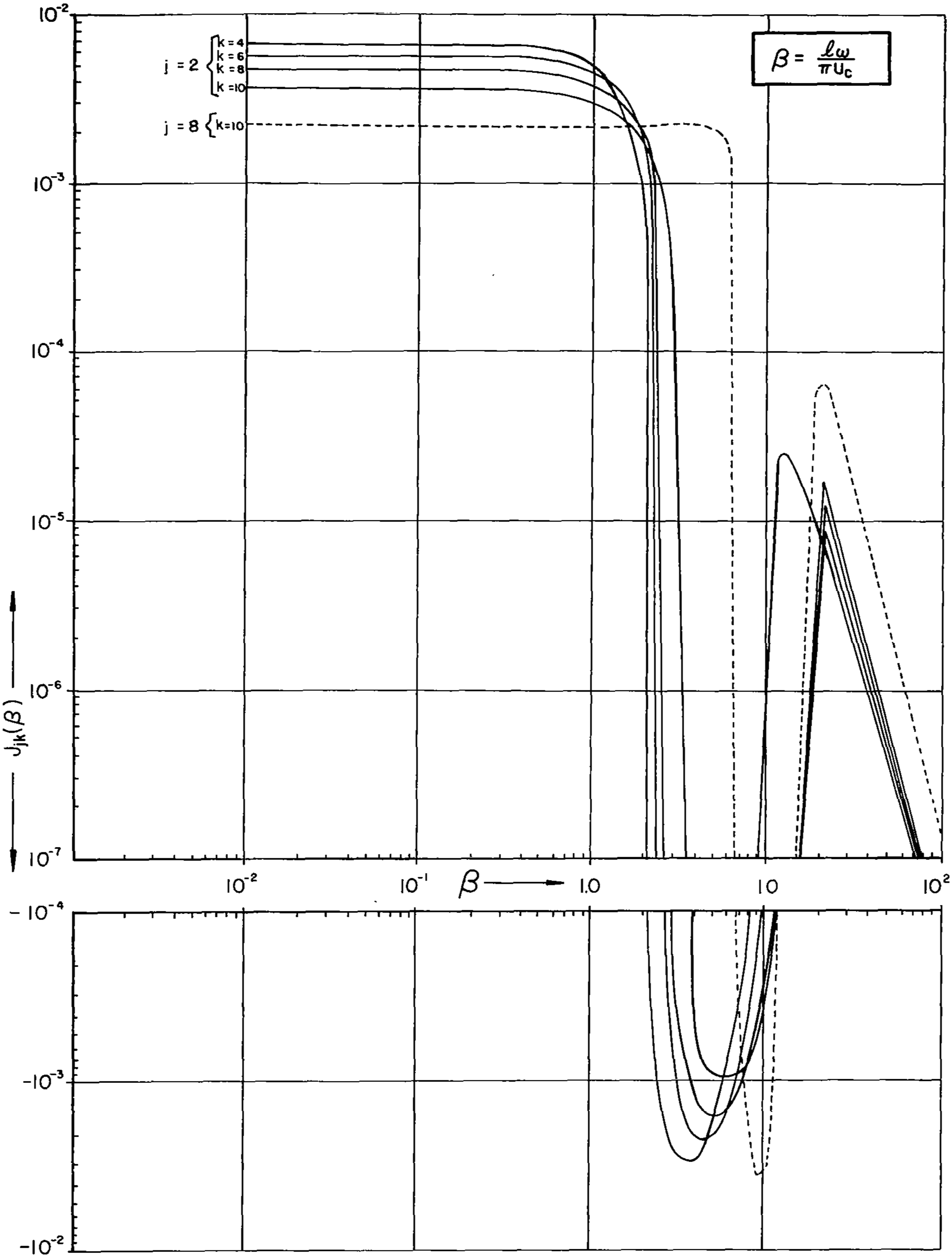

FIGURE 3.15 CROSS ACCEPTANCE FUNCTIONS FOR AERODYNAMIC TURBULENCE, ℓ/δ_b = 30 (EVEN TERMS ONLY)

over some portion of the range $1 \leq \beta \leq 20$. The magnitude and behavior of such values are shown by the curves referenced to the lower log scale in the cross acceptance plots.

Figures 3.9, 3.12 and 3.13 intimate the spatial selectivity characteristics of the system in a turbulent field as well as the relative effect of boundary layer depth on the joint acceptance functions. The system acts as a more selective filter in β for the thicker boundary layers and tends to suppress, in particular, the contributions from the even-numbered modes for $\beta \leq .5$. Over the range $.01 \leq \beta \leq 1$, the acceptance magnitude for the $j = 1$ mode dominates the values of the other modes; for $\beta > 1$, a curve which connects the acceptance values at spatial resonance for each of the modes envelopes (practically speaking) the major contributions. Note that the thicker boundary layers spread the range of acceptance values over $01. \leq \beta \leq 1$; the $j = 1$ term increases from $\simeq 0.11$ to $\simeq .379$ while the $j = 10$ term decreases from $\simeq 0.0009$ to $\simeq 0.0007$.

3.1.4 Approximate Representations

Upon inspection of the mathematical forms which govern the acceptance functions for both the reverberant field and turbulence, it is clear their substitution into Equation (3.5) will yield rather complicated integrands for the integrals of the mean square response. To carry out such integrations over β in closed form is an enormous mathematical task both in complexity and in tedium. One then seeks refuge by specifying simpler, approximate representations for the acceptance functions. We examine here two approximate forms which rely upon application of

- the Schwartz inequality
- simple filter theory

The Schwartz inequality is given by [9]

$$\int_0^{\ell} C(x, x') \, \phi_j(x') dx' \le \left[\int_0^{\ell} \phi_j^2 (x') \, dx' \right]^{1/2} \left[\int_0^{\ell} C^2(x, x') dx' \right]^{1/2} \tag{3.58}$$

so that a bound on the cross acceptance becomes

$$J_{jk}(\omega) \le \frac{1}{\ell^2} \left[\int_0^{\ell} \phi_k^2(x) \, dx \right]^{1/2} \int_0^{\ell} \phi_j(x) \left[\int_0^{\ell} C_f^2(x, x', \omega) dx' \right]^{1/2} dx \tag{3.59}$$

By the Schwartz inequality applied to the bracketed term containing $C_f^2(x, x', \omega)$,

$$J_{jk}(\omega) \le \frac{1}{\ell^2} \left[\int_0^{\ell} \phi_j^2(x) \, dx \right]^{1/2} \left[\int_0^{\ell} \phi_k^2(x) dx \right]^{1/2} I_f \, (\omega) \tag{3.60}$$

where

$$I_f(\omega) = \left[\int_0^{\ell}\int_0^{\ell} C_f^2\,(x, x', \omega)dx\,dx' \right]^{1/2} \tag{3.61}$$

If we assume

$$C_f^2(x, x', \omega) = C_f^2\,(x-x', \omega), \tag{3.62}$$

then

$$I_f^2(\omega) = \int_{-\ell/2}^{\ell/2} \left[\int_{-\ell/2\,-\,x}^{\ell/2\,-\,x} C_f^2(u, \omega)\,du \right] dx \tag{3.63}$$

$$I_f^2(\omega) = 2 \int_0 (\ell-u)\,C_f^2\,(u, \omega)\,du \tag{3.64}$$

so that

$$J_{jk}(\omega) \le \frac{1}{\ell^2} \left[2 \int_0^{\ell} \phi_j^2(x)dx \int_0^{\ell} \phi_k^2(x)dx \int_0^{\ell} (\ell-u)\,C_f^2(u,\omega)du \right]^{1/2} \tag{3.65}$$

which agrees with that already established [16].

For the harmonic mode shapes of Equation (3.7), the bound becomes

$$J_{jk}(\omega) \le \frac{1}{\left[2\,\ell^2\right]^{1/2}} \left[\int_0^{\ell} (\ell-u)\,C_f^2(u,\omega)\,du \right]^{1/2} \tag{3.66}$$

and, for the three fields of concern to us,

- plane pressure wave

$$J_{jk}(\beta) \leq \frac{1}{2\pi\beta\left[2\right]^{1/2}} \left[(\beta\pi)^2 + \sin^2 \beta\pi\right]^{1/2} \tag{3.67}$$

- reverberant field

$$J_{jk}(\beta) \leq \frac{1}{\pi\beta\left[2\right]^{1/2}} \left[\sin 2\pi\beta + \beta\pi \, \mathrm{Si}(2\pi\beta) - \frac{1}{2} \, \mathrm{Cin}\,(2\pi\beta)\right]^{1/2} \tag{3.68}$$

- turbulence

$$J_{jk}(\beta) \leq \frac{1}{4\pi\alpha\beta} \left\{ 2\pi\alpha\beta\left[\frac{2\alpha^2+1}{\alpha^2+1}\right] - \left[1 + \frac{\alpha^2(\alpha^2-1)}{(\alpha^2+1)^2}\right] + e^{-2\pi\alpha\beta}\left[1 + \frac{\alpha^2(\alpha^2-1)}{(\alpha^2+1)^2} \cos 2\pi\beta - \frac{2\alpha^3}{(\alpha^2+1)^2} \sin 2\pi\beta\right]\right\}^{1/2} \tag{3.69}$$

where α is given by Equation (3.57). Practically, the use of these expresions in developing closed form mean square response results is limited severely due to the mathematical complexities introduced by the radicals. To avoid such problems, simple filter functions in β are suggested which can be made to approximate the acceptance functions as well as lend themselves mathematically to evaluation.

We choose to derive filters which can be made to envelope approximately the maxima of the reverberant and turbulence excitations. Such filters also can be used to match approximately the individual acceptance functions. From Figures 3.5 through 3.15, we note the maxima are governed by the values for the various joint acceptances. By inspection, the envelope functions for the odd-numbered modes of the reverberant field and the turbulence appear to have low-pass characteristics of the form

$$J_I(\beta) = \frac{r}{\beta^2 + q^2} \tag{3.70}$$

where r and q are constants. The envelope for the even-numbered modes of the reverberant field seemingly have the band-pass characteristics

$$J_{II}(\beta) = \frac{r\beta^2}{\beta^4 + 2p^2\beta^2 + q^4} \tag{3.71}$$

where p, as with r and q, is a constant. By selecting values for these constants, the filter characteristics can be set to match (approximately) those of the acceptance envelopes.

Table 3.1 cites the numerical values for the filter constants used in this study. Figures 3.16, 3.17 and 3.18 provide a comparison of the acceptance envelope function, the Schwartz inequality and filter approximation for the reverberant field and turbulence. Except for the range $2 \le \beta \le 12$ in Figure 3.16, the filters provide a tighter bound on the joint acceptance envelopes than do the Schwartz inequalities. This exception can be eliminated by an alternate selection of filter constants.

Although conservative, the filter roll-offs at the higher frequencies do not provide a satisfactory fit to the acceptance envelopes. This can be corrected by introducing higher-order polynomial filters with effective rolloffs somewhat less than $1/\beta^2$. It must be remembered the filters should not be designed solely to match the acceptance envelope. Equally important is that their mathematical form be amenable to integration over β, preferably, by residue theory.

DESCRIPTION		FILTERS
REVERBERANT FIELD $\left(\beta = \frac{\ell \omega}{\pi c}\right)$	ODD TERMS	$J_I(\beta) = \dfrac{50.6}{\beta^2 + (11.3)^2}$
	EVEN TERMS	$J_{II}(\beta) = \dfrac{(51.52)\ \beta^2}{\beta^4 + 2\,(12.32)^2\,\beta^2 + 3^4}$
TURBULENCE $\left(\beta = \frac{\ell \omega}{\pi U_c}\right)$	ALL TERMS	$J_I(\beta) = \dfrac{6.92}{\beta^2 + (7.84)^2}$

TABLE 3.1 FILTERS FOR JOINT ACCEPTANCE ENVELOPES

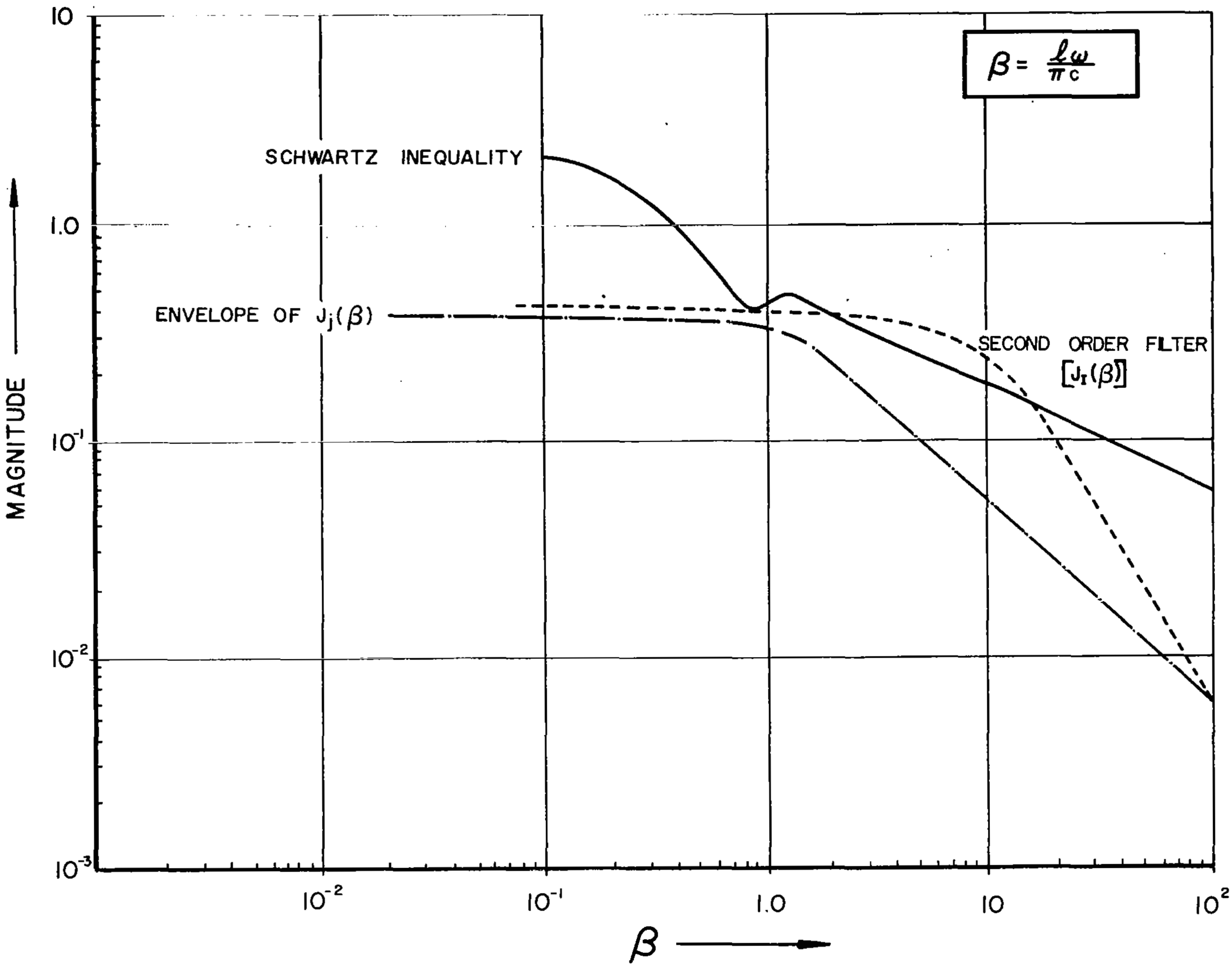

FIGURE 3.16 JOINT ACCEPTANCE APPROXIMATIONS FOR THE REVERBERANT FIELD (ODD TERMS ONLY)

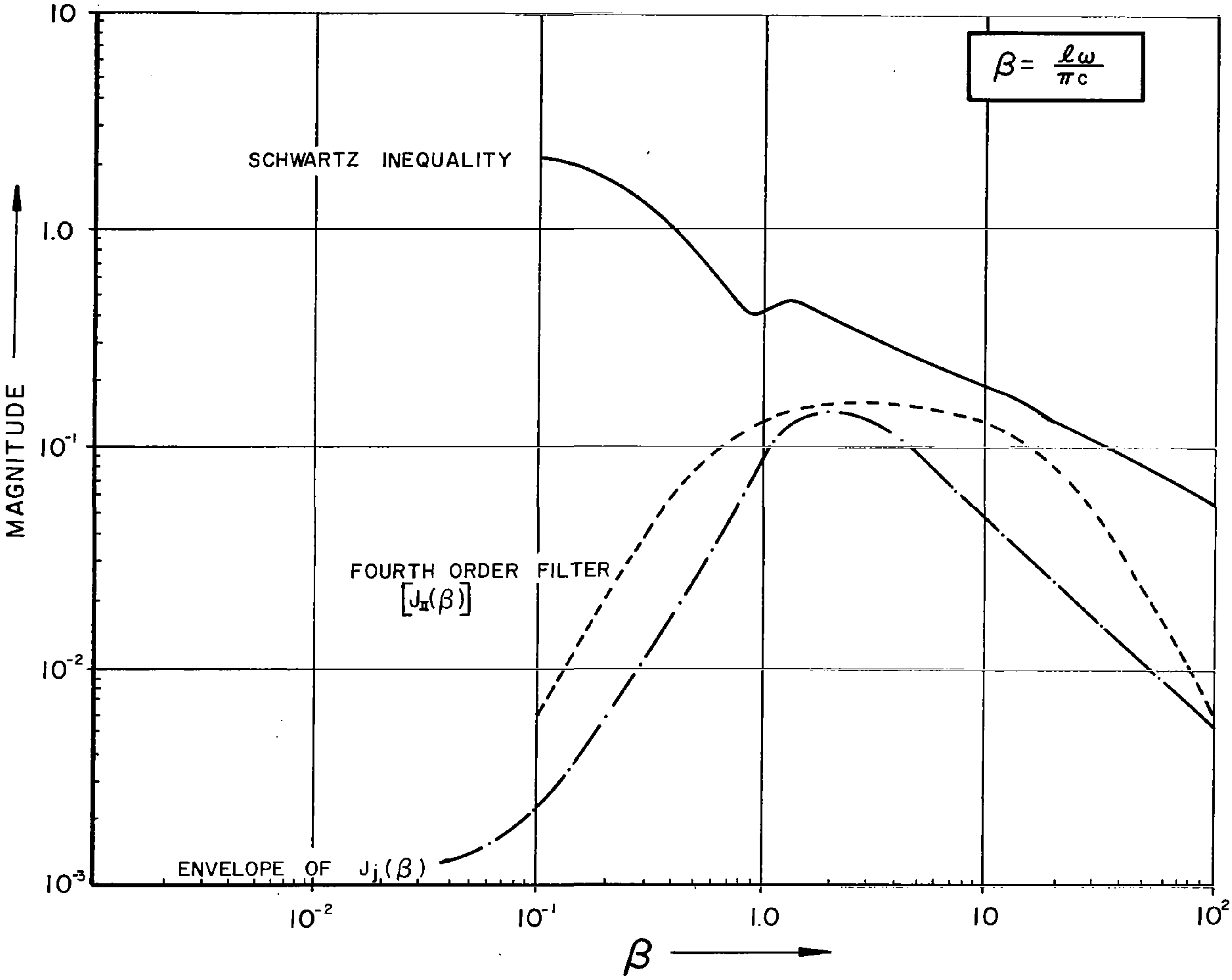

FIGURE 3.17 JOINT ACCEPTANCE APPROXIMATIONS FOR THE REVERBERANT FIELD (EVEN TERMS ONLY)

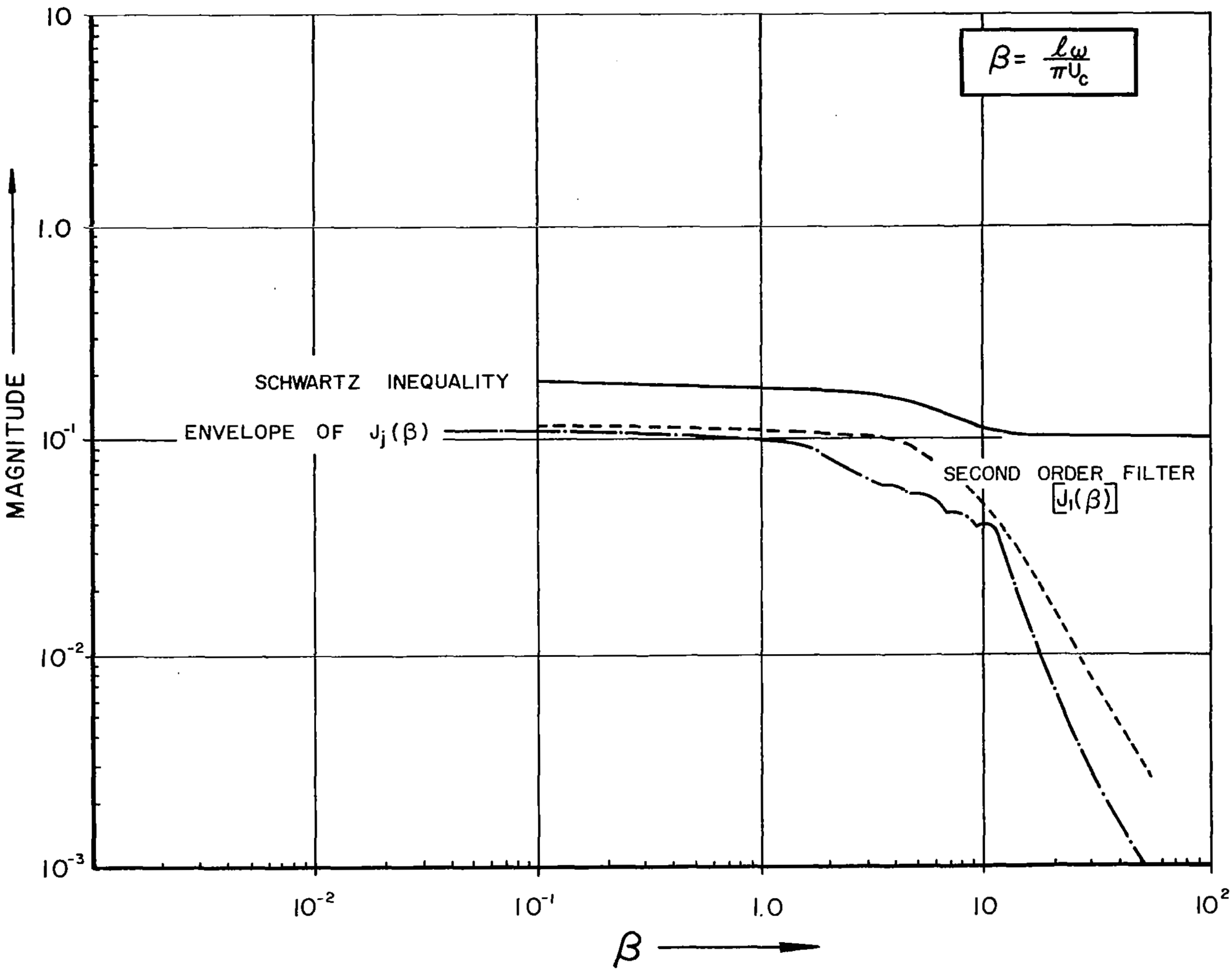

FIGURE 3.18 JOINT ACCEPTANCE APPROXIMATIONS FOR AERODYNAMIC TURBULENCE, $\ell/\delta_b = 30$

3.2 MEAN SQUARE RESPONSE RESULTS

In this section, we examine mean square results for the three previously mentioned pressure fields and the three system functions

$$
\begin{aligned}
\bullet\quad & H_j^{(1)}(\omega) = H_j(\omega) = \frac{1}{m_j \omega_j^2 \left[1 - \left(\frac{\omega}{\omega_j}\right)^2 + i\, 2\, \zeta_j \left(\frac{\omega}{\omega_j}\right)\right]} \\
\bullet\quad & H_j^{(2)}(\omega) = m_j \omega_j^2 H_j(\omega) = \frac{1}{1 - \left(\frac{\omega}{\omega_j}\right)^2 + i\, 2\, \zeta_j \left(\frac{\omega}{\omega_j}\right)} \\
\bullet\quad & H_j^{(3)}(\omega) = m_j \omega^2 H_j(\omega) = \frac{\left(\frac{\omega}{\omega_j}\right)^2}{1 - \left(\frac{\omega}{\omega_j}\right)^2 + i\, 2\, \zeta_j \left(\frac{\omega}{\omega_j}\right)}
\end{aligned}
\tag{3.72}
$$

Numerical integration results are presented for all combinations of these pressure fields and system functions. Emphasis however, is upon closed form results for all system functions wherein filter approximations are used for the reverberant and turbulence excitations. Exact closed form expressions are shown in Appendix B for the progressive field and the first two system functions; such expressions are evaluated, then displayed here in graphical form.

3.2.1 General Formulations

As stated earlier, the mean square response is given by the integral

$$
\sigma_y^2(x) = \int_{-\infty}^{\infty} S_y(x,\omega)\, d\omega \tag{3.73}
$$

This can be expressed as the double summation

$$\sigma_y^2(x) = \sum_{j=1}^{\infty} \sum_{k=1}^{\infty} \phi_j(x) \; \phi_k(x) \; I_{jk} \tag{3.74}$$

where I_{jk} is the integral

$$I_{jk} = \ell^2 S_o \int_{-\infty}^{\infty} H_j^*(\omega) \, H_k(\omega) \; J_{jk}(\omega) \, d\omega \tag{3.75}$$

and $S(x_o, \omega) \to S_o$. In terms of the variable β, we can write I_{jk} in the form

$$I_{jk} = C_1 \; I_{jk}^{(1)} \tag{3.76}$$

where the coefficient C_1 is given by

$$C_1 = \frac{4 \, G_o \mu}{m^2 \omega_1^3} \tag{3.77}$$

and the one-sided form of the integral $I_{jk}^{(1)}$ by

$$I_{jk}^{(1)} = \int_0^{\infty} R_{jk}^{(1)} \; (\beta) \; J_{jk} \; (\beta) \; d\beta \tag{3.78}$$

with

$$R_{jk}^{(1)} \; (\beta) = m_j m_k \omega_1^4 \; \mathrm{Re} \left[H_j^*(\beta) \;\; H_k(\beta) \right] \tag{3.79}$$

For the modal damping $\zeta_j = \zeta_k = \zeta$,

$$R_{jk}^{(1)} \; (\beta) = \frac{A(\beta)}{A^2(\beta) \; + \; B^2(\beta)} \tag{3.80}$$

where

$$A(\beta) = (j^4 - \mu^2 \beta^2)(k^4 - \mu^2 \beta^2) + (2jk \zeta \mu \beta)^2$$
$$B(\beta) = 2 \zeta \mu \beta \left[j^2(k^4 - \mu^2 \beta^2) - k^2(j^4 - \mu^2 \beta^2) \right] \tag{3.81}$$

and

$$\mu = \frac{\pi c}{\ell \omega_1}$$
$$\omega_j = j^2 \omega_1 \tag{3.82}$$

For turbulence, the speed of sound c simply is replace by U_c.

For the second system function $H_j^{(2)}(\omega)$

$$I_{jk} = C_2 I_{jk}^{(2)} \tag{3.83}$$

where

$$C_2 = G_o \ell^2 \mu \omega_1$$
$$I_{jk}^{(2)} = j^4 k^4 I_{jk}^{(1)} = \int_0^\infty R_{jk}^{(2)}(\beta) J_{jk}(\beta) d\beta \tag{3.84}$$

with

$$R_{jk}^{(2)}(\beta) = j^4 k^4 R_{jk}^{(1)}(\beta) \tag{3.85}$$

Finally, for the third system function $H_j^{(3)}(\omega)$,

$$I_{jk} = C_3 \, I_{jk}^{(3)} \tag{3.86}$$

where

$$C_3 = G_o \, \ell^2 \, \mu^5 \, \omega_1$$

$$I_{jk}^{(3)} = \int_0^{\infty} R_{jk}^{(3)}(\beta) \, J_{jk}(\beta) \, d\beta \tag{3.87}$$

and

$$R_{jk}^{(3)}(\beta) = \beta^4 \, R_{jk}^{(1)}(\beta) \tag{3.88}$$

With the three integrals forms related to the I_{jk} integral, we now write the mean square response in the forms

$$\sigma_y^2(x) = C_1 \sum_j \sum_k \phi_j(x) \, \phi_k(x) \, I_{jk}^{(1)}$$

$$\sigma_y^2(x) = C_2 \sum_j \sum_k \phi_j(x) \, \phi_k(x) \, I_{jk}^{(2)} \tag{3.89}$$

$$\sigma_y^2(x) = C_3 \sum_j \sum_k \phi_j(x) \, \phi_k(x) \, I_{jk}^{(3)}$$

These expressions are used in the numerical integration.

3.2.2 Filter Approximation Formulations

For practical reasons, prime concern here centers upon the evaluation of the I_{jk} integral for both the reverberant field and the aerodynamic turbulence. Although the progressive wave is of interest and response results calculated in closed form for the system functions $H_j^{(1)}(\omega)$ and $H_j^{(2)}(\omega)$, the details of the response calculations will not be elaborated upon here. Rather a separate discussion is presented as Appendix B.

Using the exact expressions for the cross acceptance terms of either the reverberant or the turbulence excitation, the integration of I_{jk} is a formidable task. In seeking closed form results, the mathematics is not entirely simple and the algebra abundant so that meaningful and concise expressions are not easy to establish. In fact, such expressions have yet to be determined. In carrying out such (exact) integrations numerically, it is difficult to develop an accurate understanding of the parametric effects without using a great deal of computer time. This is due largely to numerical accuracy problems which are introduced because the system and acceptance functions do not vary smoothly and slowly over the range of integration.

Faced with these analytical and computational difficulties, yet driven by the need for a "compromise" solution, we explore the use of well behaved polynomial filters to establish estimates of the response in mean square of multi-mode distributed systems. Central to this idea is the system response described by Figure 3.19. This model implies the output response is accounted for by contributions from

- j distinct normal modes
- a residual impedance for the mid-frequency range
- a residual impedance for the high frequency range

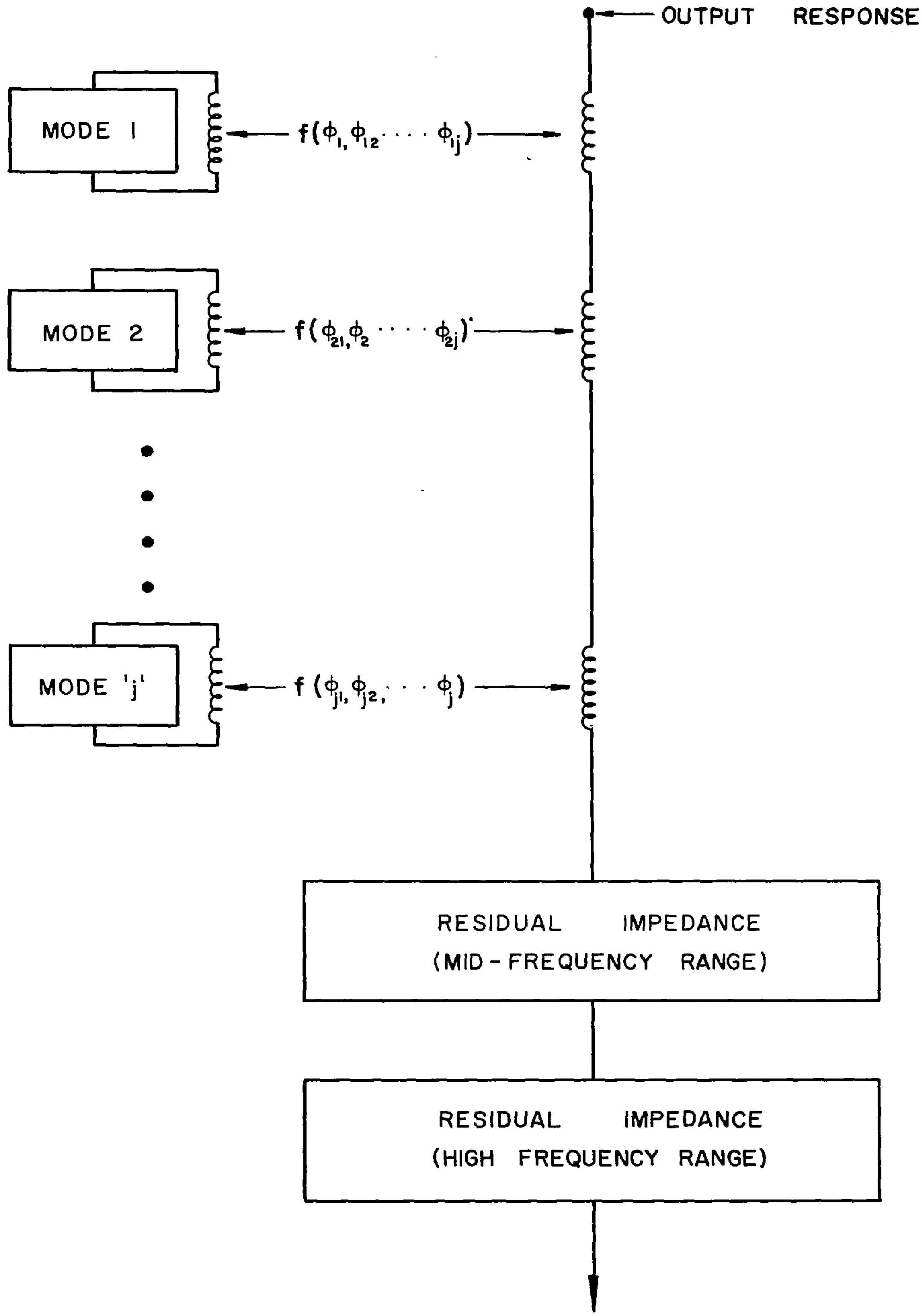

FIGURE 3.19 MODEL FOR RESPONSE OF MULTIMODE SYSTEM

We concentrate here upon the output due to the normal modes although these same filter concepts can be applied to include the residual impedances. Let it be clearly understood that in this report we strive not for accuracy over the range of modes considered. Instead, we concentrate upon simple filter forms which have approximately the characteristics of the desired acceptance functions, and at the same time, are amenable to integration by residue theory. By adjusting the numerical values of the filter constants, the accuracy of the filter approximations can be improved at will.

Let us consider an abbreviated derivation of the mean square response for the filters $J_I(\beta)$ and $J_{II}(\beta)$, and the first system function $H_j(\omega)$. Clearly, results for the system function $H_j^{(2)}(\omega)$ then can be developed by simple multiplication. Thus, for the second order filter,

$$J_I(\beta) = \frac{r}{(\beta + iq)(\beta - iq)} \tag{3.90}$$

where for the reverberant field

$$\beta = \frac{K\ell}{\pi} = \omega t_o, \qquad t_o = \frac{\ell}{\pi c} \tag{3.91}$$

and for turbulence

$$\beta = \frac{\bar{K}\ell}{\pi} = \omega t_o, \qquad t_o = \frac{\ell}{\pi U_c} \tag{3.92}$$

The product of the system functions are given by

$$H_j^*(\omega)\, H_k(\omega) = \frac{1}{m_j m_k(\omega - s_1)(\omega - s_2)(\omega + s_1)(\omega + s_2)} \tag{3.93}$$

where

$$s_1 = a_j + ib_j = -s_2^* \tag{3.94}$$

with

$$\begin{aligned} a_j &= \omega_j (1 - \zeta_j^2)^{1/2} \\ b_j &= \zeta_j \ \omega_j \end{aligned} \tag{3.95}$$

The I_{jk} integral then may be written as

$$I_{jk} = \ell^2 S_o \int_{-\infty}^{\infty} H_j^* (\omega) H_k(\omega) J_I(\omega) \, d\omega \tag{3.96}$$

and by residue theory

$$I_{jk} = \ell^2 S_o(2\pi i) \sum_{r=1}^{3} R_r \tag{3.97}$$

where R_r is the rth residue of $H_j^*(\omega) H_k(\omega) J_I(\omega)$ at its poles in the upper-half plane. The poles are given by

$$\begin{aligned} p_1 &= a_j + ib_j \\ p_2 &= -a_j + ib_j \\ p_3 &= i \frac{\pi c q}{\ell} \end{aligned} \tag{3.98}$$

and, after some labor,

$$I_{jk} = \frac{4\pi \ \ell^2 S_o r}{m_j m_k t_o^2 (\omega_j^2 - 2b_j q' + q'^2)} A_{jk} \tag{3.99}$$

where

$$A_{jk} = \frac{b_j(a_j^2 - a_k^2 - (b_j+b_k)^2) + (b_j+b_k)(a_j^2 - b_j^2 + q'^2)}{(\omega_j^2 + 2b_j q' + q'^2)\left(\left[b_j^2 - a_k^2 - (b_j+b_k)^2\right]^2 + 4a_j^2(b_j+b_k)^2\right)} + \frac{1}{4q'(\omega_k^2 + 2b_k q' + q'^2)} \tag{3.100}$$

with the symbol q' defined as the ratio

$$q' = \frac{q}{t_o} \tag{3.101}$$

The main diagonal terms with $I_{jj} = I_j$ reduce to

$$I_j = \frac{\pi \ell^2 S_o r}{2m_j^2 \omega_j^2 b_j t_o^2 q'} \cdot \left[\frac{q'(a_j^2 - 3b_j^2 + q'^2) + 2b_j \omega_j^2}{\omega_j^4 + 2(a_j^2 - b_j^2) q'^2 + q'^4}\right] \tag{3.102}$$

For the fourth order filter,

$$J_{II}(\beta) = \frac{r\beta^2}{[\beta - i(c+d)][\beta - i(c-d)][\beta + i(c+d)][\beta + i(c-d)]} \tag{3.103}$$

where the coefficients c and d are related to the filter constants by

$$c^2 = \frac{1}{2}(p^2 + q^2), \quad d^2 = \frac{1}{2}(p^2 - q^2) \tag{3.104}$$

The integral I_{jk} becomes

$$I_{jk} = \ell^2 S_o \int_{-\infty}^{\infty} H_j^*(\omega)\, H_k(\omega)\, J_{II}(\omega)\, d\omega \tag{3.105}$$

and by residue theory

$$I_{jk} = \ell^2 S_o (2\pi i) \sum_{r=1}^{4} R_r \tag{3.106}$$

where the poles in the upper-half plane are given by

$$\begin{aligned} p_1 &= a_j + ib_j \\ p_2 &= -a_j + ib_j \\ p_3 &= i\,\frac{(c+d)}{t_o} \\ p_4 &= i\,\frac{(c-d)}{t_o} \end{aligned} \tag{3.107}$$

After some additional labor,

$$\begin{aligned} I_{jk} = \frac{2\pi\,\ell^2 S_o r'}{m_j m_k t_o} \Bigg\{ & \frac{2}{B_{jk} C_j} \Big[b_j(\omega_j^4 - q'^4)(a_j^2 - a_k^2) - (b_j + b_k)^2 \\ & + (b_j + b_k)\left(\omega_j^4 (a_j^2 - b_j^2 + 2p'^2) + (a_j^2 - b_j^2)\, q'^4\right) \Big] \\ & + \frac{c'+d'}{8c'd'} \left[\frac{1}{(a_j^2 + (b_j - c' - d')^2)(a_k^2 + (b_k + c' + d')^2)} \right] \\ & - \frac{c'-d'}{8c'd'} \left[\frac{1}{(a_j^2 + (b_j - c' + d')^2)(a_k^2 + (b_k + c' - d')^2)} \right] \Bigg\} \end{aligned} \tag{3.108}$$

where

$$B_{jk} = \left[(a_j^2 - a_k^2) - (b_j + b_k)^2 \right]^2 + 4\, a_j^2 \left[b_j + b_k \right]^2 \tag{3.109}$$

$$C_j = \left[(a_j^2 - b_j^2)(a_j^2 - b_j^2 + 2p'^2) - 4\, a_j^2 b_j^2 + q'^4 \right]^2$$

$$+ \; 16\, a_j^2 b_j^2 \left[a_j^2 - b_j^2 + p'^2 \right]^2$$

Division by t_o is noted by a prime superscript so that

$$c' = c/t_o \qquad p' = p/t_o \tag{3.110}$$

$$d' = d/t_o \qquad q' = q/t_o$$

For the main diagonal terms,

$$I_j = \frac{2\pi\, \ell^2 S_o r'}{m_j^2\ t_o} \left\{ \frac{4b_j}{B_j C_j} \left[\omega^4 (a_j^2 - b_j^2 + 2p'^2) + (a_j^2 - b_j^2) q'^4 - 2b_j^2 (\omega_j^4 - q'^4) \right] \right.$$

$$+ \frac{c'+d'}{8c'd'} \left[\frac{1}{\omega_j^4 + (c'+d')^2 ((c'+d')^2 + 2(a_j^2 - b_j^2))} \right]$$

$$\left. - \frac{c'-d'}{8c'd'} \left[\frac{1}{\omega_j^4 + (c'-d')^2 ((c'-d')^2 + 2(a_j^2 - b_j^2))} \right] \right\} \tag{3.111}$$

where

$$B_j = 16\, b_j^2\, \omega_j^2 \tag{3.112}$$

$$C_j = \left[(a_j^2 - b_j^2)(a_j^2 - b_j^2 + 2\, p'^2) - 4\, a_j^2 b_j^2 + q'^4 \right]^2 + 16\, a_j^2 b_j^2 \left[a_j^2 - b_j^2 + p'^2 \right]^2$$

In much the same manner, we derive closed form I_{jk} results for the third system function $H_j^{(3)}(\omega)$ and the filters $J_I(\beta)$ and $J_{II}(\beta)$. The desired integral is written as

$$I_{jk} = \ell^2 S_o \int_{-\infty}^{\infty} H_j^{*(3)}(\omega)\, H_k^{(3)}(\omega)\, J_{jk}(\omega)\, d\omega \tag{3.113}$$

where $J_{jk}(\omega)$ is represented by either $J_I(\omega)$ or $J_{II}(\omega)$. For the first filter, the residues are governed by Equation (3.97) so that

$$I_{jk} = \frac{4\pi \ell^2 S_o\, r}{t_o^2\, B_{jk} C_j} \left[b_j (\omega_j^4 + 2(a_j^2 - b_j^2)\, q'^2)^2\, \omega_k^2 \right.$$
$$\left. + (\omega_j^4 + (a_j^2 - 3b_j^2)\, q'^2)\, \omega_j^2\, b_k - b_j \omega_j^4\, q'^2 \right] \tag{3.114}$$
$$+ \frac{\pi \ell^2 S_o}{t_o^2} \quad \frac{r q'^3}{\left[a_j^2 + (b_j - q')^2 \right] \left[a_k^2 + (b_k + q')^2 \right]}$$

where

$$B_{jk} = (a_j^2 - a_k^2)^2 + 2(a_j^2 + a_k^2)(b_j + b_k)^2 + (b_j + b_k)^4$$

$$C_j = \left[a_j^2 + (b_j - q')^2\right]\left[a_j^2 + (b_j + q')^2\right] \tag{3.115}$$

For j = k, the I_{jk} expression reduces to

$$I_j = \frac{\pi \ell^2 S_o r}{2t_o^2 b_j}\left[\frac{\omega_j^4 + (a_j^2 - 3b_j^2)q'^2 + 2b_j q'^3}{\omega_j^4 + 2(a_j^2 - b_j^2)\,q'^2 + q'^4}\right] \tag{3.116}$$

For the second filter, the residues are treated according to Equation (3.106) so that

$$\begin{aligned} I_{jk} = \frac{2\pi\ell^2 S_o r}{t_o^2}\Bigg\{ & -\frac{2}{B_{jk}C_j}\Bigg[2b_j\omega_j^4\left[\omega_j^4 p'^2 + (a_j^2 - b_j^2)q'^4\right] \\ & - \left[\omega_j^8 + 2\omega_j^4(a_j^2 - b_j^2)p'^2 + (a_j^4 - 10a_j^2 b_j^2 + 5b_j^4)q'^4\right] b_k \omega_j^2 \\ & - \left[\omega_j^8 + 4\omega_j^4(a_j^2 - b_j^2)p'^2 + (3a_j^2 - b_j^2)(a_j^2 - 3b_j^2)q'^4\right] b_j \omega_k^2\Bigg] \\ & + \frac{(c'+d')^5}{8c'd'}\left[\frac{1}{\left[a_j^2 + (b_j - c' - d')^2\right]\left[a_k^2 + (b_k + c' + d')^2\right]}\right] \\ & - \frac{(c'-d')^5}{8c'd'}\left[\frac{1}{\left[a_j^2 + (b_j - c' + d')^2\right]\left[a_k^2 + (b_k + c' - d')^2\right]}\right]\Bigg\} \end{aligned} \tag{3.117}$$

where

$$B_{jk} = (a_j^2-b_j^2 - 2b_jb_k-\omega_k^2)^2 + 4a_j^2(b_j+b_k)^2$$

$$C_j = \left[(a_j^2-b_j^2)^2 - 4a_j^2b_j^2 + 2p'^2(a_j^2-b_j^2) + q'^4\right]^2 \qquad (3.118)$$

$$+ 16\, a_j^2b_j^2\,(a_j^2 - b_j^2 + p'^2)^2$$

For j = k, the resultant diagonal term becomes

$$I_j = \frac{\pi \ell^2 S_o r}{4\, t_o^2} \left\{ \frac{2}{b_j C_j}\left[\omega_j^8 + 2\,\omega_j^4\,(a_j^2-2b_j^2)p'^2 + (a_j^4-10a_j^2b_j^2+5b_j^4\right]\right.$$

$$+ \frac{(c'+d')^5}{c'd'}\left[\frac{1}{\left[a_j^2 + (b_j-c'-d')^2\right]\left[a_j^2 + (b_j+c'+d')^2\right]}\right] \qquad (3.119)$$

$$\left. - \frac{(c'-d')^5}{c'd'}\left[\frac{1}{\left[a_j^2 + (b_j-c'+d')^2\right]\left[a_j^2 + (b_j+c'-d')^2\right]}\right]\right\}$$

The coefficient t_o is given by either Equation (3.91) or Equation (3.92) and C_j is that quoted above.

3.2.3 Results

In the preceeding sections, we have considered formulations intrinsically related to determining mean square response values of a structural system. The first sections deals with forms compatible with numerical integration while the second section concerns filter approximations results in closed form. Let us now examine a numerical evaluation of these theoretical results.

The three system functions evaluated are those defined by Equation (3.72). For light values of damping, say $\zeta_j \leq .1$, all of the systems display selective band-pass characteristics. The first expression corresponds to the familiar displacement-to-force frequency response functions; the second, modal magnification factors; and the third, acceleration-to-force system functions. Here, we assume the equal modal damping $\zeta_j = 0.025$. Accordingly, the characteristics of the three systems are shown by Figures 3.20 through 3.22 where $R_j^{(1)}(\beta)$ is given by Equation (3.80) with j = k. The remaining two system functions are defined in Section 3.2.1.

The output response in mean square of systems with these filter characteristics are governed by the modal summations of Equation (3.89). For the reverberant field, integrands proportional to I_{jk} (for j = k and j = 1, 2, 3. . . 10) for each system are shown by Figures 3.26 through 3.28, respectively. Tables 3.2 through 3.7 show the integrated values for each mode and each system; these values correspond to the contribution of the main diagonal terms to the mean square response.

By comparing the filter approximation tabular values from the numerical integration with the closed form results, confidence is eatablished in the validity of the analytical work. Also, by an exercise of this sort, we are led to respect that general class of numerical accuracy problems associated with the integration of sharply fluctuating functions. Such problems are particularly severe for the cross term integrations. After numerous trials, the increments used in the

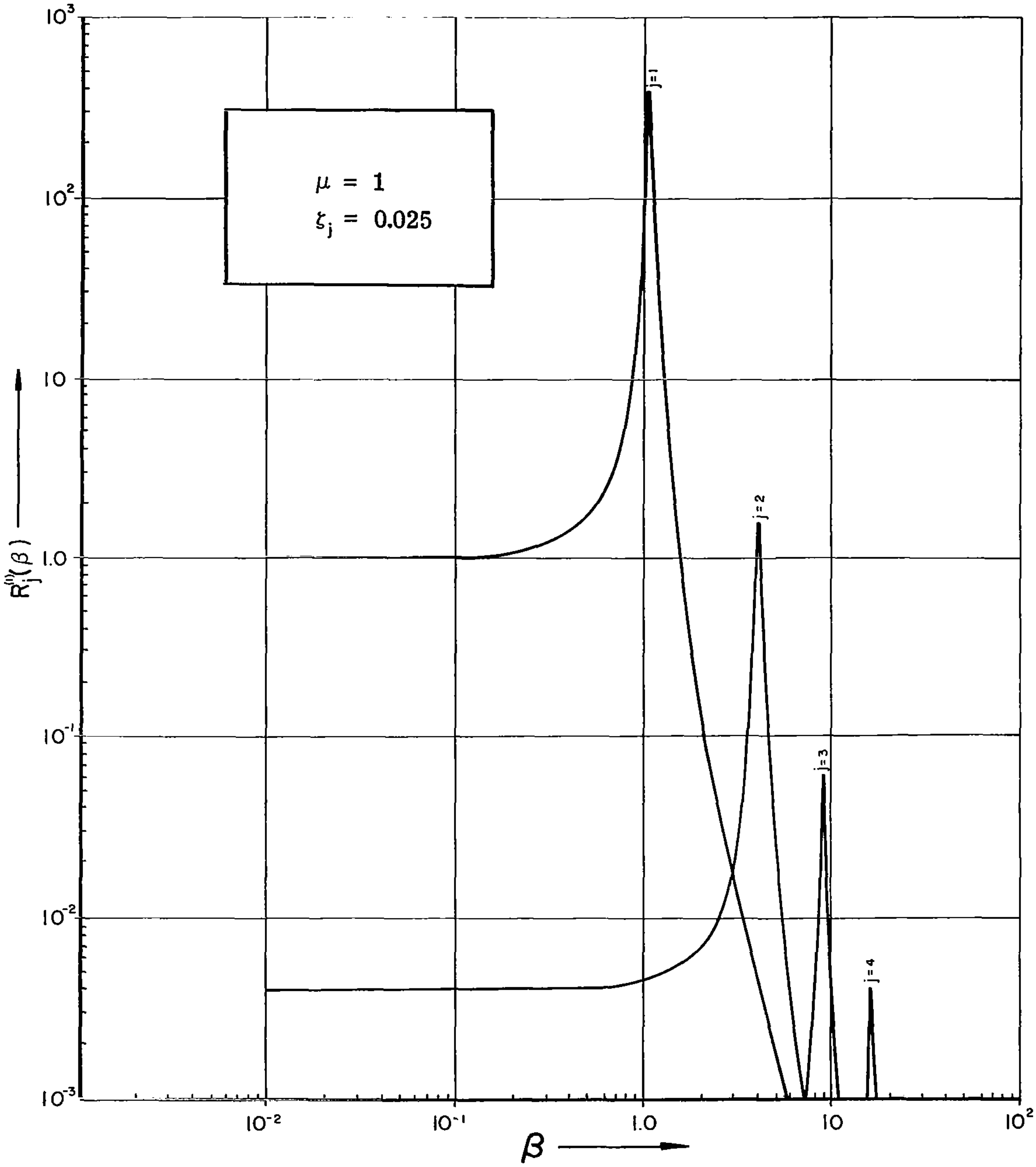

FIGURE 3.20 SYSTEM CHARACTERISTICS FOR $|H_j(\omega)|^2$

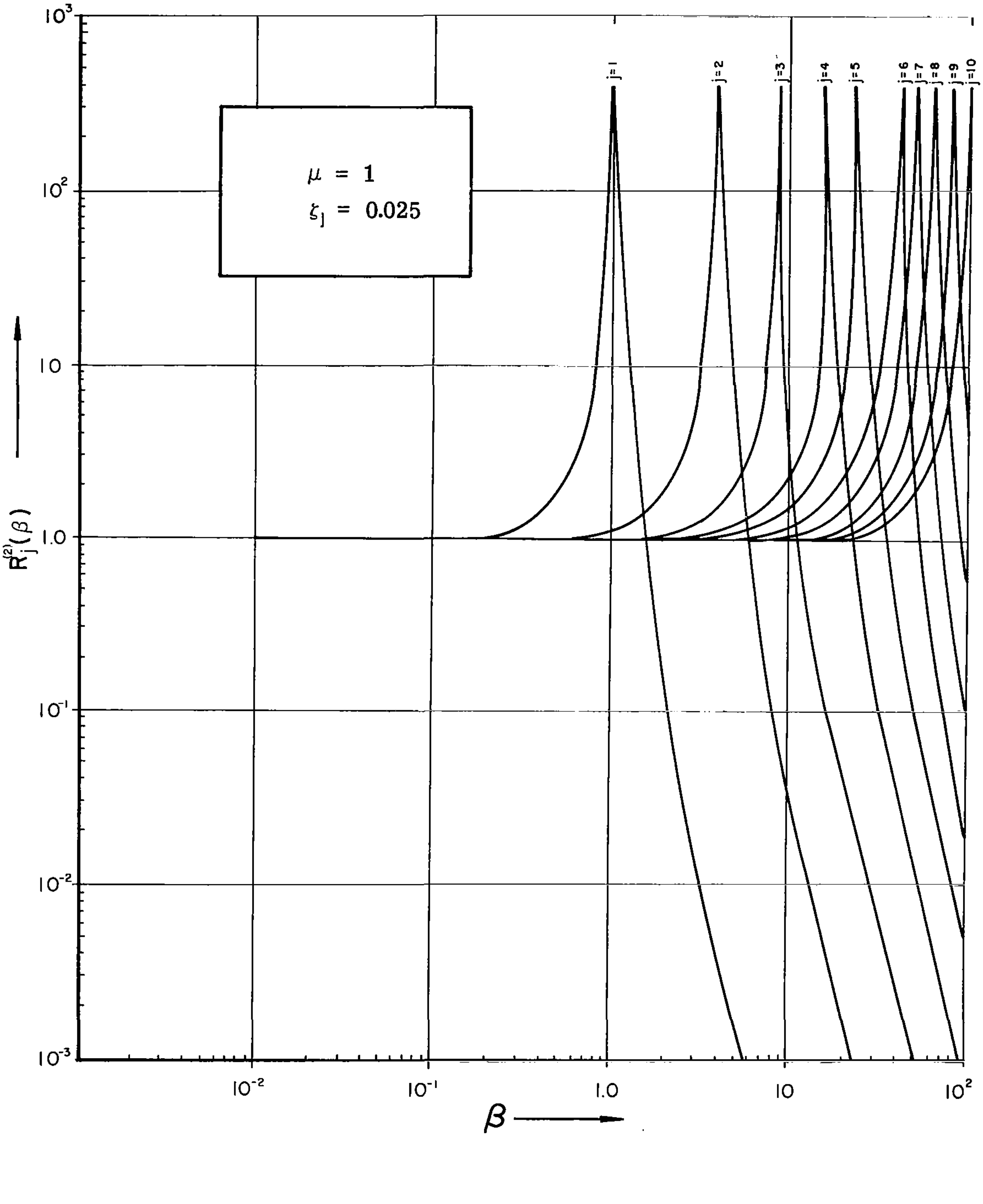

FIGURE 3.21 SYSTEM CHARACTERISTICS FOR $|m_j\omega_j^2 H_j(\omega)|^2$

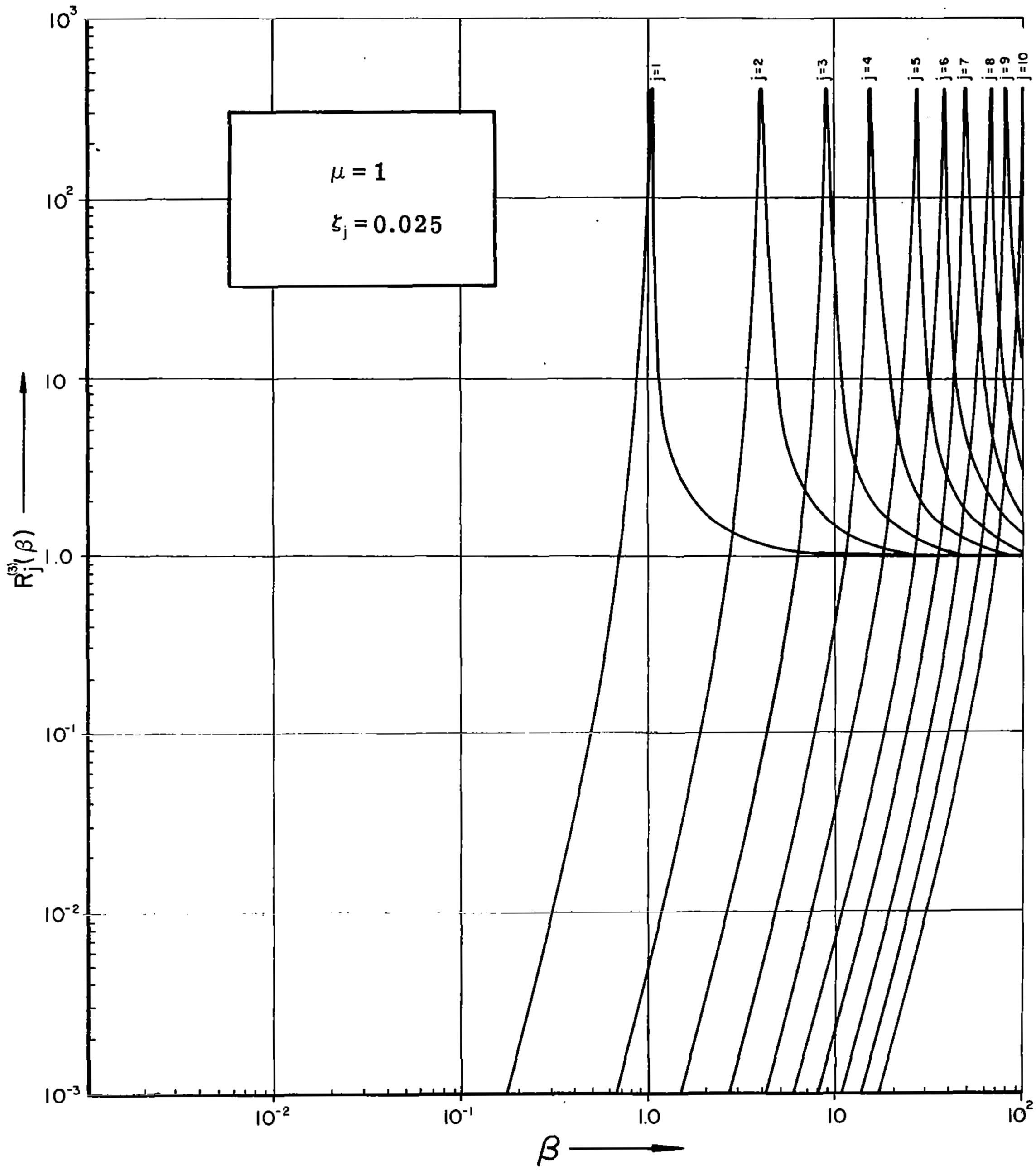

FIGURE 3.22 SYSTEM CHARACTERISTICS FOR $\left|m_j\omega^2 H_j(\omega)\right|^2$

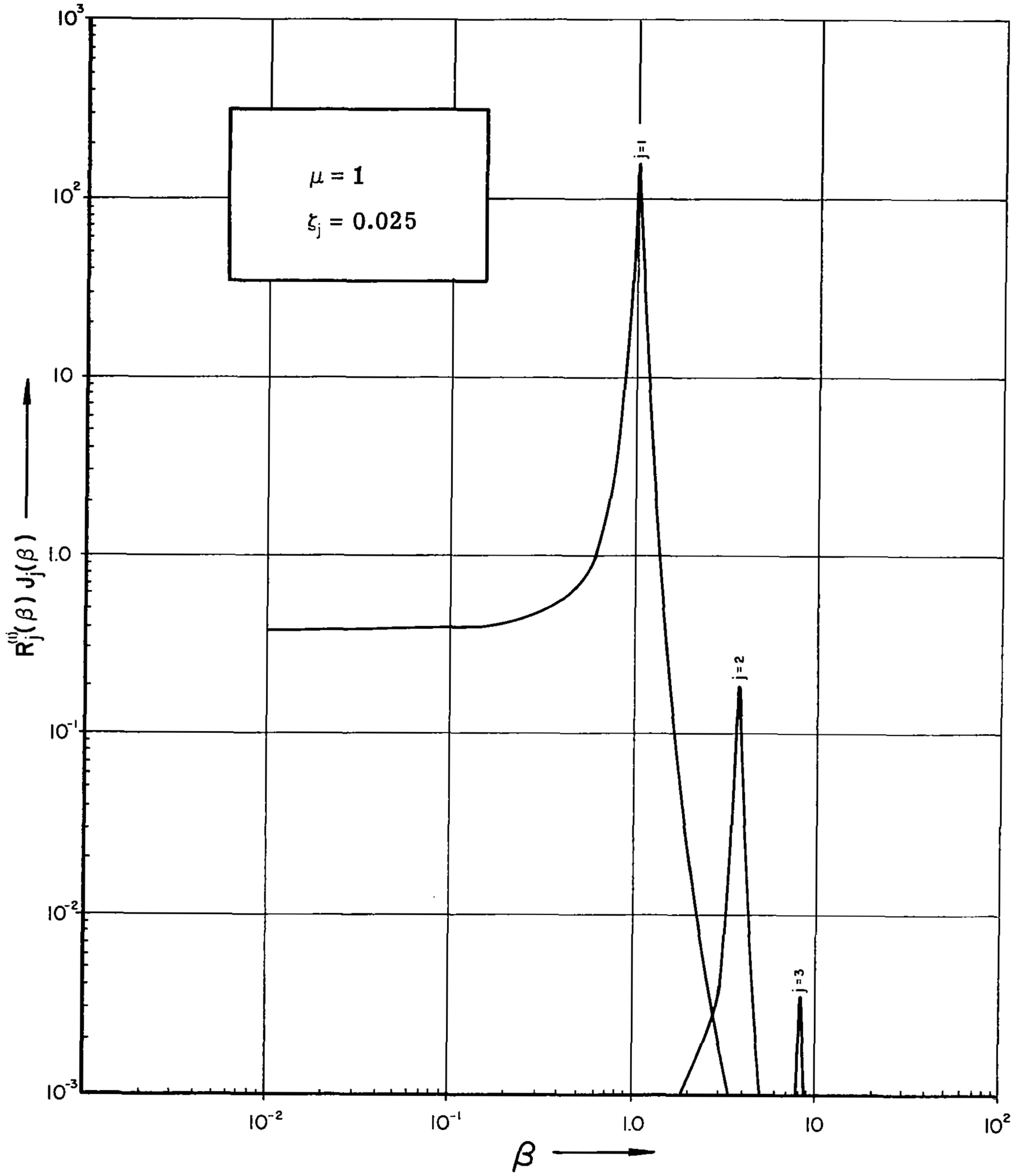

FIGURE 3.23 INTEGRAND FOR $\left|H_j(\omega)\right|^2$ AND THE REVERBERANT FIELD

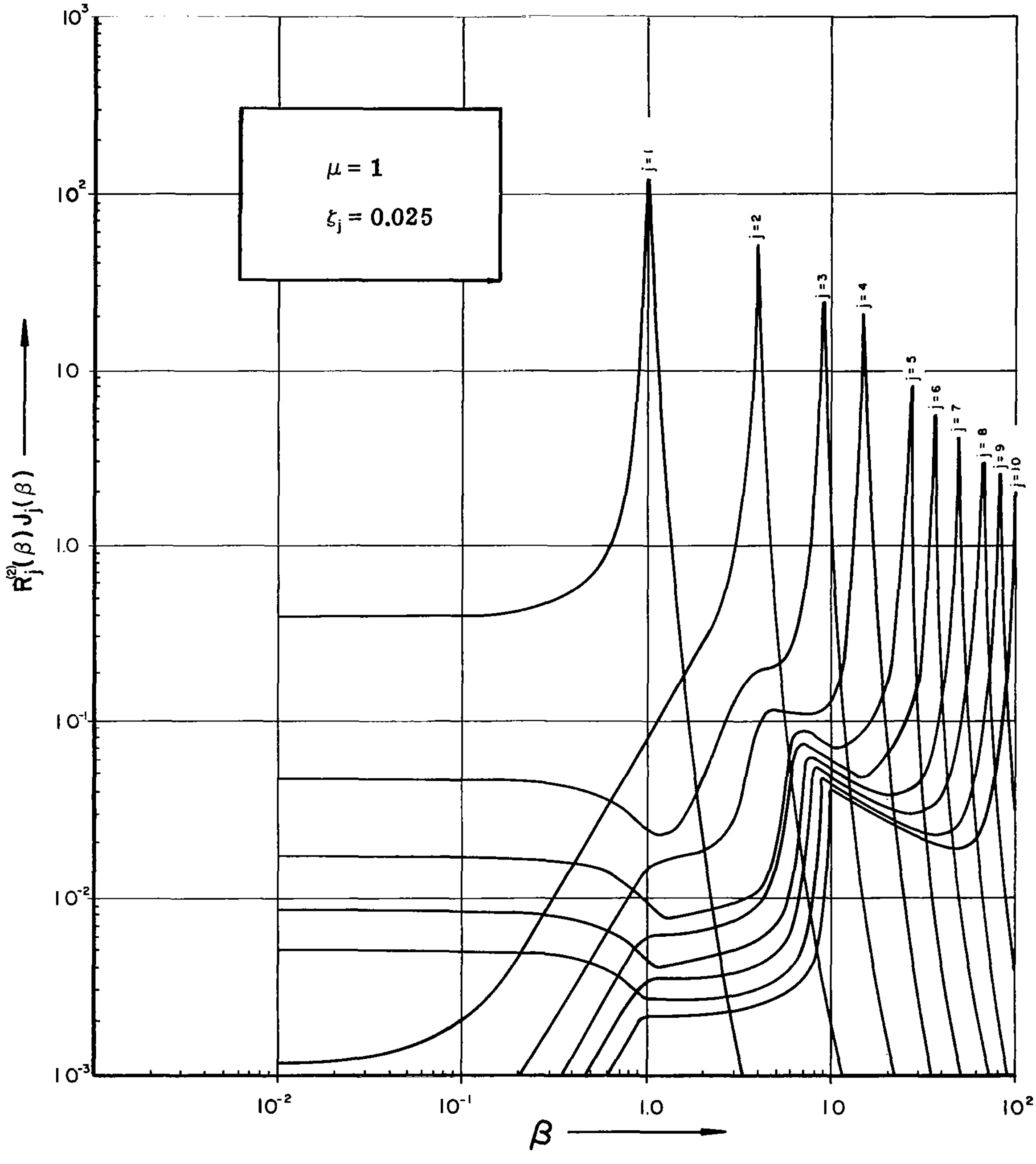

FIGURE 3.24 INTEGRAND FOR $\left| m_j \omega_j^2 H_j(\omega) \right|^2$ AND THE REVERBERANT FIELD

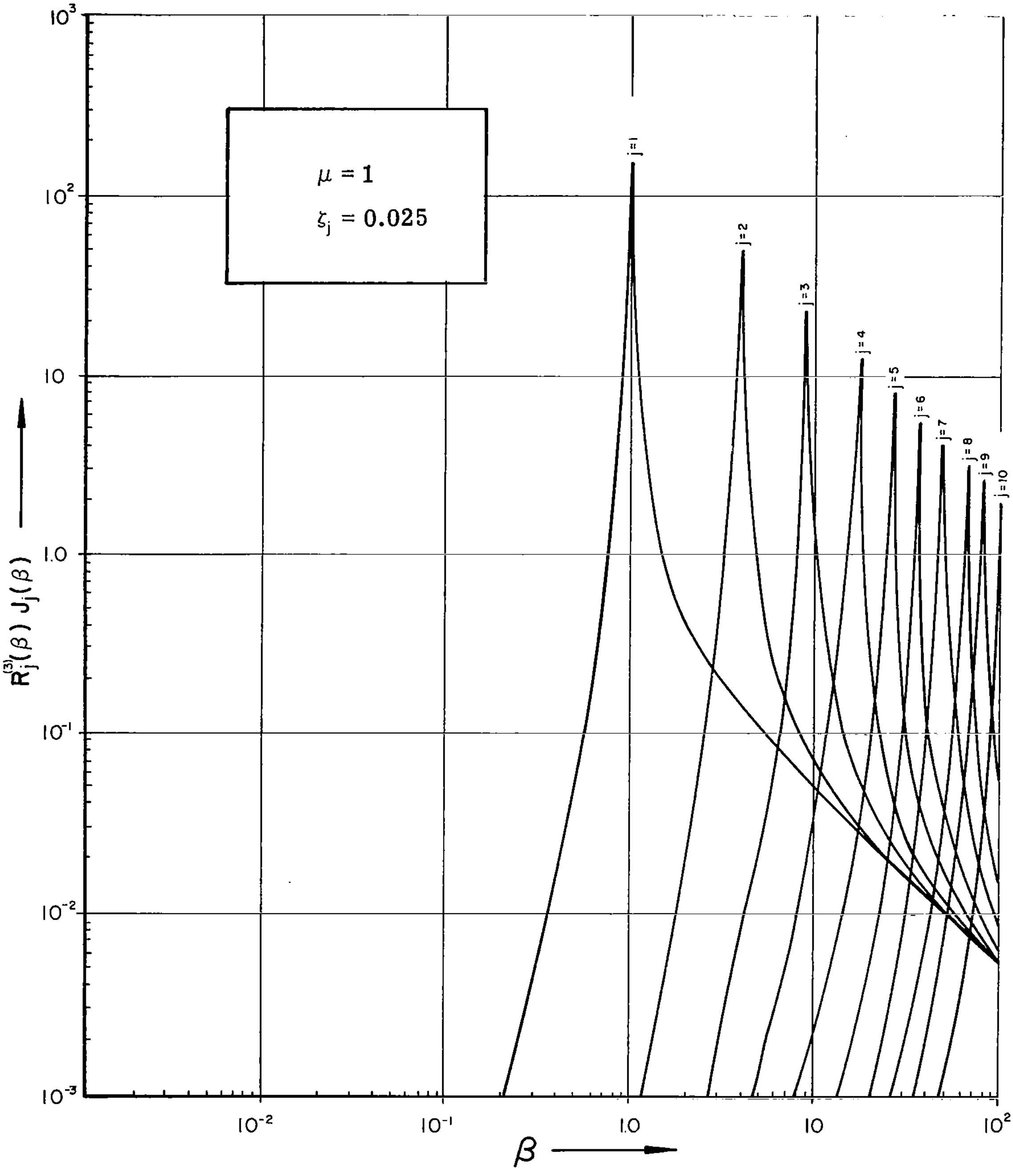

FIGURE 3.25 INTEGRAND FOR $\left|m_j \omega^2 H_j(\omega)\right|^2$ AND THE REVERBERANT FIELD

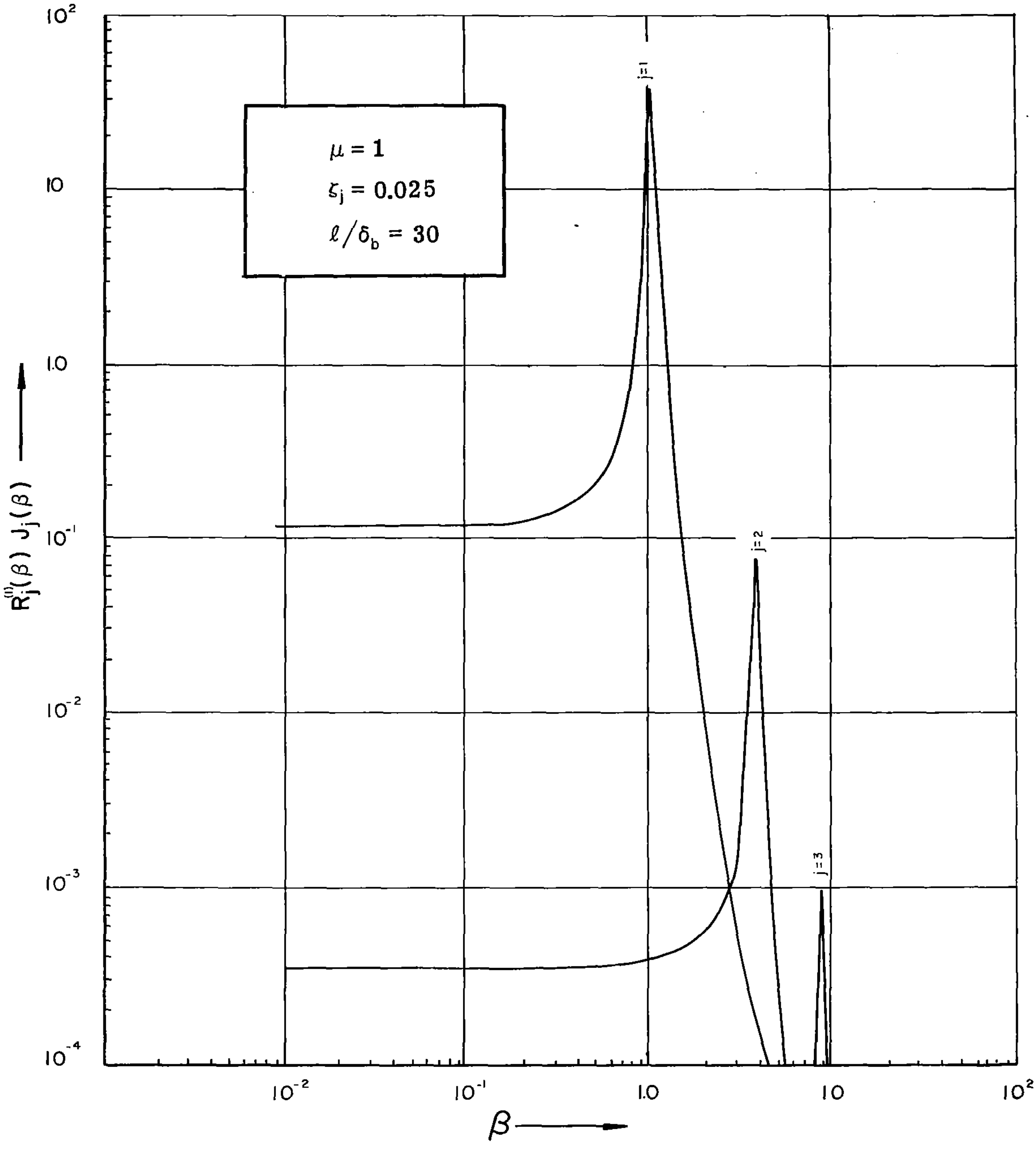

FIGURE 3.26 INTEGRAND FOR $|H_j(\omega)|^2$ AND AERODYNAMIC TURBULENCE

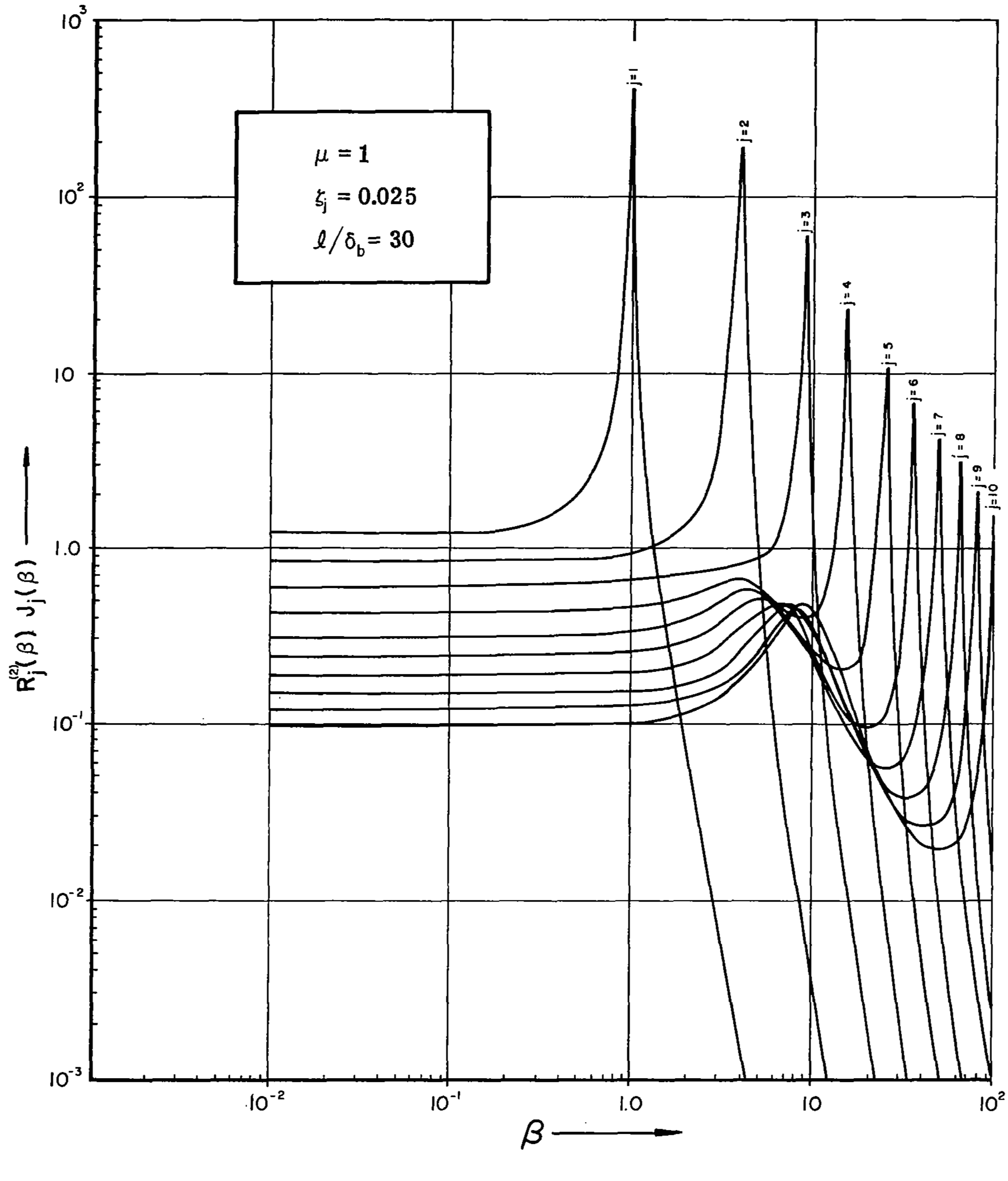

FIGURE 3.27 INTEGRAND FOR $\left| m_j \omega_j^2 H_j(\omega) \right|^2$ AND AERODYNAMIC TURBULENCE

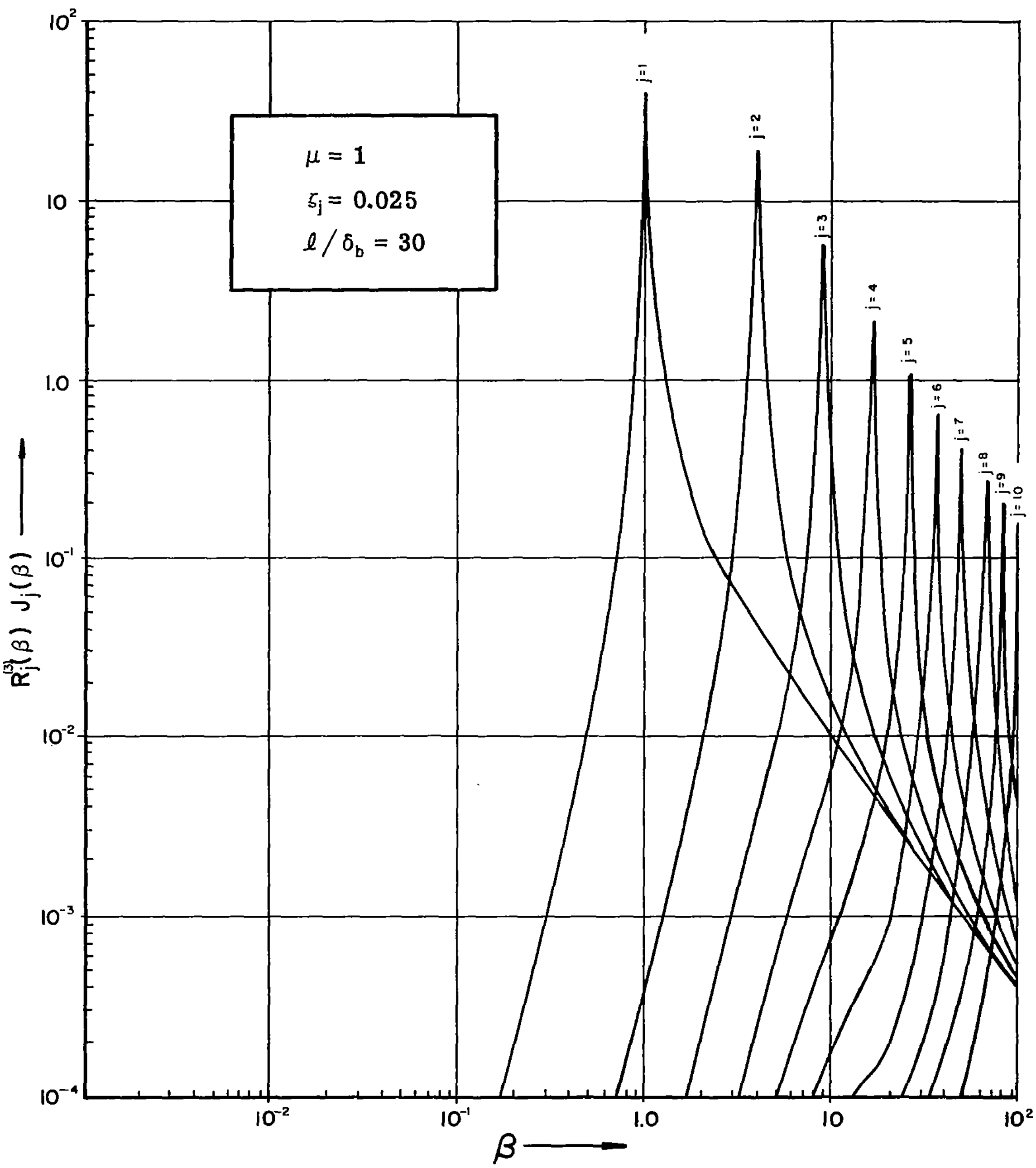

FIGURE 3.28 INTEGRAND FOR $\left| m_j \omega^2 H_j(\omega) \right|^2$ AND AERODYNAMIC TURBULENCE

SYSTEM $\mu = 1$, $\zeta_j = 0.025$		$\lvert H_j(\omega) \rvert^2$, n = 1	$\lvert m_j \omega_j^2 H_j(\omega) \rvert^2$, n = 2	$\lvert m_j \omega^2 H_j(\omega) \rvert^2$, n = 3
$\int_0^\infty R_j^{(n)}(\beta)\ J_j(\beta)\ d\beta$	j = 1	8.958	8.958	13.128
	j = 2	6.094 (-2)	15.606	16.959
	j = 3	2.423 (-3)	16.020	16.697
	j = 4	2.732 (-4)	16.423	16.591
	j = 5	4.192 (-5)	16.376	16.251
	j = 6	9.891 (-6)	16.613	16.056
	j = 7	2.860 (-6)	16.493	15.675
	j = 8	9.834 (-7)	16.499	15.371
	j = 9	3.808 (-7)	16.394	14.831
	j = 10	1.009 (-7)	10.663	9.149

TABLE 3.2 MAIN DIAGONAL CONTRIBUTIONS TO THE MEAN SQUARE RESPONSE (REVERBERANT FIELD - NUMERICAL INTEGRATION OF INTEGRAND)

SYSTEM $\mu = 1,\ \zeta_j = 0.025$		$\lvert H_j(\omega)\rvert^2,\ n=1$	$\lvert m_j \omega_j^2 H_j(\omega)\rvert^2,\ n=2$	$\lvert m_j \omega^2 H_j(\omega)\rvert^2,\ n=3$
$\int_0^\infty R_j^{(m)}(\beta)\ J_j(\beta)\ d\beta$; $J_j(\beta) = J_{I}(\beta)$ for j odd, $J_j(\beta) = J_{II}(\beta)$ for j even	j = 1	12.642	12.642	26.096
	j = 2	7.774 (-2)	19.901	23.939
	j = 3	1.058 (-2)	69.704	70.966
	j = 4	7.302 (-4)	47.858	47.801
	j = 5	1.482 (-4)	59.601	52.910
	j = 6	2.376 (-5)	39.913	36.448
	j = 7	6.465 (-6)	37.273	30.260
	j = 8	1.636 (-6)	27.449	22.847
	j = 9	5.603 (-7)	25.927	18.199
	j = 10	1.438 (-7)	14.377	8.278

TABLE 3.3 MAIN DIAGONAL CONTRIBUTION TO THE MEAN SQUARE RESPONSE (REVERBERANT FIELD- NUMERICAL INTEGRATION OF FILTER APPROXIMATION)

SYSTEM $\mu = 1,\ \zeta = 0.025$		$\lvert H_j(\omega)\rvert^2,\ n=1$	$\lvert m_j\omega_j^2 H_j(\omega)\rvert^2,\ n=2$	$\lvert m_j\omega^2 H_j(\omega)\rvert^2,\ n=3$
$\int_0^\infty R_j^{(n)}(\beta)\ J_j(\beta)\ d\beta$; $J_j(\beta)\ \ J_I(\beta)$ for j odd, $J_j(\beta)\ \ J_{II}(\beta)$ for j even	j = 1	12.361	12.361	19.247
	j = 2	7.758 (-2)	19.860	24.106
	j = 3	1.061 (-2)	69.616	71.126
	j = 4	7.197 (-4)	47.168	47.832
	j = 5	1.474 (-4)	57.565	52.998
	j = 6	2.344 (-5)	39.373	36.594
	j = 7	6.432 (-6)	37.077	30.821
	j = 8	1.636 (-6)	27.470	23.568
	j = 9	6.033 (-7)	25.972	19.253
	j = 10	1.488 (-7)	14.876	15.713

TABLE 3.4 MAIN DIAGONAL CONTRIBUTIONS TO THE MEAN SQUARE RESPONSE (REVERBERANT FIELD - FILTER APPROXIMATION IN CLOSED FORM)

SYSTEM $\mu=1$, $\ell/\delta_b=30$, $\zeta_j=0.025$		$\left\|H_j(\omega)\right\|^2$, n = 1	$\left\|m_j\omega_j^2 H_j(\omega)\right\|^2$, n = 2	$\left\|m_j\omega^2 H_j(\omega)\right\|^2$, n = 3
$\int_0^\infty R_j^{(m)}(\beta)\ J_j(\beta)\ d\beta$	j = 1	3.037	3.037	3.459
	j = 2	2.329 (-2)	5.961	6.028
	j = 3	7.038 (-4)	4.607	4.283
	j = 4	5.917 (-5)	3.878	3.502
	j = 5	7.066 (-6)	2.788	2.243
	j = 6	1.391 (-6)	2.337	1.807
	j = 7	3.653 (-7)	2.106	1.561
	j = 8	1.170 (-7)	1.962	1.399
	j = 9	4.310 (-8)	1.856	1.264
	j = 10	1.328 (-8)	1.328	0.652

TABLE 3.5 MAIN DIAGONAL CONTRIBUTIONS TO THE MEAN SQUARE RESPONSE (TURBULENCE - NUMERICAL INTEGRATION OF INTEGRAND)

SYSTEM $\mu = 1,\ \ell/\delta_b = 30,\ \zeta_j = 0.025$		$\lvert H_j(\omega) \rvert^2_{,n=1}$	$\lvert m_j \omega_j^2 H_j(\omega) \rvert^2_{,n=2}$	$\lvert m_j \omega^2 H_j(\omega) \rvert^2_{,n=3}$
$\int_0^\infty R_j^{(m)}(\beta)\ J_r(\beta)\ d\beta$	j = 1	3.592	3.592	4.772
	j = 2	4.427 (-2)	11.238	12.073
	j = 3	2.151 (-3)	14.194	13.977
	j = 4	1.822 (-4)	12.039	11.109
	j = 5	2.296 (-5)	9.107	7.922
	j = 6	4.245 (-6)	7.130	5.760
	j = 7	9.831 (-7)	5.669	4.250
	j = 8	2.825 (-7)	4.705	3.249
	j = 9	9.322 (-8)	4.031	2.514
	j = 10	2.763 (-8)	2.763	1.142

TABLE 3.6 MAIN DIAGONAL CONTRIBUTIONS TO THE MEAN SQUARE RESPONSE (TURBULENCE–NUMERICAL INTEGRATION OF FILTER APPROXIMATION)

SYSTEM $\mu = 1,\ \ell/\delta_b = 30,\ \zeta_j = 0.025$		$\lvert H_j(\omega) \rvert^2_{,\, n=1}$	$\lvert m_j \omega_j^2 H_j(\omega) \rvert^2_{,\, n=2}$	$\lvert m_j \omega^2 H_j(\omega) \rvert^2_{,\, n=3}$
$\int_0^\infty R_j^{(n)}(\beta)\ J_I(\beta)\, d\beta$	j = 1	3.483	3.483	4.821
	j = 2	4.410 (-2)	11.289	12.080
	j = 3	2.160 (-3)	14.175	13.987
	j = 4	1.807 (-4)	11.842	11.024
	j = 5	2.317 (-5)	9.051	7.982
	j = 6	4.177 (-6)	7.016	5.777
	j = 7	9.773 (-7)	5.634	4.333
	j = 8	2.792 (-7)	4.684	3.352
	j = 9	9.323 (-8)	4.013	2.663
	j = 10	2.763 (-8)	2.763	2.164

TABLE 3.7 MAIN DIAGONAL CONTRIBUTIONS TO THE MEAN SQUARE RESPONSE (TURBULENCE — FILTER APPROXIMATION IN CLOSED FORM)

numerical integrations over the range $.01 < \beta < 100$ follows: the incremental size of β over $.01 \leq \beta \leq 1$ was $\Delta = .05$; over $1 \leq \beta = 12$, $\Delta = .1$; over $12 \leq \beta \leq 30$, $\Delta = .5$; and over $30 \leq \beta \leq 100$, $\Delta = 1$.

The relative contributions of the off-diagonal terms to the mean square response for both the reverberant field and turbulence are shown by the tables in Appendix C. In this study, the modal frequencies vary according to $\omega_k/\omega_j = (k/j)^2$ and the modal damping has the same magnitude for all modes, $\zeta = 0.025$. Consistent with these properties, the off-diagonal terms should (and do) contribute little to the mean square response relative to the diagonal terms. For more closely spaced modal frequencies, say when the frequency spacing is within 1.414, and/or damping values on the order of $\zeta_j = 0.1$, the effect of the off-diagonal terms will become more pronounced. Due to the crude filter representation used, the integral contributions of the off diagonal terms are accentuated, in particular, for the higher order terms.

We note the accuracy of the filter approximations is lax. Such is expected inasmuch as the filters shapes were set to match somewhat the envelope maxima of the acceptance functions rather than the acceptance shape for each of the individual modes. If the filter constants are made dependent upon the mode numbers, the accuracy of the filter approximations can be improved by an order of magnitude. By retaining the analytical filter results in parametric form, this modal dependent filter scheme can be implemented with negligible analytical effort.

Normalized plots of the mean square response to the reverberant field are represented by Figures 3.29 through 3.31; and to the aerodynamic turbulence by Figures 3.32 through 3.34. For completeness, the mean square response to the plane progressive wave is repeated here as Figure 3.35. Since the variation of $\sigma_y^2(x)$ is symmetric relative to the mid-span of the structure, the plots are constructed only over the range $0 \leq x/\ell \leq .5$. The coefficients C_n, where $n = 1, 2, 3$, are those defined in Section 3.2.1.

Of note is the decisive difference in form and magnitude between the response for the system function $H_j(\omega)$ and the response for the other two system functions in the reverberant field and turbulence. The response for $H_j(\omega)$ essentially is that of a unimodal system at ω_1 since the other integral contributions are minor relative to the $j = k = 1$ term; thus, $\sigma_y^2(x)$ varies over x approximately as $\sin^2 \pi x/\ell$. The response for both $m_j\omega_j^2 H_j(\omega)$ and $m_j\omega^2 H_j(\omega)$ are influenced predominantly by the main diagonal terms. All ten terms are important for the range of parameters selected here; those beyond $j = 10$ would be considerably less important due to the rapid roll-off of the acceptance functions.

The variation in $\sigma_y^2(x)$ over x for the plane wave excitation is similar for all of the system functions; it is unimodal in its behavior. We note this variation is similar to that of $H_j(\omega)$ in either the reverberant field or/and the turbulence. For the system functions $m_j\omega_j^2 H_j(\omega)$ and $m_j\omega^2 H_j(\omega)$ in either the reverberant field or/and the turbulence, the mean square response variations are markedly similar; the $\sigma_y^2(x)$ rises rapidly over the range $0 \leq x/\ell \leq .1$ and fluctuates only modestly over $.1 \leq x/\ell \leq .5$. If a larger number of terms were used (we recall $j = 1, 2 \ldots 10$ and $k = 1, 2 \ldots 10$), their contributions would tend to smooth the fluctuations so that $\sigma_y^2(x)$ over $.1 \leq x/\ell \leq .9$ would be nearly constant.

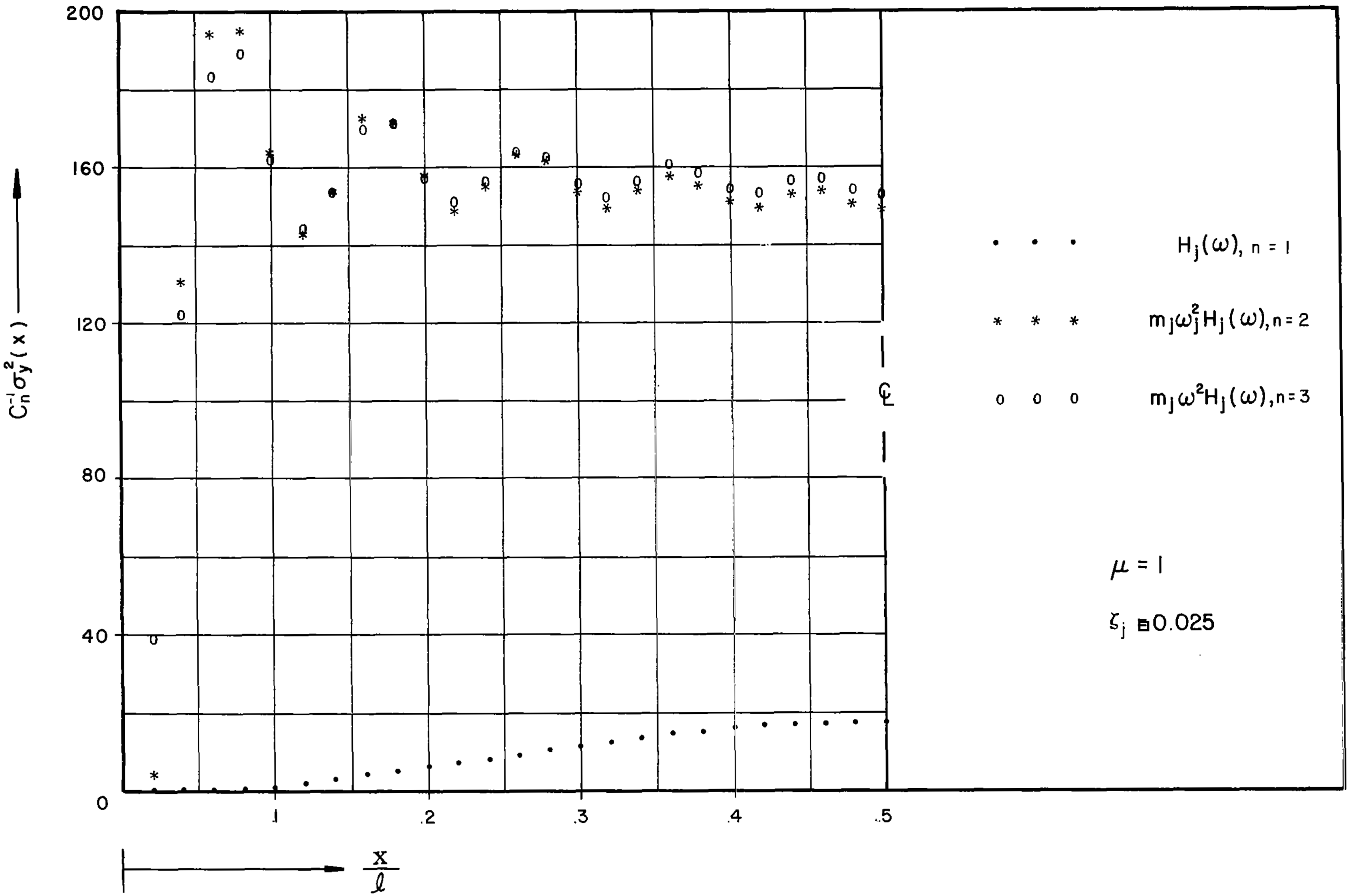

FIGURE 3.29 MEAN SQUARE RESPONSE TO THE REVERBERANT FIELD

(NUMERICAL INTEGRATION OF INTEGRAND)

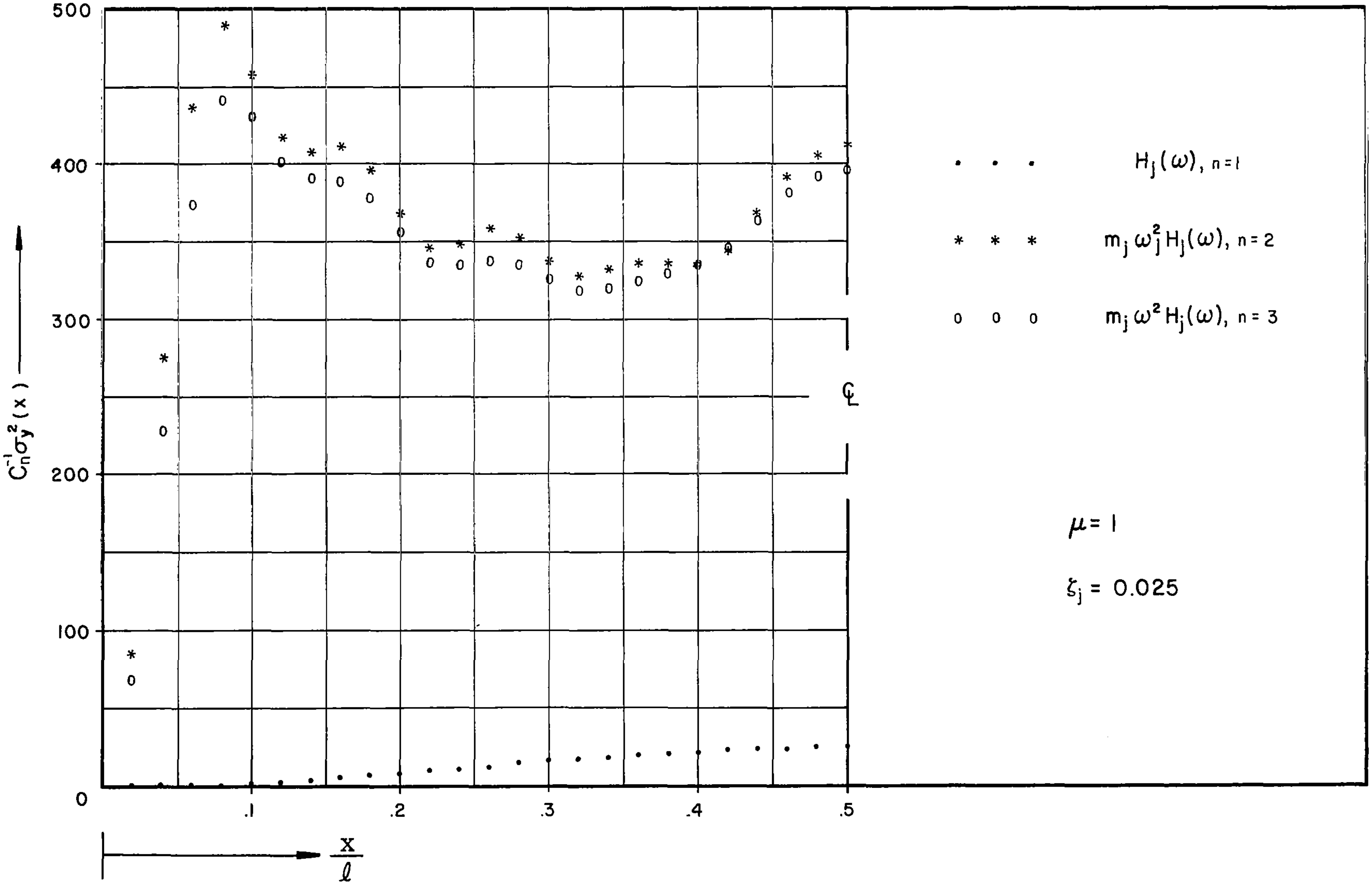

FIGURE 3.30 MEAN SQUARE RESPONSE TO THE REVERBERANT FIELD

(NUMERICAL INTEGRATION OF FILTER APPROXIMATION)

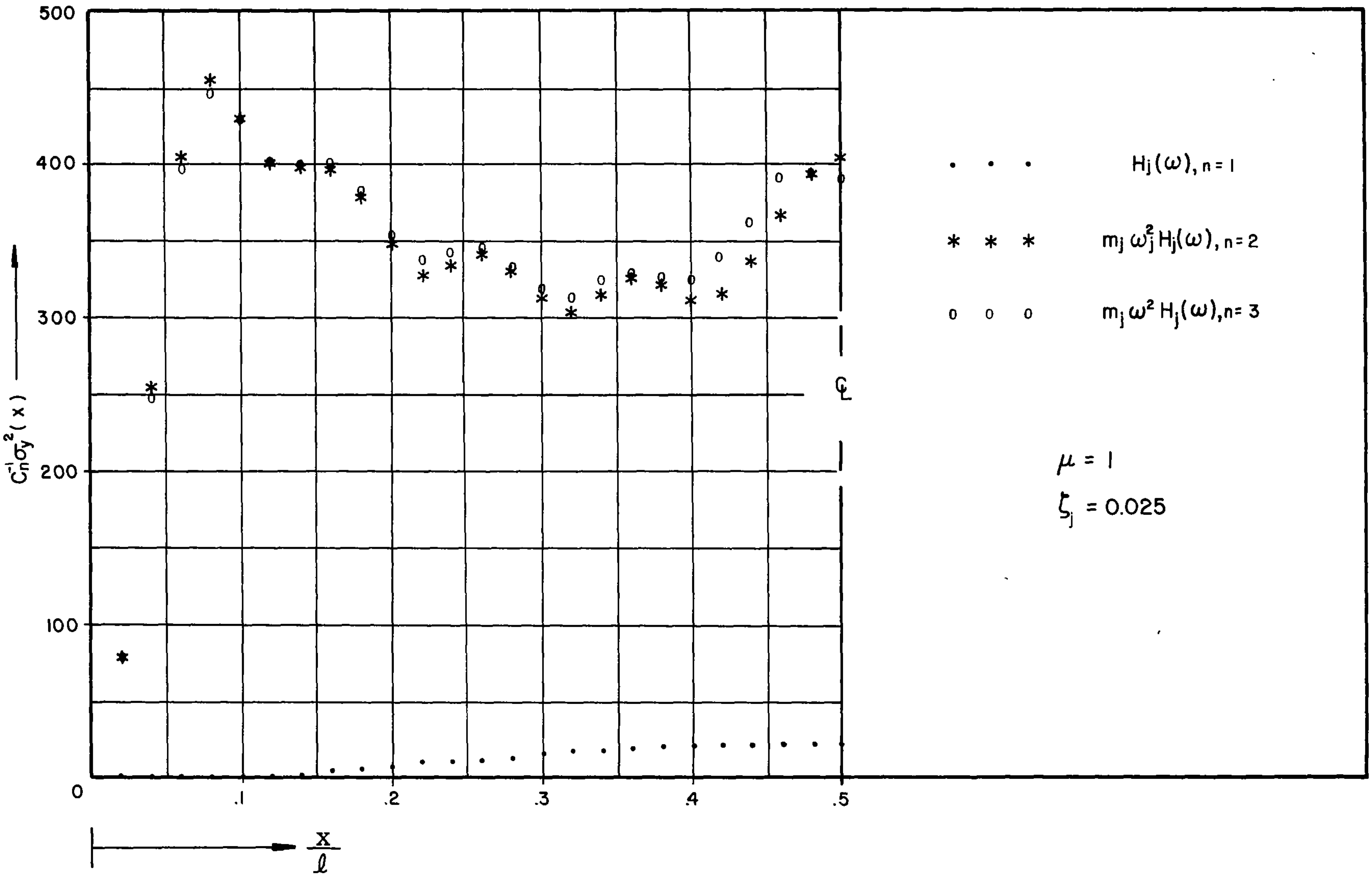

FIGURE 3.31 MEAN SQUARE RESPONSE TO THE REVERBERANT FIELD

(FILTER APPROXIMATION IN CLOSED FORM)

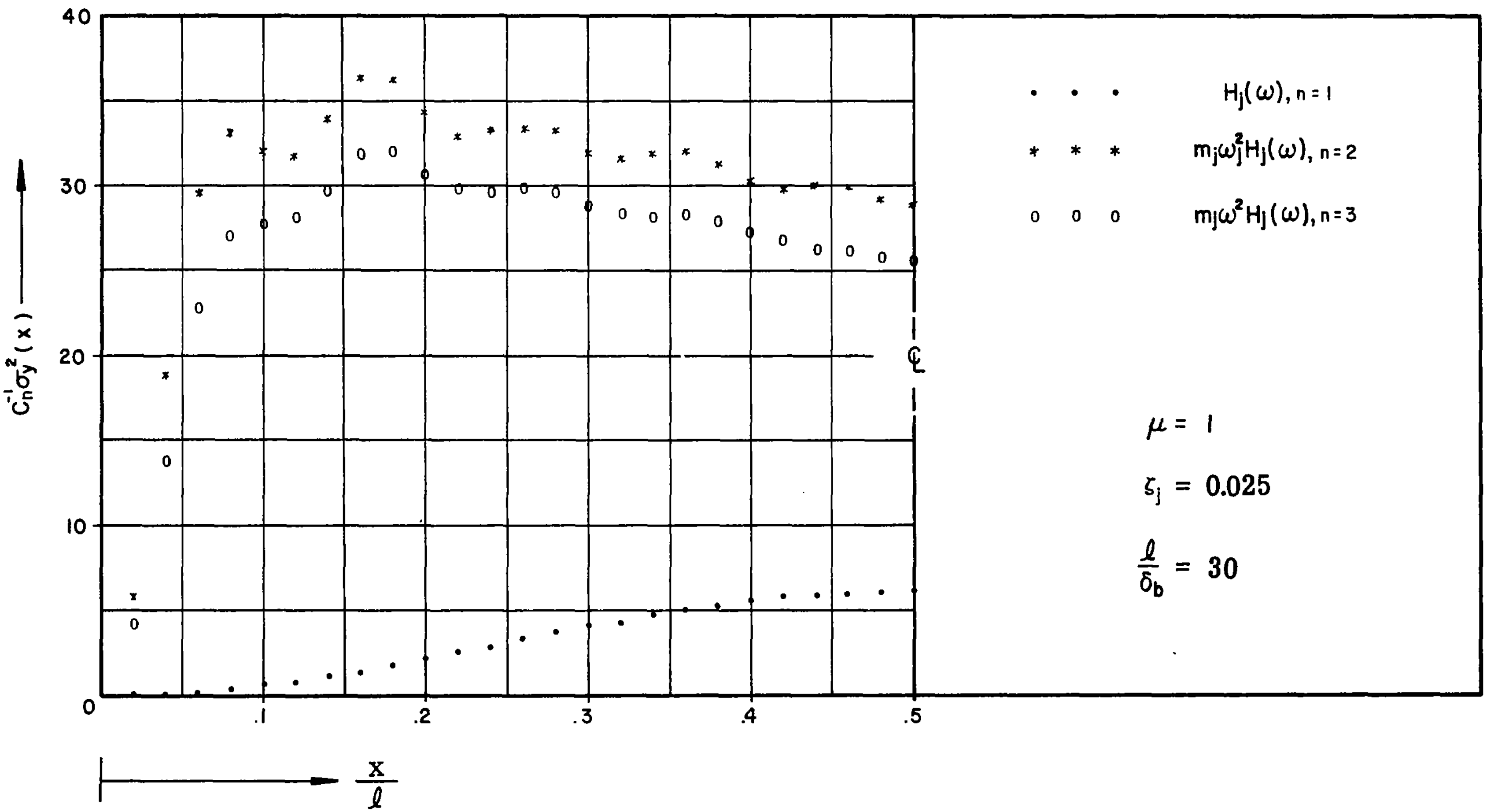

FIGURE 3.32 MEAN SQUARE RESPONSE TO AERODYNAMIC TURBULENCE (NUMERICAL INTEGRATION OF INTEGRAND)

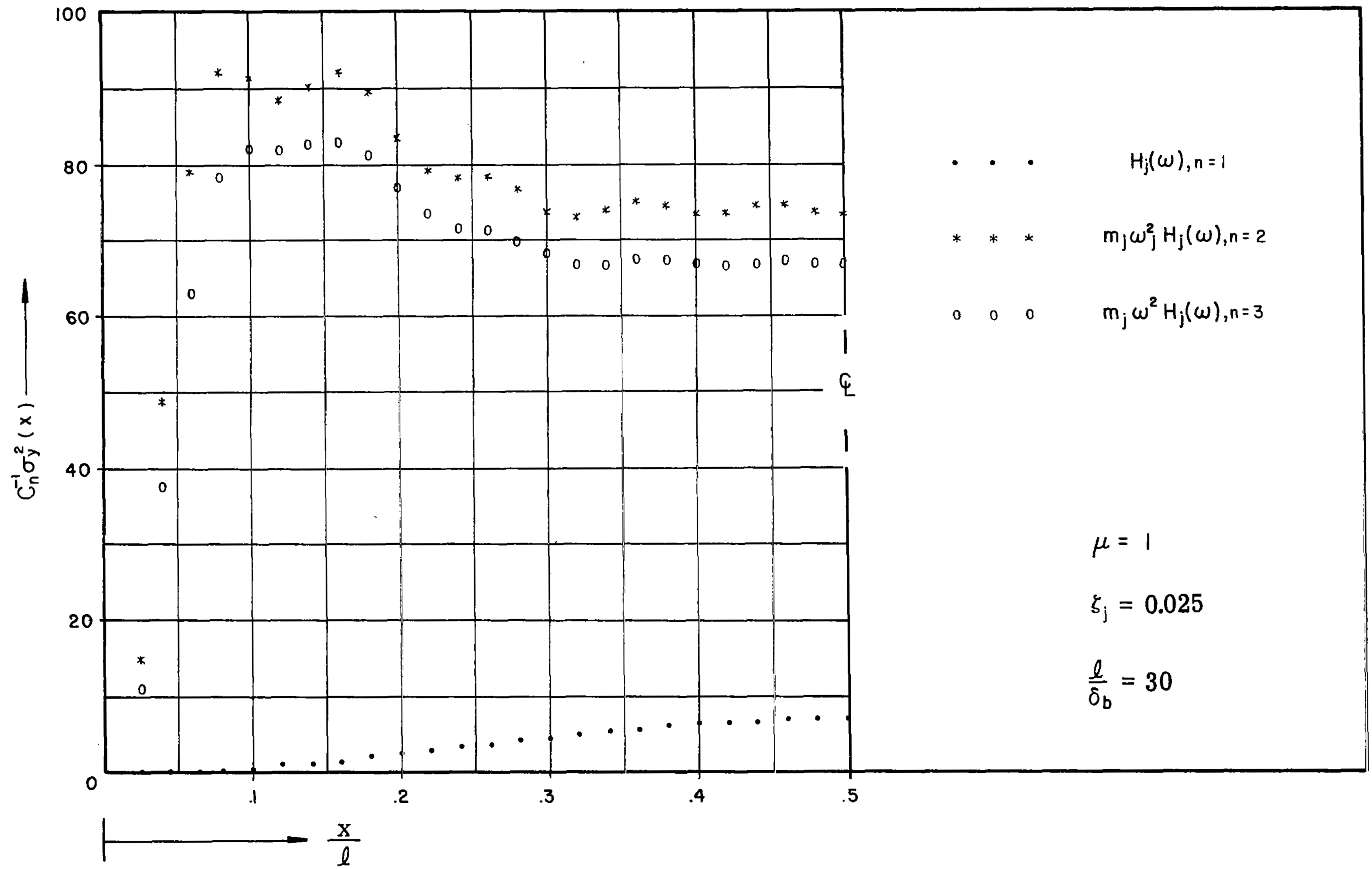

FIGURE 3.33 MEAN SQUARE RESPONSE TO AERODYNAMIC TURBULENCE (NUMERICAL INTEGRATION OF FILTER APPROXIMATION)

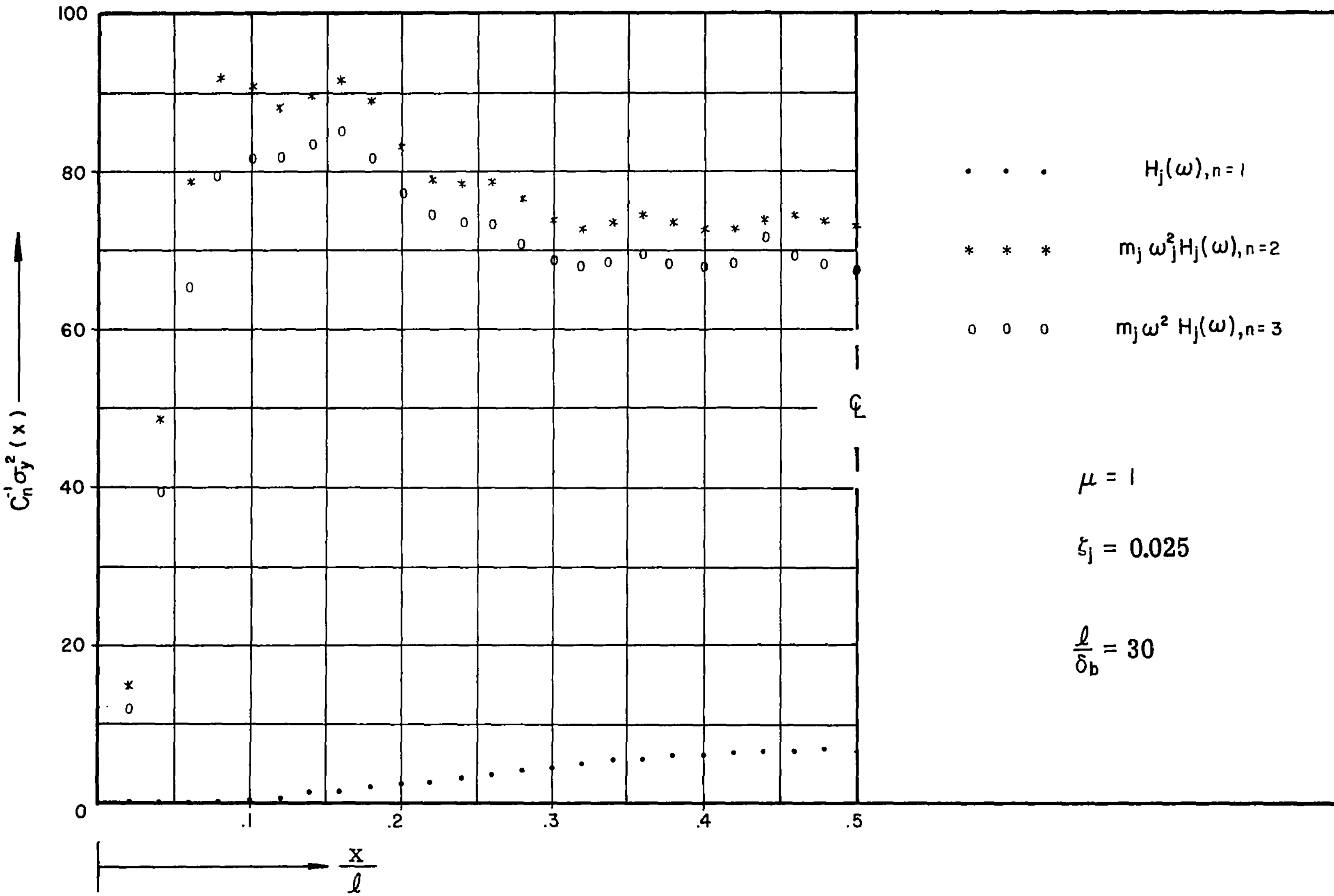

FIGURE 3.34 MEAN SQUARE RESPONSE TO AERODYNAMIC TURBULENCE (FILTER APPROXIMATION IN CLOSED FORM)

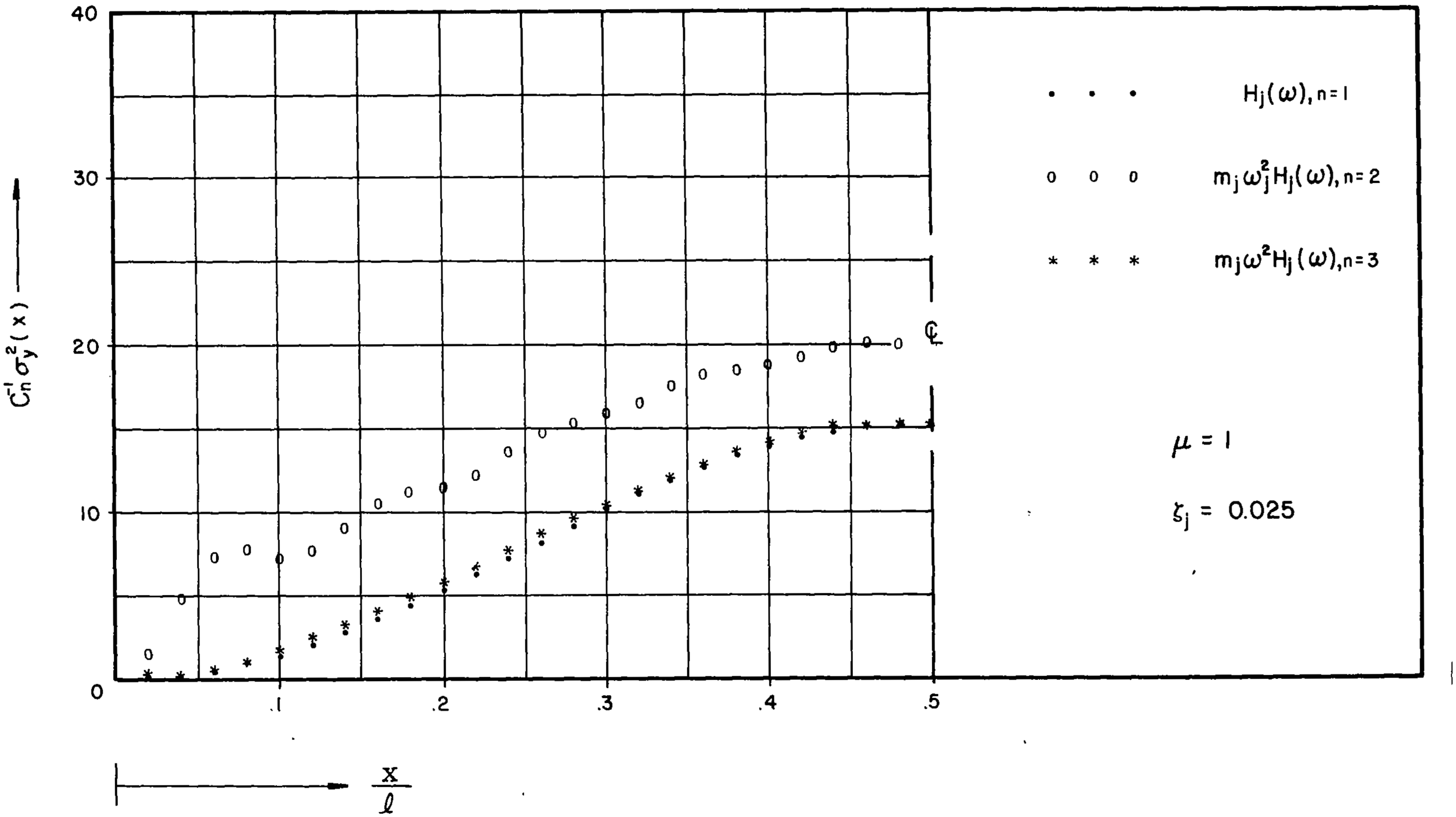

FIGURE 3.35 MEAN SQUARE RESPONSE TO THE PROGRESSIVE WAVE FIELD (NUMERICAL INTEGRATION OF INTEGRAND)

4.0 SUMMARY REMARKS

In this report, we reviewed briefly the theory fundamental to assessing the mean square response of distributed linear systems in a random environment. The theory emphasized favors a modal series representation and spectral analysis; hence, attention is focused upon formulations which lead to response spectral density functions. Nonhomogeneous, nonstationary excitations are mentioned; homogeneous, stationary excitations are examined in depth. Point-wise loadings are treated as well.

To promote insight into the physical meaning of the theory, some of the formulations presented in the text are used to compute mean square response values of representative structural systems to each of three distributed random excitations. The basic structural system is a very simple one. It is a one dimensional system, and assumed to have harmonic mode shapes, well separated modal frequencies, and equal damping ($\zeta_j = 0.025$) in all modes. Such assumptions do not necessarily compromise the generality of the results and, at the same time, serve to simplify enormously the mathematics. The excitations examined, three in number, are all homogeneous and stationary acoustic pressure fields. Chief interest concerns those excitations representative of a reverberant field and aerodynamic turbulence, although a random progressive wave field is treated.

We examined three system functions with frequency characteristics designated by $H_j(\omega)$, $m_j \omega_j^2 H_j(\omega)$ and $m_j \omega^2 H_j(\omega)$. For each system function and each excitation, the response contributions are determined for the jk terms where $j = 1, 2 \ldots 10$ and $k = 1, 2 \ldots 10$. These data are shown in Appendices B and C only for $j = 1, 2 \ldots 9$ and $k = 1, 2 \ldots 9$.

In the text, the contributions for $j = k = 1, 2. . . 10$ are considered in detail for the reverberant field and turbulence; that is, the system functions, the acceptance functions, and the products of these functions (response spectral densities) are all displayed. Similar detail is given to the progressive wave in Appendix B.

Of note are the filter approximation formulations. The filters are designed so that their frequency characteristics can be set to match the joint acceptance functions for the reverberant and turbulence excitations. In addition, and equally important, these filter forms (after multiplication by the system functions) are amenable to integration by residue theory so that parametric mean square response results can be obtained in closed form with but a moderate mathematical effort. Closed form results are shown for all three system functions. When compared with the values computed by numerical integration of the filter approximations, these theoretical results agree very closely so that validity in the theoretical work is established. Of use also are the closed form results for the progressive wave excitation; the details of this analytical effort is shown as Appendix B.

For a consistent set of system-excitation parameters, the variations of $\sigma_y^2(x)$ in x display similar patterns in behavior although the accuracy of the filter approximations relative to numerical integration of the exact integrands is not satisfactory. However, the filter results can be made to match almost exactly the numerical integration results simply by selecting other filter coefficient values (note that with the closed form results, this matching activity reduces to but an exercise in algebra). Having set the coefficients in this way, we then can plot the filter characteristics and observe what constitutes a "good" approximation of the force field acceptance functions. Perhaps less crudely, we can establish a dependency of the filter coefficient values on the mode numbers and use this form of model in the response calculations. These are but two plausible approximation schemes; others certainly can be devised by the reader.

As with all work of this nature, the results collectively point out a number of additional tasks fundamental to not only understanding the subtleties of the underlying theory, but developing theoretically proper response predictions as well. Some of these follow:

- for the turbulence and reverberant field, formulate a modal dependency relationship for the filter coefficients in the filter approximation response model
- develop residual impedance concepts so that response predictions can be made when modal concepts are inappropriate or inordinately complicated
- examine the variation of $\sigma_y^2(x)$ for structural configurations with random system functions
- examine the variation of $\sigma_y^2(x)$ for variations in μ and/or nonconstant modal damping
- consider estimates of $\sigma_y^2(x)$ for system functions with modal frequency spacings other than $\omega_k/\omega_j = (k/j)^2$
- consider acceptance functions for orthogonal functions other than simple harmonic mode shapes
- consider acceptance functions for systems with statistical variation in the mode shapes

This list is by no means exhaustive, although such results would go far to answer questions of immediate practical interest to the analyst.

Perhaps the greatest value of this report is the implicit generality of the results; the true worth, however, depends to no small extent on the resourcefulness of the user. If nothing else, the included plots, tables, and theoretical expressions all serve one extremely important purpose. They provide a latent "feel" for the nature, complexity and expected forms of solutions for problems indigenous to structural response predictions in random environments. Radical departure from the general behavior shown here would be suspect even for more complicated structural systems. The results shown thus provide solid theoretical bases from which to establish, however simple, response predictions.

The direct extension of these results to structural configurations of more than one dimension is not unreasonable, though not without additional effort. Such an extension requires a formulation which makes repetitive use of the integral forms presented here. This approach has precedence in classical treatments of plate and shell structures and in more practical applications as well [4, 17].

The reader is urged to examine the various appendices in a manner something other than that of a cursory inspection. Although not profound, the problems of Appendix A should promote physical insight into the theory and clarify some of the symbolism of the text. Appendix B concerns in detail the response calculations associated with random progressive waves. The integral forms here should prove of interest to the reader who is more analytically inclined. Appendix C shows the modal cross terms for all three system functions and both the reverberant field and turbulence. Appendix D represents a small collection of integral results important to the work of this report as well as fundamental to non-stationary excitation problems. For the serious analyst, time spent in becoming acquainted with the integral forms in this brief table should prove a very worthwhile investment indeed.

5.0 REFERENCES

1. Barnoski, R. L. and J. R. Maurer, "Mean-Square Response of Simple Mechanical Systems to Nonstationary Random Excitation", Transactions of the AMSE, Series E, Journal of Applied Mechanics, Vol. 36, No. 2, June 1969.

2. Barnoski, R. L., "The Maximum Response of Rectangular Plates to Random Excitations", NASA CR-853, September 1967.

3. Bendat, J. S. and A. G. Piersol, Measurement and Analysis of Random Data, John Wiley and Sons, Inc., New York, 1966.

4. Bozich, D. J., "Spatial Correlation in Acoustic-Structural Coupling," The Journal of the Acoustical Society of America, Vol. 36, No. 1, January 1964.

5. Crandall, S. H. and W. D. Mark, Random Vibration in Mechanical Systems, Academic Press, New York, 1963.

6. Hurty, W. C. and M. F. Rubinstein, Dynamics of Structures, Prentice-Hall, Inc., New Jersey, 1964.

7. Jacobs, L. D. and D. R. Lagerquist, "Finite-Element Analysis of Complex Panel Response to Random Loads", AFFDL-TR-68-44, Wright-Patterson Air Force Base, Ohio, October 1968.

8. Maestrello, L., "Design Criterion for Minimum Structural Response and Sound Radiation of a Panel Excited by a Turbulence Boundary Layer", AIAA Paper No. 67-12, AIAA 5th Aerospace Sciences Meeting, New York, January 1967.

9. Papoulis, A., The Fourier Integral and Its Applications, McGraw-Hill Book Company, Inc., 1962.

10. Powell, A., "On the Response of Structures to Random Pressure and to Jet Noise in Particular", Chapter 8 of Random Vibration, edited by S. H. Crandall, John Wiley and Sons, Inc., New York, 1968.

11. Robson, J. D., An Introduction to Random Vibration, Elsevier Publishing Company, New York, 1964.

12. Schweiker, J. S. and R. E. Davis, "Response of Complex Shell Structures to Aerodynamic Noise", NASA CR-450, April 1966.

13. Sokolnikoff, I. S., Advanced Calculus, McGraw-Hill Book Company, Inc., New York, 1939, page 151.

14. Trubert, M. R. P., "Response of Elastic Structures to Statistically Correlated Multiple Random Excitations", The Journal of the Acoustical Society of America, Vol. 35, No. 7, July 1963.

15. Wilby, J. F., "The Response of Simple Panels to Turbulent Boundary Layer Excitation", AFFDL-TR-67-70, Wright-Patterson Air Force Base, Ohio, October 1967.

16. White, P. H., "Some Useful Approximations for Determining the Vibration of Structures Excited by Random Pressures", The Journal of the Acoustical Society of America, Vol. 36, No. 4, April 1964.

17. White, R. W., "Theoretical Study of Acoustic Simulation of In-Flight Environments", The Shock and Vibration Bulletin No. 37, Part 5, January 1968.

18. AMS 55, Handbook of Mathematical Functions, U. S. Department of Commerce, National Bureau of Standards, edited by M. Abramowitz and I. A. Stegun, June 1964.

19. Gradshteyn, I. S. and I. M. Ryzhik, Table of Integrals Series and Products, Academic Press Inc., New York, 1965.

20. Roberts, G. E. and H. Kaufman, Table of Laplace Transforms, W. B. Sanders Co., Philadelphia, 1966.

6.0 APPENDICES

- A - Illustrative Problems
- B - Mean Square Response to a Progressive Wave Field
- C - Integral Contributions to the Mean Square Response
- D - Table of Selected Integrals

APPENDIX A

Here, example problems and their solutions are presented to illustrate some of the theory presented in the text of this report. The equation numbers refer to each problem separately; no confusion should result even though some of these numbers are used elsewhere in the text.

Example Problem 1

Calculate the response y(t) of a mechanical oscillator to the rectangular step function of Figure A. 1.

Solution: The system equation of motion is

$$m\ddot{y} + c\dot{y} + ky = f(t) \tag{1.1}$$

or, alternatively,

$$\ddot{y} + 2\zeta\omega_n\dot{y} + \omega_n^2 y = \frac{1}{m} f(t) \tag{1.2}$$

where

$$\omega_n^2 = \frac{k}{m}$$

$$2\zeta\omega_n = \frac{c}{m} \tag{1.3}$$

$$\zeta = \frac{c}{c_c}$$

The input force excitation may be written as

$$f(t) = f_0\left[U(t) - U(t-t_0)\right] \tag{1.4}$$

where U(t) is the unit step function.

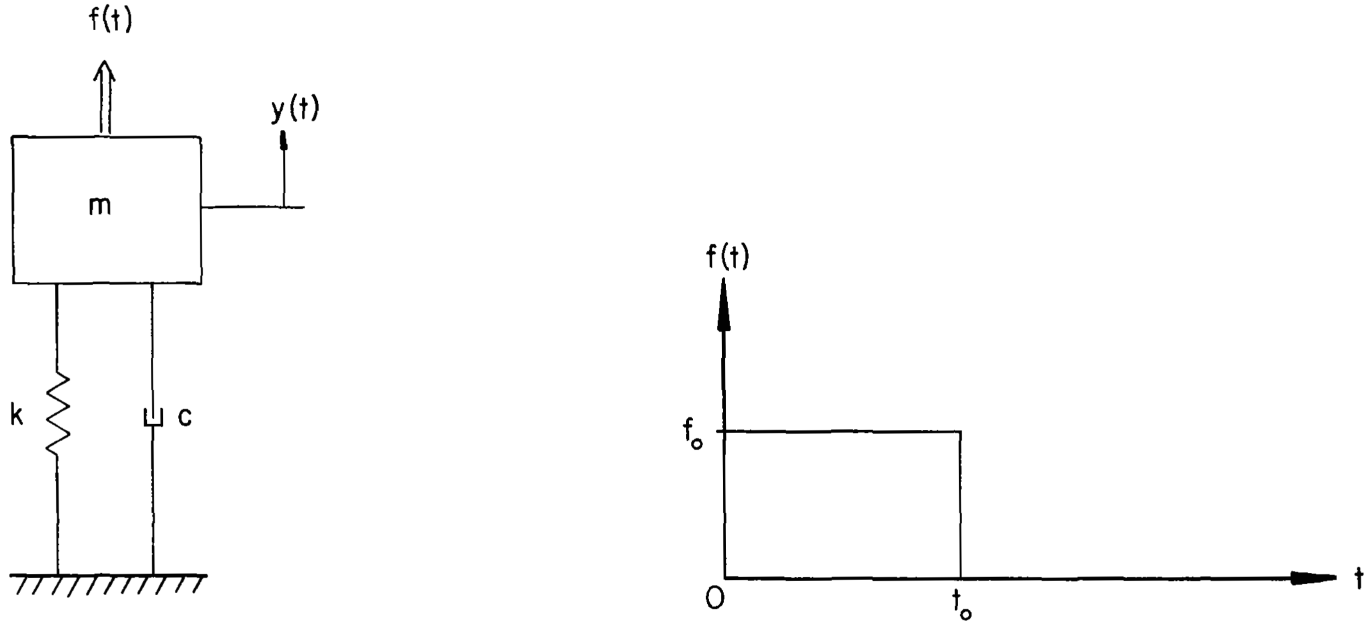

Mechanical System

Force Excitation

FIGURE A.1 MECHANICAL SYSTEM AND INPUT EXCITATION

By Fourier transform methods, the response y(t) is given by [9]

$$y(t) = \frac{1}{2\pi}\int_{-\infty}^{\infty} Y(\omega)\, e^{i\omega t}\, d\omega \tag{1.5}$$

and the Fourier transform (F. T.) of the response by

$$Y(\omega) = H(\omega)\, F(\omega) \tag{1.6}$$

where

$$H(\omega) = \frac{1}{m\omega_n^2} \cdot \frac{1}{1 - \left(\frac{\omega}{\omega_n}\right)^2 + i2\varsigma\frac{\omega}{\omega_n}} \tag{1.7}$$

Now the F. T. of the excitation f(t) is noted by

$$f(t) \longleftrightarrow F(\omega) \tag{1.8}$$

and [9]

$$U(t) \longleftrightarrow \pi\delta(\omega) + \frac{1}{i\omega} \tag{1.9}$$

so that

$$F(\omega) = f_o\left[\pi\delta(\omega) + \frac{1}{i\omega}\right]\left[1 - e^{-it_o\omega}\right] \tag{1.10}$$

The response given by Equation (1.5) may be expressed as the sum

$$y(t) = I_1(t) + I_2(t) + I_3(t) + I_4(t) \tag{1.11}$$

where

$$I_1(t) = \frac{f_o}{2} \int_{-\infty}^{\infty} H(\omega) e^{i\omega t} \cdot \delta(\omega) \, d\omega$$

$$I_2(t) = \frac{f_o}{2\pi i} \int_{-\infty}^{\infty} \frac{1}{\omega} H(\omega) e^{i\omega t} \, d\omega$$

$$I_3(t) = - I_1(t - t_o), \quad \text{for } t \geq t_o$$

$$I_4(t) = - I_2(t - t_o), \quad \text{for } t \geq t_o \tag{1.12}$$

Upon integration

$$I_1(t) = \frac{f_o}{2k}$$

$$I_2(t) = \frac{f_o}{2\pi m i} \int_{-\infty}^{\infty} \frac{e^{i\omega t}}{(\omega_n^2 - \omega^2 + i 2\zeta\omega_n \omega)\, \omega} \, d\omega$$

$$= - \frac{f_o}{m \omega_n a} e^{-bt} \sin(at + \phi) + \frac{f_o}{2k} \tag{1.13}$$

where

$$\phi = \tan^{-1} \frac{a}{b}$$

$$a = \omega_n (1 - \zeta^2)^{1/2}$$

$$b = \zeta \omega_n \tag{1.14}$$

Thus,

$$y(t) = I_1(t) + I_2(t), \quad \text{for } 0 \le t \le t_0$$

$$y(t) = I_1(t) + I_2(t) - U(t-t_0)\left[I_1(t-t_0) + I_2(t-t_0)\right], \quad \text{for } t \ge t_0 \tag{1.15}$$

or, in expanded form,

$$y(t) = \frac{f_0}{k}\left[1 - \frac{e^{-bt}}{(1-\varsigma^2)^{1/2}} \sin\left[at + \phi\right]\right], \quad \text{for } 0 \le t \le t_0$$

$$y(t) = \frac{f_0}{k}\left[\frac{e^{-b(t-t_0)}}{(1-\varsigma^2)^{1/2}} \sin\left[a(t-t_0) + \phi\right] - \frac{e^{-bt}}{(1-\varsigma^2)^{1/2}} \sin\left[at + \phi\right]\right] \quad \text{for } t \ge t_0 \tag{1.16}$$

$$\phi = \tan^{-1} \frac{(1-\varsigma^2)^{1/2}}{\varsigma}$$

An alternative approach is to reconsider Equation (1.5) beginning with the form

$$y(t) = \frac{1}{2\pi}\int_{-\infty}^{\infty} H(\omega)\, F(\omega)\, e^{i\omega t}\, d\omega \tag{1.17}$$

Since

$$h(t) \longleftrightarrow H(\omega)$$

$$f(t) \longleftrightarrow F(\omega) \tag{1.18}$$

the time convolution theorem allows us to express this equation as

$$y(t) = \int_{-\infty}^{\infty} h(n)\, f(t-n)\, dn \tag{1.19}$$

which may be written as

$$y(t) = \int_{0}^{t} h(n)\, f(t-n)\, dn = \int_{0}^{t} h(t-n)\, f(n)\, dn \tag{1.20}$$

since

$$h(t-n) = 0 \quad \text{for} \quad 0 \leq t \leq n.$$

For this problem,

$$h(t) = \frac{1}{a} e^{-bt} \sin at \tag{1.21}$$

and subsequent integration according to Equation (1.20) produces the results shown by Equation (1.16).

Yet another approach (and possibly the least tedious for this problem) is by the use of Laplace transforms. By the L. T. of Equation (1.2),

$$Y(s) = H(s)\, F(s) \tag{1.22}$$

where

$$H(s) = \frac{1}{m} \frac{1}{\omega_n^2 - s^2 + 2\varsigma\omega_n s}$$

$$F(s) = \frac{f_0}{s}\left(1 - e^{-st_0}\right) \tag{1.23}$$

Now rearranging Y(s) gives

$$Y(s) = \frac{f_0}{m}\left[\left(\frac{1}{(s+b)^2 + a^2}\right)\frac{1}{s} - \left(\frac{1}{(s+b)^2 + a^2}\right)\frac{e^{-st_0}}{s}\right] \tag{1.24}$$

so that, from Laplace transform tables [20],

$$y(t) \longleftrightarrow Y(s) \tag{1.25}$$

where

$$\frac{1}{a^2 + b^2} - \frac{e^{-bt}\sin(at + \phi)}{a(a^2 + b^2)^{1/2}} \longleftrightarrow \frac{1}{s} \cdot \frac{1}{(s+b)^2 + a^2}$$

$$f(t)\,U(t - t_0) \longleftrightarrow f(s)\,e^{-st_0} \tag{1.26}$$

After some algebra, y(t) may be written as shown by Equations (1.16).

Example Problem 2

Determine the forced response of a simple supported beam to the harmonic loading shown in Figure A.2.

Solution: The equation of motion is

$$m\ddot{y}(x,t) + c\dot{y}(x,t) + D_x y(x,t) = f(x,t) \tag{2.1}$$

where

$$D_x = EI \frac{\partial^4}{\partial x^4}$$

$$f(x,t) = f_0 \sin \omega t \tag{2.2}$$

For this problem, we seek a particular solution to Equation (2.1) subject to the boundary conditions

$$\left.\begin{matrix} y(0,t) \\ M(0,t) \end{matrix}\right\rangle = 0 \qquad \left.\begin{matrix} y(\ell,t) \\ M(\ell,t) \end{matrix}\right\rangle = 0 \tag{2.3}$$

where the bending moment is given by

$$M(x,t) = EI \frac{\partial^2 y(x,t)}{\partial x^2} \tag{2.4}$$

From modal theory, the desired response is written as

$$y(x,t) = \sum_{j=1}^{\infty} \phi_j(x)\, q_j(t) \tag{2.5}$$

where the mode shapes $\phi_j(x)$ is computed from the solution to the

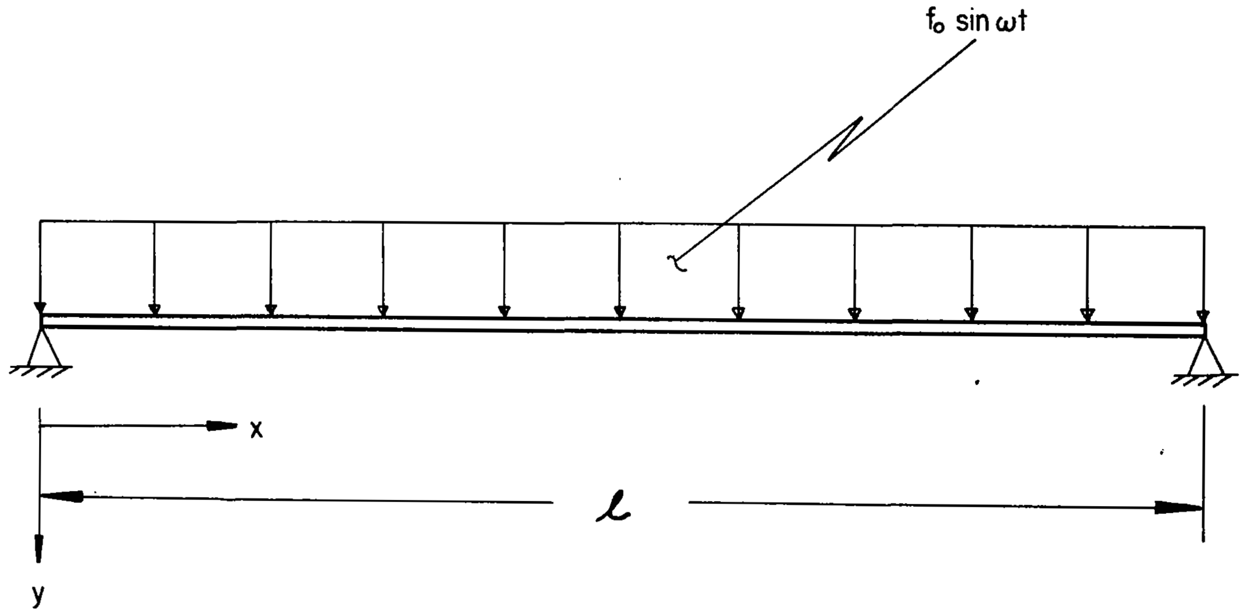

FIGURE A.2 SIMPLY SUPPORTED BEAM EXCITED BY A UNIFORMLY DISTRIBUTED HARMONIC LOADING homogeneous equation

$$m\ddot{y}(x,t) + EI\frac{\partial^4 y(x,t)}{\partial x^4} = 0 \tag{2.6}$$

and $q_j(t)$ is the particular solution to

$$\ddot{q}_j(t) + 2\zeta_j\omega_j\dot{q}_j(t) + \omega_j^2 q_j(t) = \frac{1}{m_j} f_j(t) \tag{2.7}$$

If the loading can be expressed as the product $f(x, t) = f(x) f(t)$, the generalized force is of the form

$$f_j(t) = f_j(x) f(t) \tag{2.8}$$

where

$$f_j(x) = \int_0^{\ell} f(x)\phi_j(x)\,dx \tag{2.9}$$

The modal participation factor is defined according to

$$\Gamma_j = \frac{1}{\ell}\int_0^{\ell} f(x)\phi_j(x)\,dx \tag{2.10}$$

so that

$$\ddot{q}_j(t) + 2\zeta_j\omega_j\dot{q}_j(t) + \omega_j^2 q_j(t) = \frac{f_0\ell}{m_j}\Gamma_j f(t) \tag{2.11}$$

The quantity Γ_j may be considered as a measure of the extent to which the jth mode participates in exciting the structural system. If we interpret the structure as a system with selectivity characteristics both in space and frequency, this quantity provides an estimate of the spatial selectivity of the structural system in affecting a response.

Upon substituting (2.5) into Equation (2.6) with the input excitation at $\omega = \omega_j$,

$$(D^4 - k_j^4)\, \phi_j(x) = 0 \tag{2.12}$$

where

$$D = \frac{\partial}{\partial x}$$

$$k_j^4 = \omega_j^2 \frac{m}{EI} \tag{2.13}$$

Thus,

$$\phi_j(x) = C \cos k_j x + D \sin k_j x + E \cosh k_j x + F \sinh k_j x \tag{2.14}$$

where C, D, E, and F are constant coefficients with values dependent upon the boundary conditions.

For the boundary conditions of Equation (2.3) the coefficients C, E, and F reduce to zero and the frequency equation reduces to the simple transcendental equation

$$D \sin k_j \ell = 0 \tag{2.15}$$

Since we will not admit the trivial solution D = 0, the frequency equation is satisfied by

$$k_j \ell = j\pi, \qquad j = 1, 2, 3 \ldots \tag{2.16}$$

and the system modal (natural) frequencies are given by

$$\omega_j^2 = \frac{EI}{m\ell^4} (k_j \ell)^4 \tag{2.17}$$

With the coefficient D arbitrarily set to unity, the modes shapes $\phi_j(x)$ which correspond to the modal frequencies ω_j are given by

$$\phi_j(x) = \sin k_j x = \sin \frac{j\pi x}{\ell} \tag{2.18}$$

Let us consider now the particular solution to Equation (2.7). With the above jth mode shape,

$$m_j = m \int_0^{\ell} \sin^2 k_j x \, dx = \frac{m\ell}{2} \tag{2.19}$$

$$f_j(t) = f_0 \sin \omega t \int_0^{\ell} \sin k_j x \, dx \begin{cases} = 0, & j = 2, 4, 6 \cdots \\ = \dfrac{2f_0}{k_j} \sin \omega t, & j = 1, 3, 5 \cdots \end{cases} \tag{2.20}$$

By the substitution of these quantities into Equation (2.7), the modal equation of motion becomes

$$\ddot{q}_j(t) + 2\zeta_j \omega_j \dot{q}_j(t) + \omega_j^2 q_j(t) = \frac{4f_0}{m k_j \ell} \sin \omega t \tag{2.21}$$

Note the generalized force points out the intuitive fact that loadings distributed antisymmetric with respect to the mid-span of the beam contribute nothing to the overall response. In other words, the system acts spatially to accept energy only in the odd-numbered modes; it rejects all contributions with wave numbers that correspond to the even-numbered modes. By any one of a number of elementary differential equation methods,

$$q_j(t) = \frac{4 f_0}{m \ell \omega_j^2 k_j} \left| H_j(\omega) \right| \sin(\omega t - \phi_j) \tag{2.22}$$

where

$$H_j(\omega) = \frac{1}{1 - \left(\frac{\omega}{\omega_j}\right)^2 + i\,2\zeta_j \frac{\omega}{\omega_j}} \tag{2.23}$$

$$\phi_j = \tan^{-1} \frac{2\zeta_j \frac{\omega}{\omega_j}}{1 - \left(\frac{\omega}{\omega_j}\right)^2}$$

From Equation (2.5) with (2.18) for $\phi_j(x)$ and (2.22) for $q_j(t)$,

$$y(x,t) = \frac{4f_0}{m\pi} \sum_{j=1,3,5}^{\infty} \frac{1}{j\omega_j^2} \left| H_j(\omega) \right| \sin \frac{j\pi x}{\ell} \sin(\omega t - \phi_j) \tag{2.24}$$

Since this series is rapidly convergent in j, the higher order terms become vanishingly small and may be discarded with little error. If the system function were of the form

$$\hat{H}_j(\omega) = -\omega^2 H_j(\omega) \tag{2.25}$$

then

$$y(x,t) = \frac{4f_0}{m\pi} \sum_{j=1,3,5}^{\infty} \frac{1}{j} \left(\frac{\omega}{\omega_j}\right)^2 \left| H_j(\omega) \right| \sin \frac{j\pi x}{\ell} \sin(\omega t - \phi_j + \pi) \tag{2.26}$$

and the higher order terms become important for $\omega \gg \omega_j$.

Example Problem 3

Estimate the mean square response of a lightly damped, simply supported beam to a homogeneous random pressure field created by a speaker excited with bandlimited white noise and directed at normal incidence to the structure. Assume a sound pressure level of 143 db, a spectral bandwidth $10 \leq \omega \leq 1110$, and the following beam properties:

$$m = 1.298 \times 10^{-4} \text{ lb. sec}^2/\text{inch}^2$$

$$\omega_1 = 100 \text{ rad/sec.}$$

$$\ell = 20 \text{ inches}$$

Solution: We seek an approximate value for the mean square response

$$\sigma_y^2(x) = \int_0^\infty G_y(x, \omega)\, d\omega \tag{3.1}$$

where

$$G_y(x,\omega) = \sum_j \sum_k \phi_j(x)\, \phi_k(x)\, H_j^*(\omega)\, H_k(\omega)\, G_{jk}(\omega) \tag{3.2}$$

since

$$G_y(x,\omega) = 2\, S_y(x,\omega) \tag{3.3}$$

From the preceeding problem

$$\phi_j(x) = \sin \frac{j\pi x}{\ell}, \qquad j = 1, 2, 3 \ldots$$

$$2 m_j = m\ell \tag{3.4}$$

$$\omega_j^2 = \frac{EI}{m\ell^4} (k_j \ell)^4$$

where

$$k_j \ell = j\pi \tag{3.5}$$

The higher modal frequencies are related to ω_1 by

$$\omega_j = \omega_1 j^2 \tag{3.6}$$

so that $\omega_2/\omega_1 = 4$, $\omega_3/\omega_1 = 9$, $\omega_4/\omega_1 = 16$, etc.

A spectral description of this problem now can be constructed as Figure A.3. The spectrum of the input is a constant over the first three modal frequencies of the system. From Figure 2.3, we find the $j \neq k$ terms can be ignored so that

$$\sigma_y^2(x) = G_0 \sum_j \varphi_j^2(x) \left[\int_0^{\ell} \varphi_j(x)\,dx \right]^2 \int_0^{\omega_c} \left| H_j(\omega) \right|^2 d\omega \tag{3.7}$$

For simple harmonic mode shapes and the use of (2.88) for the finite integral,

$$\sigma_y^2(x) = \frac{16 G_0}{\pi m^2} \sum_{j=1,3} \frac{Q_j}{j^2 \omega_j^3} \sin^2 \frac{j\pi x}{\ell} I_j \tag{3.8}$$

From Figure 2.4, we let $I_j = 1$ for light damping.

Now the pressure field in db, per unit width, is related to G_0 by

$$SPL(db) = 20 \log_{10} \left(\frac{p}{p_0} \right)$$

$$p^2 = G_0 (1110 - 10) \tag{3.9}$$

where p_0 is the rms pressure level 0.0002 dynes/cm^2 (or zero db).

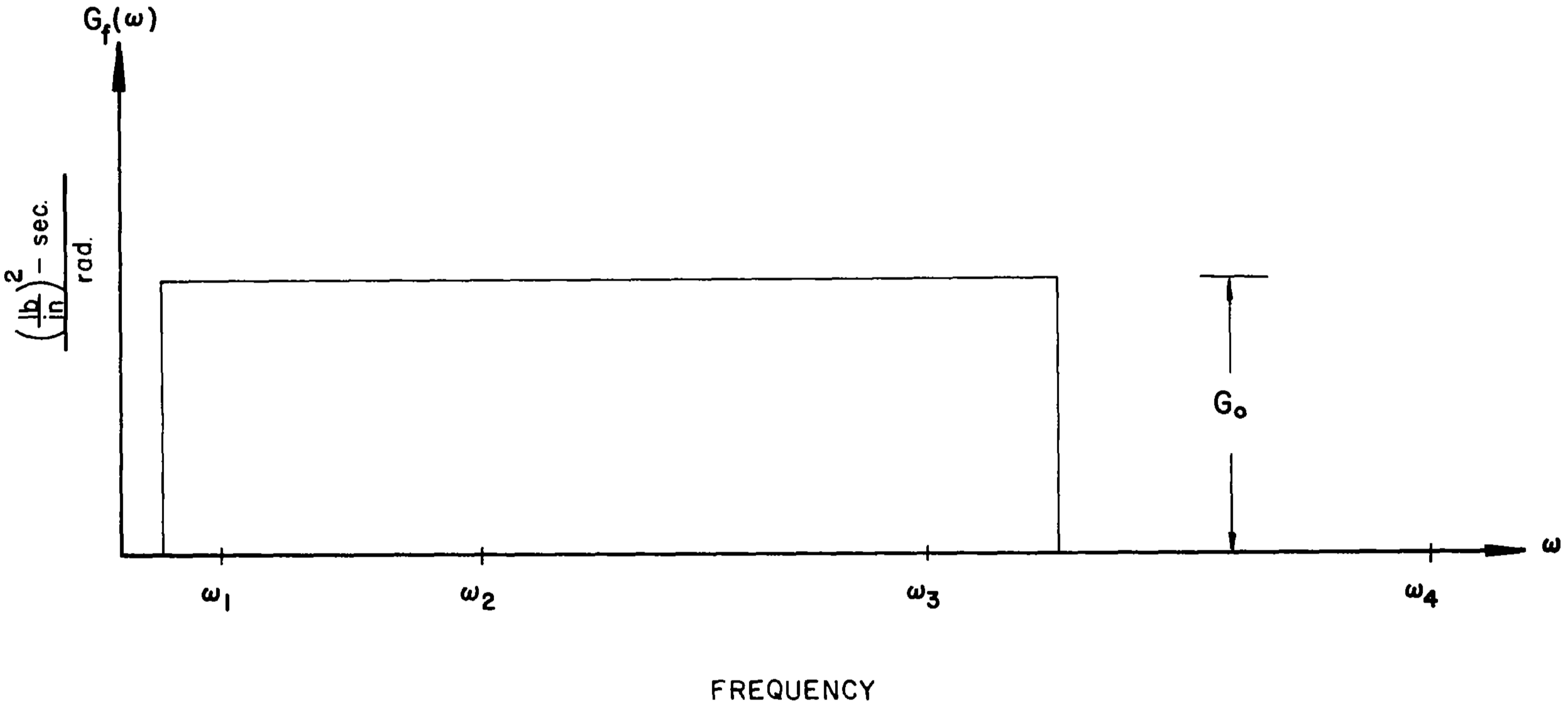

FIGURE A.3 SPECTRAL CHARACTERISTICS OF BEAM PROBLEM

Since 1 dyne/cm^2 = 1.4504×10^{-5} lb/in^2,

$$143 \text{ db} = 20 \log_{10} \left[\frac{(1100\, G_0)^{1/2}}{(2 \times 10^{-4})(1.4504 \times 10^{-5})} \right] \tag{3.10}$$

and

$$G_0 \simeq 1.54 \times 10^{-6} \; \frac{\text{lb}^2\text{-sec}}{\text{in}^2\text{-rad}} \tag{3.11}$$

By assuming $Q_j = 50$, we find at the mid-span that

$$\sigma_y^2\left(\frac{\ell}{2}\right) \simeq 0.0464 \text{ in}^2 \tag{3.12}$$

APPENDIX B

We examine the response characteristics of the three system functions to excitation categorized as a progressive wave field. The mean square response is determined numerically for all system functions; it is determined analytically only for the systems $H_j(\omega)$ and $m_j \omega_j^2 H_j(\omega)$.

The acceptance function for a plane progressive wave may be expressed in the form

$$J_{jk}(\beta) = A_{jk}(\beta)\left[1-(-1)^j \cos \pi\beta\right]; \quad \text{for } j \neq k,\ (j+k) \text{ even}$$

$$= 0; \quad \text{for } j \neq k,\ (j+k) \text{ odd}$$

$$J_j(\beta) = A_j(\beta)\left[1-(-1)^j \cos \pi\beta\right] \tag{B.1}$$

$$A_{jk}(\beta) = \frac{2j^2}{\pi^2(\beta^2-j^2)(\beta^2-k^2)}$$

$$A_j(\beta) = \frac{2j^2}{\pi^2(\beta^2-j^2)^2}$$

$$\beta = \omega t_0$$

$$t_0 = \frac{l \cos\theta}{\pi c}$$

For this acceptance function, it is convenient to express the integral I_{jk} in terms of the normalized frequency parameter, β. Thus,

$$I_{jk} = \frac{\ell^2 S_o}{t_o} \int_{-\infty}^{\infty} A_{jk}(\beta)\, H_{jk}(\beta) \left[1 - (-1)^j \cos \pi\beta\right] d\beta \tag{B.2}$$

where

$$H_{jk}(\beta) = \frac{t_o^4}{m_j m_k (\beta - r_{j1})(\beta - r_{j2})(\beta + r_{j1})(\beta + r_{j2})} \tag{B.3}$$

$$r_{j1} = t_o s_{j1} = t_o(a_j + i b_j) = c_j + i d_j$$

$$r_{j2} = t_o s_{j2} = t_o(-a_j + i b_j) = -c_j + i d_j$$

In order to evaluate this integral, the function $A_{jk}(\beta)H_{jk}(\beta)$ is expanded by partial fractions. Then, I_{jk} can be expressed as the sum of the three separate integrals,

$$I_{jk} = I_{jk}^{(1)} + I_{jk}^{(2)} + I_{jk}^{(3)} \tag{B.4}$$

Each of these integrals is now evaluated separately. The first integral

$$I_{jk}^{(1)} = \frac{\ell^2 S_o}{\pi^2 t_o (j+k)(j-k)} \int_{-\infty}^{\infty} \left[1 - (-1)^j \cos \pi\beta\right] \left[\frac{H_{jk}(j)}{(\beta - j)} - \frac{H_{jk}(-j)}{(\beta + j)}\right] d\beta \tag{B.5}$$

so that

$$I_{jk}^{(1)} = \frac{\ell^2 S_o}{\pi^2 t_o (j+k)(j-k)} \left[H_{jk}(j) \int_{-\infty}^{\infty} \frac{1-(-1)^j \cos \pi\beta}{\beta - j} d\beta \right.$$

$$\left. - H_{jk}(-j) \int_{-\infty}^{\infty} \frac{1-(-1)^j \cos \pi\beta}{\beta + j} d\beta \right] \tag{B. 6}$$

Now by letting $\mu = \beta - j$ in the first integral and $\mu = \beta + j$ in the second integral,

$$I_{jk}^{(1)} = \frac{\ell^2 S_o}{\pi^2 t_o (j+k)(j-k)} \left[H_{jk}(j) - H_{jk}(-j) \right] \int_{-\infty}^{\infty} \frac{1 - \cos u}{u} du \tag{B. 7}$$

This integral is equal to zero so that $I_{jk}^{(1)} = 0$. The second integral $I_{jk}^{(2)}$ is given by

$$I_{jk}^{(2)} = \frac{\ell^2 S_o}{\pi^2 t_o (j+k)(j-k)} \int_{-\infty}^{\infty} \left[1 - (-1)^j \cos \pi\beta \right] \left[\frac{H_{jk}(k)}{(\beta + k)} - \frac{H_{jk}(-k)}{(\beta - k)} \right] d\beta \tag{B. 8}$$

This expression can be reduced to the same form as the first integral; thus $I_{jk}^{(2)} = 0$.

With $I_{jk}^{(1)}$ and $I_{jk}^{(2)}$ both equal to zero,

$$I_{jk} = I_{jk}^{(3)} = \frac{\ell^2 S_o}{t_o} \int_{-\infty}^{\infty} \left[1 - (-1)^j \cos \pi\beta \right] \cdot$$

$$\left[\frac{A_{jk}(r_{j1}) R_1}{(\beta - r_{j1})} + \frac{A_{jk}(r_{j2}) R_2}{(\beta - r_{j2})} + \frac{A_{jk}(-r_{j1}) R_{-1}}{(\beta + r_{j1})} + \frac{A_{jk}(-r_{j2}) R_{-2}}{(\beta + r_{j2})} \right] d\beta \tag{B. 9}$$

where R_1 is the residue of $H_{jk}(\beta)$ at $\beta = r_{j1}$. This integral may be evaluated by using residue theory and complex integration in the upper half of the complex β plane. Since the last two terms in this expression have no poles in the upper half plane, they contribute nothing to the value of the integral. Therefore,

$$I_{jk} = \frac{\ell^2 S_0}{t_0}\Big\{2\pi i\left[A_{jk}(r_{j1})R_1 + A_{jk}(r_{j2})R_2\right] + (-1)^j\left[2\pi\, \mathrm{Im}\left(A_{jk}(r_{j1})R_1 e^{i\pi r_{j1}} + A_{jk}(r_{j2})R_2 e^{i\pi r_{j2}}\right)\right]\Big\} \tag{B. 10}$$

Since r_{j2} is the complex conjugate of r_{j1} ($r_{j2} = r_{j1}^*$),

$$\begin{aligned} A_{jk}(r_{j2}) &= A_{jk}^*(r_{j1}) \\ R_2 &= -R_1^* \end{aligned} \tag{B. 11}$$

and the I_{jk} integral reduces to

$$I_{jk} = -\frac{4\pi \ell^2 S_0}{t_0}\left[\mathrm{Im}\left(A_{jk}(r_{j1})R_1\right) - (-1)^j\, \mathrm{Im}\left(A_{jk}(r_{j1})R_1 e^{i\pi r_{j1}}\right)\right] \tag{B. 12}$$

After much complex algebra, the results may be expressed for $j \neq k$.

$$I_{jk} = \frac{4\ell^2 S_o\, i k\, t_o^2}{\pi m_j m_k a_j B_{jk} D_j D_k} \Big[Q_{jk}\left(1-(-1)^j e^{-\pi d_j}\cos \pi c_j\right) \tag{B. 13}$$

$$+ (-1)^j P_{jk} e^{-\pi d_j} \sin \pi c_j \Big]$$

where

$$Q_{jk} = 2c_j \Big\{ \Big[b_j(3c_j^4 - 10c_j^2 d_j^2 + 3d_j^4) + (c_j^4 - 10c_j^2 d_j^2 + 5d_j^4)d_k - 2d_j(c_j^2 - d_k^2)\eta_k^2 \Big]$$
$$- \Big[2d_j(c_j^2 - d_j^2) + (c_j^2 - 3d_j^2)d_k - d_j\eta_k^2 \Big](j^2 + k^2) + (d_j + d_k) j^2 k^2 \Big\}$$

$$P_{jk} = \Big\{ \Big[(c_j^2 - d_j^2)(c_j^4 - 14c_j^2 d_j^2 + d_j^4) - 2d_j(5c_j^4 - 10c_j^2 d_j^2 + d_j^4)d_k - (c_j^4 - 6c_j^2 d_j^2 + d_j^4)\eta_k^2 \Big] \tag{B. 14}$$
$$- \Big[(c_j^4 - 6c_j^2 d_j^2 + d_j^4) - 2(3c_j^2 - d_j^2)d_j d_k - (c_j^2 - d_j^2)\eta_k^2 \Big](j^2 + k^2)$$
$$+ \Big[c_j^2 - d_j^2 - 2d_j d_k - \eta_k^2 \Big] j^2 k^2 \Big\}$$

$$B_{jk} = (c_j^2 - c_k^2)^2 + 2(c_j^2 + c_k^2)(d_j + d_k)^2 + (d_j + d_k)^4$$

$$D_j = \omega_j^4 - 2(c_j^2 - d_j^2) j^2 + j^4, \quad D_k = \omega_j^4 - 2(c_j^2 - d_j^2)k^2 + k^4$$

$$\eta_k = t_o \omega_k$$

For $j = k$, the integral becomes

$$I_j = \frac{\ell^2 S_o}{t_o} \int_{-\infty}^{\infty} \left[1 - (-1)^j \cos \pi\beta\right] A_j(\beta)\, H_j(\beta)\, d\beta \tag{B. 15}$$

where

$$H_j(\beta) = \frac{t_o^4}{m_j^2 \left[(\beta^2 - \eta_j^2)^2 + 4 d_j^2 \beta^2\right]} \tag{B. 16}$$

$$\eta_j = t_o \omega_j$$

This integral can be expressed as the sum of three integrals by a partial fraction expansion of $A_j(\beta)\, H_j(\beta)$; thus

$$I_j = I_j^{(1)} + I_j^{(2)} + I_j^{(3)} \tag{B. 17}$$

The first integral is of the form

$$I_j^{(1)} = \frac{\ell^2 S_o}{2\pi^2 t_o\, m} \int_{-\infty}^{\infty} \left[1 - (-1)^j \cos \pi\beta\right] \left[\frac{R_j}{(\beta - j)} - \frac{R_{-j}}{(\beta + j)}\right] d\beta \tag{B. 18}$$

This expression reduces as

$$I_j^{(1)} = \frac{\ell^2 S_o}{2\pi^2 t_o m}(R_j + R_{-j}) \int_{-\infty}^{\infty} \frac{1-\cos \pi u}{u}\, du = 0 \qquad \text{(B.19)}$$

The second integral is

$$I_j^{(2)} = \frac{\ell^2 S_o}{2\pi^2 t_o} \int_{-\infty}^{\infty} \left[1-(-1)^j \cos \pi\beta\right] \left[\frac{H_j(i)}{(\beta-j)^2} + \frac{H_j(-i)}{(\beta+j)^2}\right] d\beta \qquad \text{(B.20)}$$

so that

$$I_j^{(2)} = \frac{\ell^2 S_o}{\pi^2 t_o} H_j(i) \left[\int_{-\infty}^{\infty} \frac{1-\cos \pi u}{u^2}\, du\right]$$

$$= \frac{\ell^2 S_o}{\pi^2 t_o} H_j(j)\left[\pi^2\right] \qquad \text{(B.21)}$$

By Equation (B.16),

$$I_j^{(2)} = \frac{\ell^2 S_o t_o^3}{m_j^2 \left[(j^2-\eta^2)^2 + 4 d_j^2 j^2\right]} \qquad \text{(B.22)}$$

The third integral $I_j^{(3)} = I_{jk}^{(3)}$ with j = k; thus the integral I_j can be determined from Equations (B.13) and (B.22) evaluated at j = k.

After much algebra,

$$I_j = \frac{4\ell^2 S_o j^2 t_o^2}{\pi m_j^2 c_j B_j D_j^2}\Big[Q_j\left(1-(-1)^j e^{-\pi d_j}\cos\pi c_j\right)$$

$$-(-1)^j P_j\, e^{-\pi d_j}\sin\pi c_j\Big] \qquad \text{(B. 23)}$$

$$+\frac{\ell^2 S_o t_o^3}{m_j^2}\left[\frac{1}{(j^2-\eta_j^2)^2+4\,d_j^2 j^2}\right]$$

where

$$Q_j = c_j d_j\left[(c_j^4-10c_j^2d_j^2+5d_j^4)-2(c_j^2-3d_j^2)j^2+j^4\right]$$

$$P_j = d_j^2\left[(5c_j^4-10c_j^2d_j^2+5d_j^4)-2(3c_j^2-d_j^2)j^2+j^4\right]$$

$$B_j = 4\,d_j^2\eta_j^2 \qquad \text{(B. 24)}$$

$$D_j = \eta_j^4-2(c_j^2-d_j^2)j^2+j^4$$

$$\eta_j = t_o\omega_j$$

The mean square response is then

$$\sigma_y^2(x) = \sum_j \sum_k \phi_j(x)\, \phi_k(x)\, I_{jk} \qquad \text{(B. 25)}$$

and for harmonic modes

$$\sigma_y^2(x) = \sum_j \sin^2 \frac{j\pi x}{\ell}\, I_j + 2 \sum_j \sum_{k=j+1} \sin \frac{j\pi x}{\ell} \sin \frac{k\pi x}{\ell}\, I_{jk} \qquad \text{(B. 26)}$$

We note that $I_{jk} = 0$ for $j \neq k$ and $j + k$ odd. For the numerical integration, it is convenient to express the integrals I_j and I_{jk} in the form

$$C_1 I_j = \int_0^\infty R_j^{(1)}(\beta)\, J_j(\beta)\, d\beta$$

$$C_1 I_{jk} = \int_0^\infty R_{jk}^{(1)}(\beta)\, J_{jk}(\beta)\, d\beta \qquad \text{(B. 27)}$$

where $R_{jk}^{(1)}(\beta)$, $J_{jk}(\beta)$ and C_1 are as defined in the text.

For all results, $\mu = 1$ and $\zeta_j = \zeta = 0.025$; Figures B. 1 through B. 5 show a normalized form of the response spectral densities for the system functions $H_j(\omega)$, $m_j \omega_j^2 H_j(\omega)$ and $m_j \omega^2 H_j(\omega)$. Tables B-1 and B-2 show the main diagonal contributions (for the first ten modes) obtained by numerical integration and by an evaluation of the closed form results, respectively. Similarly, Tables B-3 and B-4 provide the integral results for $j = 1, 3. . . 9$ and $k = 1, 2, . . . 9$. Figure B. 6, repeated in the text as Figure 3. 35, displays the mean square response for all system functions over $0 \leq x/\ell \leq .5$. These results correspond to the analytical results for the first two systems; the last system $m_j \omega^2 H_j(\omega)$ was not evaluated in closed form.

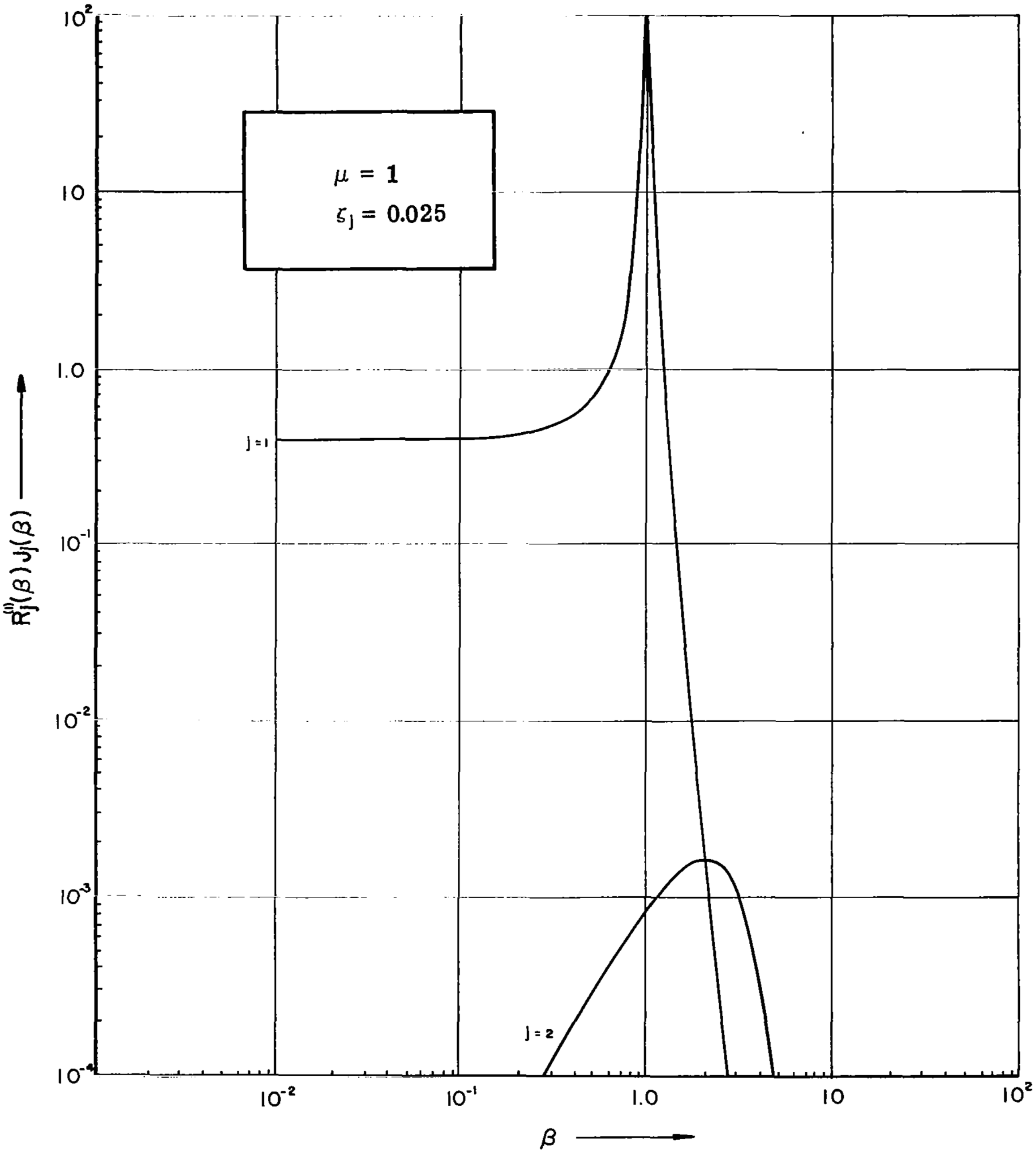

FIGURE B.1 INTEGRAND FOR $|H_j(\omega)|^2$ AND THE PROGRESSIVE WAVE

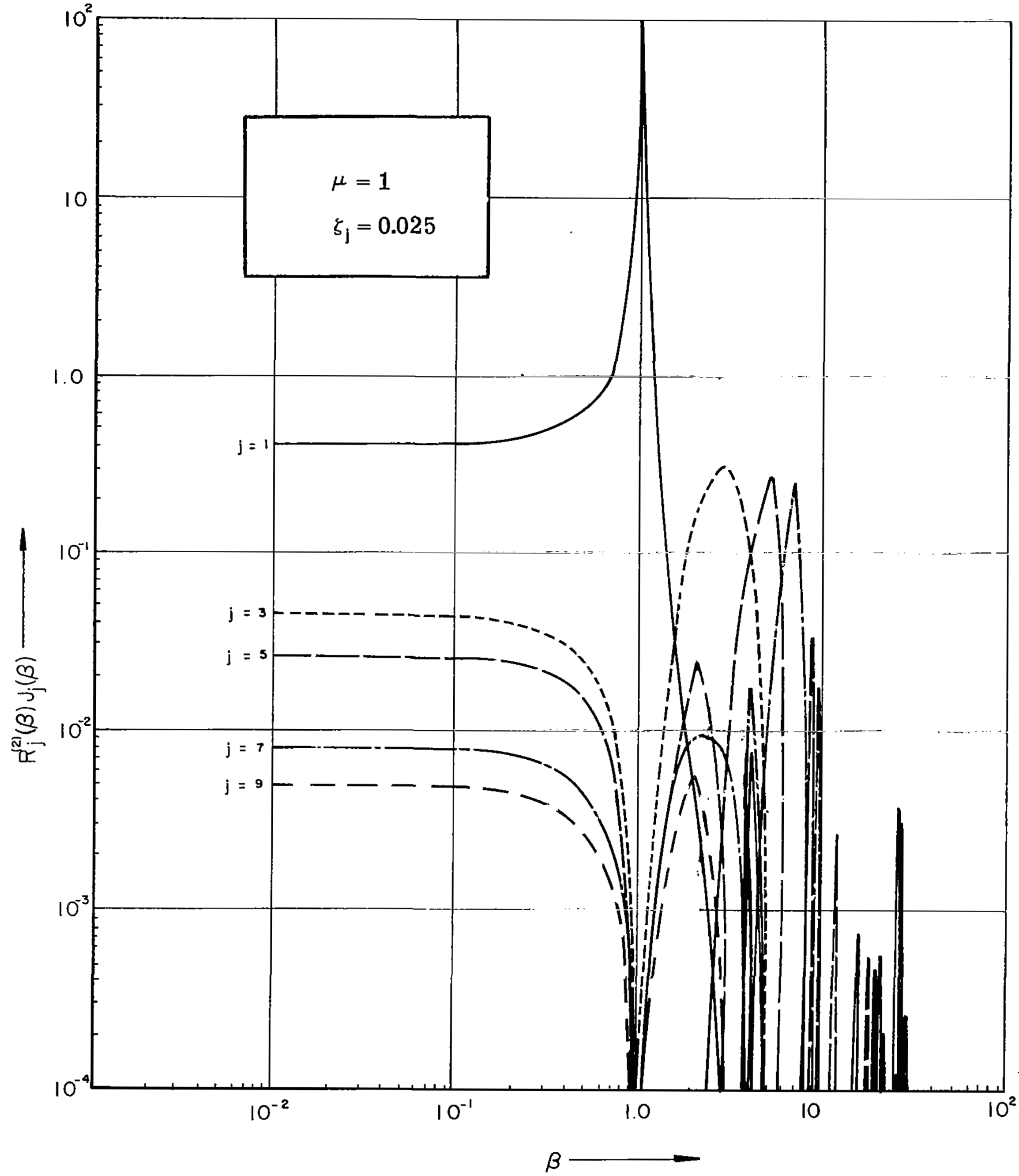

FIGURE B.2 INTEGRAND FOR $\left|m_j \omega_j^2 H_j(\omega)\right|^2$ AND THE PROGRESSIVE WAVE (ODD TERMS ONLY)

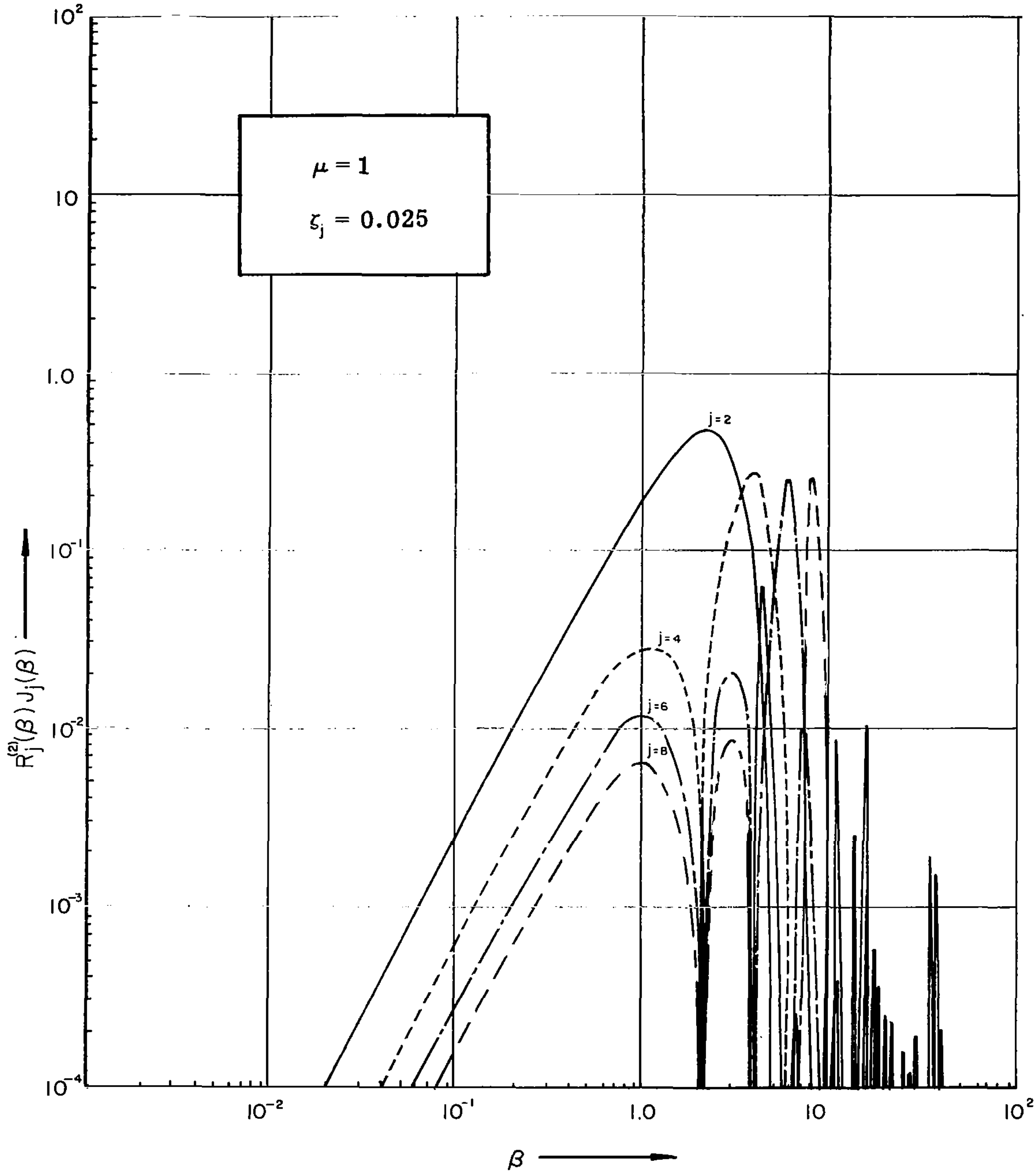

FIGURE B.3 INTEGRAND FOR $\left| m_j \omega_j^2 H(\omega) \right|^2$ AND THE PROGRESSIVE WAVE (EVEN TERMS ONLY)

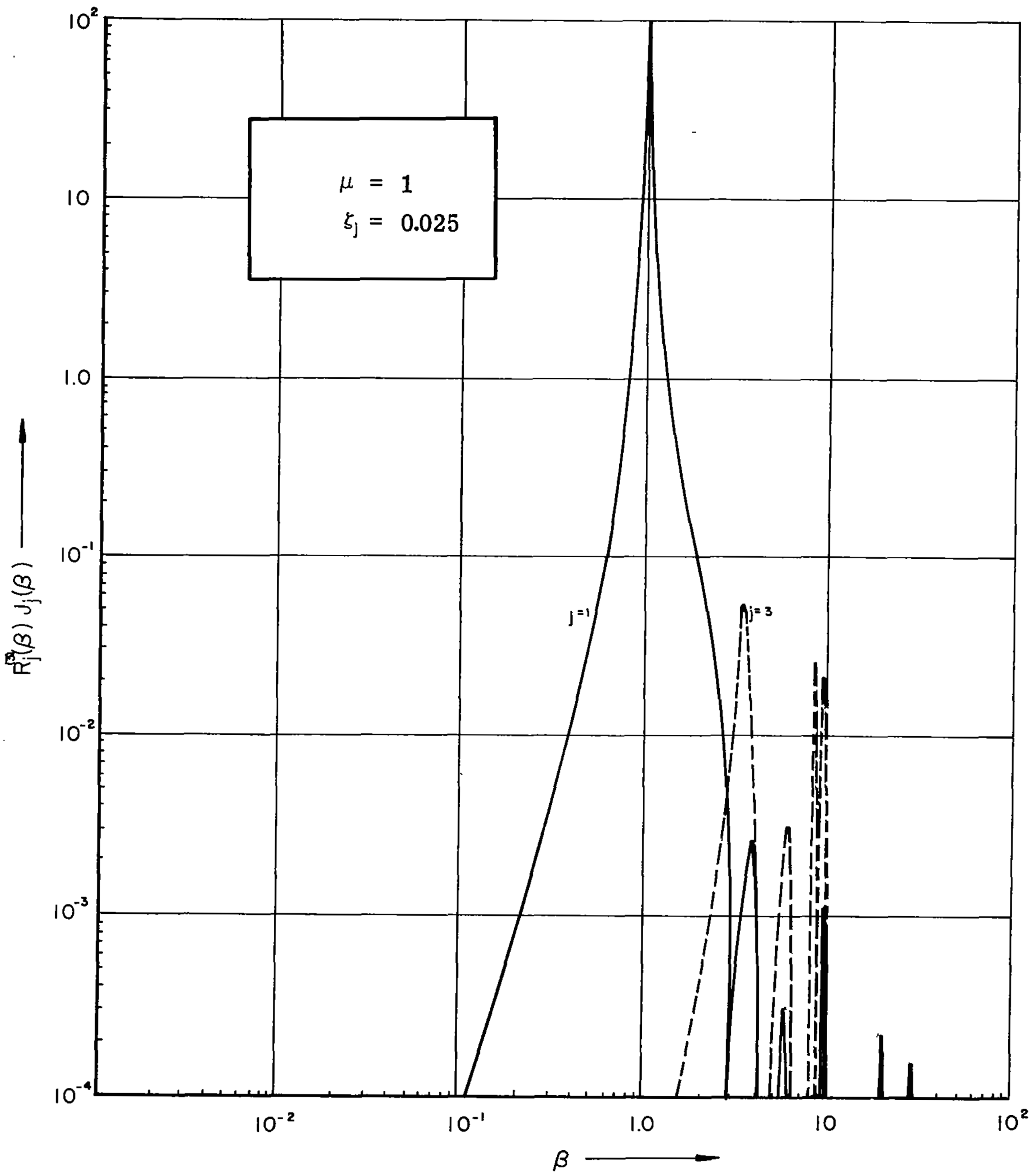

FIGURE B.4 INTEGRAND FOR $|m_j \omega^2 H_j(\omega)|^2$ AND THE PROGRESSIVE WAVE (ODD TERMS ONLY)

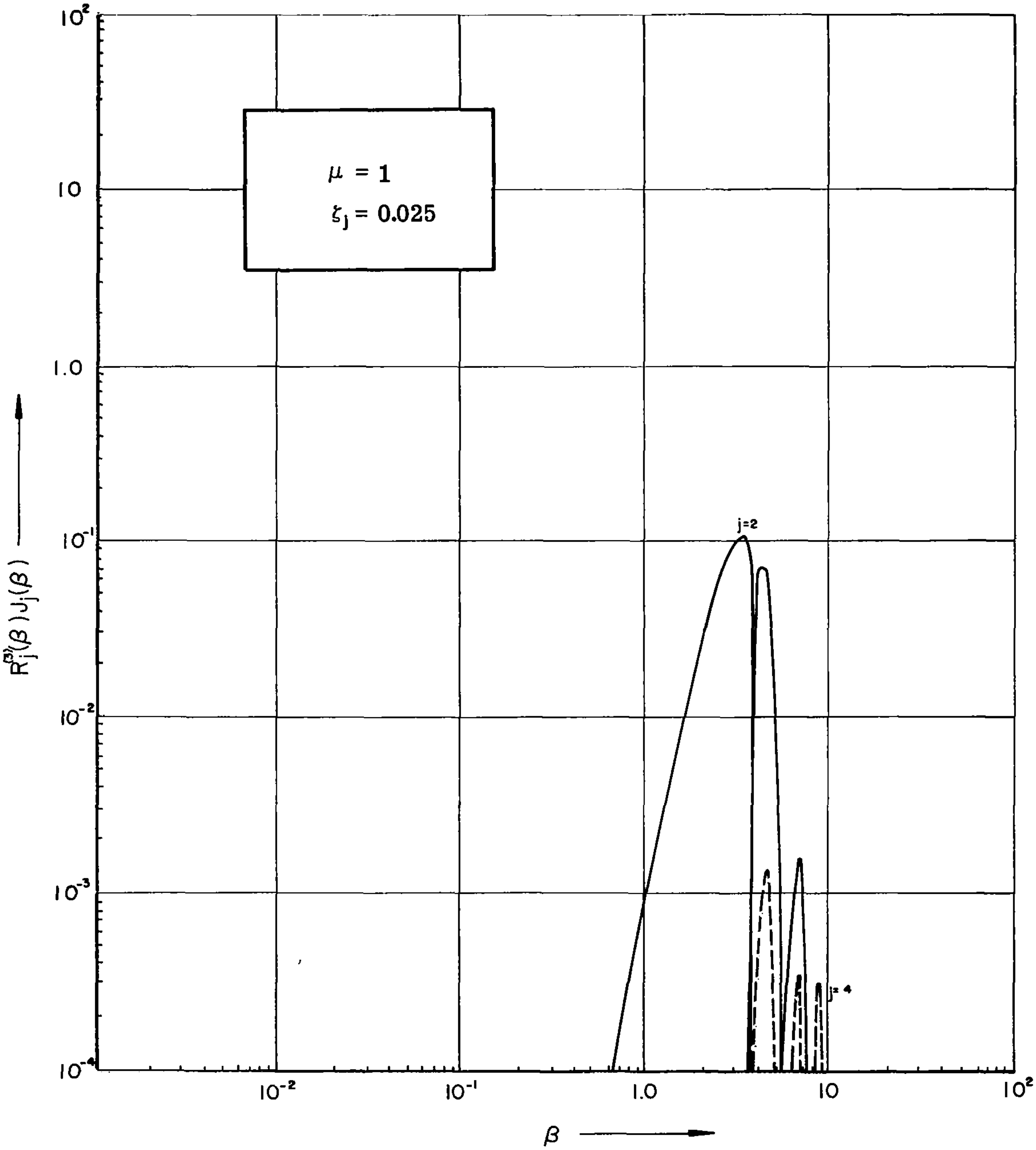

FIGURE B.5 INTEGRAND FOR $|m_j\omega^2 H_j(\omega)|^2$ AND THE PROGRESSIVE WAVE (EVEN TERMS ONLY)

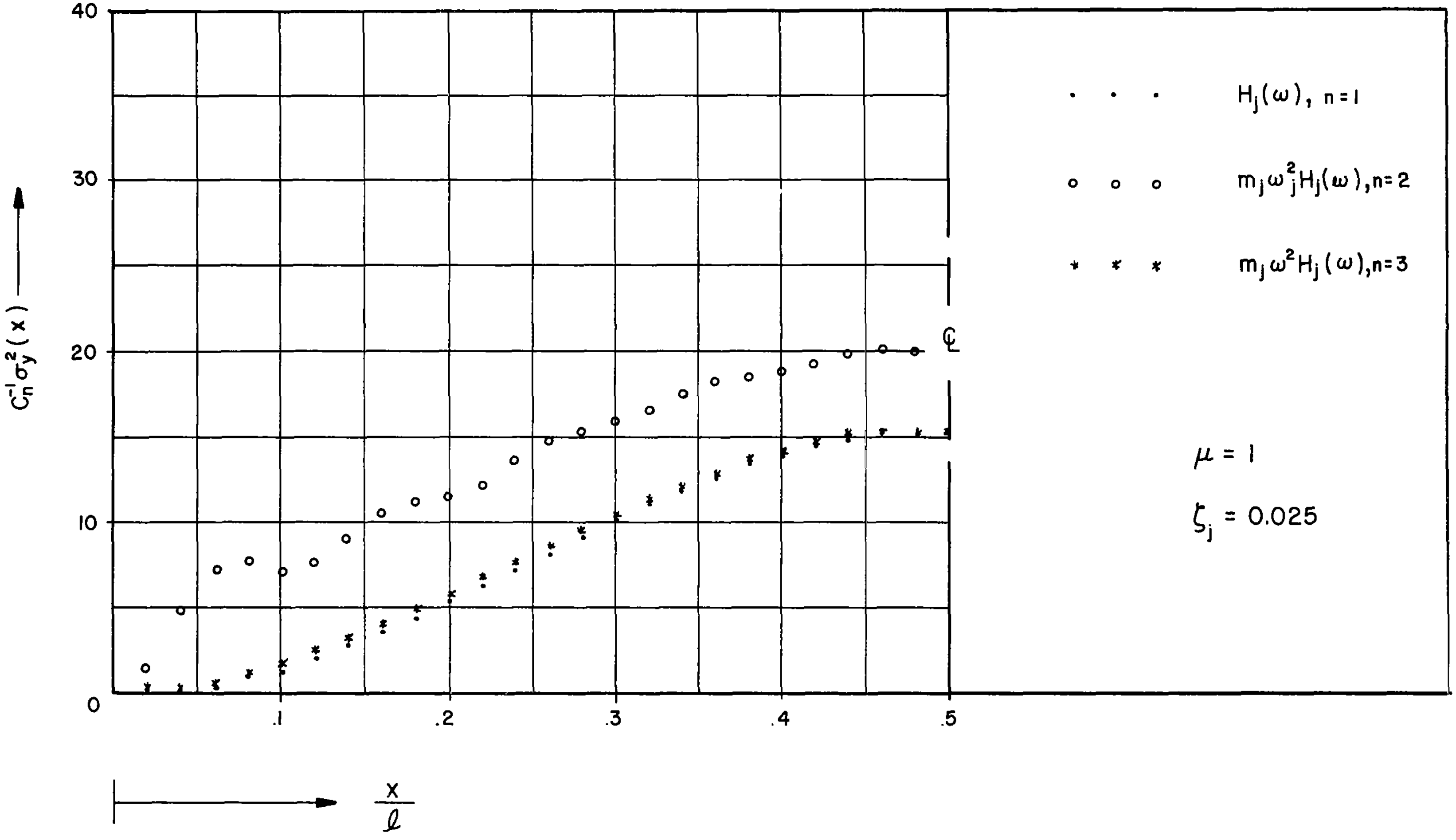

FIGURE B.6 MEAN SQUARE RESPONSE TO THE PROGRESSIVE WAVE FIELD (NUMERICAL INTEGRATION OF INTEGRAND)

SYSTEM $\mu=1$, $\zeta_j = 0.025$		$\lvert H_j(\omega)\rvert^2$, n=1	$\lvert m_j\omega_j^2 H_j(\omega)\rvert^2$, n=2	$\lvert m_j\omega^2 H_j(\omega)\rvert^2$, n=3
$\int_0^\infty R_j^{(n)}(\beta)\ J_j(\beta)\ d\beta$	j = 1	7.712	7.712	7.629
	j = 2	4.204 (-3)	1.076	2.457 (-1)
	j = 3	1.043 (-4)	.6844	5.843 (-2)
	j = 4	8.981 (-6)	.5886	2.221 (-2)
	j = 5	1.415 (-6)	.5529	1.047 (-2)
	j = 6	3.176 (-7)	.5335	5.023 (-3)
	j = 7	9.099 (-8)	.5245	2.869 (-3)
	j = 8	3.085 (-8)	.5176	1.701 (-3)
	j = 9	1.198 (-8)	.5165	1.053 (-3)
	j = 10	4.143 (-9)	.5144	7.291 (-4)

TABLE B-1 MAIN DIAGONAL CONTRIBUTIONS TO THE MEAN SQUARE RESPONSE (PROGRESSIVE WAVE — NUMERICAL INTEGRATION OF INTEGRAND)

SYSTEM $\mu = 1,\ \zeta_j = 0.025$		$\lvert H_j(\omega)\rvert^2_{,n=1}$	$\lvert m_j\omega_j^2 H_j(\omega)\rvert^2_{,n=2}$	$\lvert m_j\omega^2 H_j(\omega)\rvert^2_{,n=3}$
$\int_0^\infty R_j^{(m)}(\beta)\ J_j(\beta)\ d\beta$	j = 1	8.236	8.236	
	j = 2	4.205 (-3)	1.076	INTEGRAL NOT EVALUATED
	j = 3	1.040 (-4)	0.6826	
	j = 4	8.986 (-6)	0.5889	
	j = 5	1.413 (-6)	0.5519	
	j = 6	3.178 (-7)	0.5338	
	j = 7	9.085 (-8)	0.5237	
	j = 8	3.085 (-8)	0.5175	
	j = 9	1.193 (-8)	0.5135	
	j = 10	5.107 (-9)	0.5107	

TABLE B-2 MAIN DIAGONAL CONTRIBUTIONS TO THE MEAN SQUARE RESPONSE (PROGRESSIVE WAVE — CLOSED FORM RESULTS)

k ↓ / j →	SYSTEM: $H_j(\omega) H_k(\omega)$, $\mu = 1, \zeta_j = 0.025$				$\int_0^\infty R^{(1)}_{jk}(\beta)\, J_{jk}(\beta)\, d\beta$				
	1	2	3	4	5	6	7	8	9
1	7.712	0	2.272(-3)	0	1.623(-4)	0	2.957(-5)	0	8.445(-6)
2	0	4.204(-3)	0	-7.422(-5)	0	9.350(-9)	0	6.779(-8)	0
3		0	1.043(-4)	0	6.052(-9)	0	-8.916(-9)	0	-2.555(-7)
4	0		0	8.981(-6)	0	-3.391(-10)	0	-4.210(-9)	0
5		0		0	1.415(-6)	0	5.982(-10)	0	2.977(-10)
6	0		0		0	3.176(-7)	0	1.247(-12)	0
7		0		0		0	9.089(-8)	0	1.114(-10)
8	0		0		0		0	3.085(-8)	0
9		0		0		0		0	1.198(-8)

TABLE B-3.1 INTEGRAL CONTRIBUTIONS TO THE MEAN SQUARE RESPONSE

(PROGRESSIVE WAVE — NUMERICAL INTEGRATION OF INTEGRAND)

k ↓ / j →	SYSTEM: $m_j m_k \omega_j^2 \omega_k^2 H_j(\omega) H_k(\omega)$, $\mu = 1$, $\zeta_j = 0.025$				$\int_0^\infty R^{(2)}_{jk}(\beta)\, J_{jk}(\beta)\, d\beta$				
	1	2	3	4	5	6	7	8	9
1	7.712	0	0.1840	0	0.1015	0	7.098 (-2)	0	5.476 (-2)
2	0	1.076	0	-0.3040	0	1.969 (-4)	0	3.654 (-4)	0
3		0	0.6844	0	3.065 (-4)	0	-1.724 (-3)	0	0.1368
4	0		0	0.5886	0	-1.125 (-4)	0	-2.467 (-4)	0
5		0		0	0.5529	0	8.972 (-4)	0	1.223-3
6	0		0		0	0.5335	0	-6.111 (-6)	0
7		0		0		0	0.5245	0	1.755 (-3)
8	0		0		0		0	0.5176	0
9		0		0		0		0	0.5165

TABLE B-3.2 INTEGRAL CONTRIBUTIONS TO THE MEAN SQUARE RESPONSE

(PROGRESSIVE WAVE – NUMERICAL INTEGRATION OF INTEGRAND)

k \ j →	SYSTEM: $m_j m_k \omega^4 H_j(\omega) H_k(\omega)$, $\mu = 1$, $\zeta_j = 0.025$					$\int_0^\infty R^{(3)}_{jk}(\beta)\, J_{jk}(\beta)\, d\beta$			
	1	2	3	4	5	6	7	8	9
1	7.629	0	2.277(-4)	0	1.569(-4)	0	2.311(-5)	0	3.867(-6)
2	0	0.2457	0	-1.899(-2)	0	-1.621(-5)	0	-2.797(-6)	0
3		0	5.843(-2)	0	-2.757(-5)	0	-6.221(-5)	0	-1.704(-3)
4	0		0	2.212(-2)	0	2.887(-5)	0	-4.290(-7)	0
5		0		0	1.047(-2)	0	1.408(-6)	0	-6.547(-6)
6	0		0		0	5.023(-3)	0	1.441(-5)	0
7		0		0		0	2.869(-3)	0	1.088(-5)
8	0		0		0		0	1.701(-3)	0
9		0		0		0		0	1.053(-3)

TABLE B-3.3 INTEGRAL CONTRIBUTIONS TO THE MEAN SQUARE RESPONSE

(PROGRESSIVE WAVE – NUMERICAL INTEGRATION OF INTEGRAND)

k ↓ / j →	SYSTEM:	$H_j(\omega)\,H_k^*(\omega)$,	$\mu = 1$, $\zeta_j = 0.025$			$\int_0^\infty R_{jk}^{(1)}(\beta)\, J_{jk}(\beta)\, d\beta$			
	1	2	3	4	5	6	7	8	9
1	8.236	0	1.502(-3)	0	6.419(-5)	0	8.345(-6)	0	1.832(-6)
2	0	4.205(-3)	0	-7.423(-5)	0	-5.480(-9)	0	2.620(-9)	0
3		0	1.040(-4)	0	-1.347(-8)	0	-9.726(-9)	0	-1.703(-7)
4	0		0	8.986(-6)	0	-5.406(-10)	0	-2.493(-10)	0
5		0		0	1.413(-6)	0	-4.479(-11)	0	-2.346(-11)
6	0		0		0	3.178(-7)	0	-5.181(-12)	0
7		0		0		0	9.085(-8)	0	-6.968(-13)
8	0		0		0		0	3.085(-8)	0
9		0		0		0		0	1.193(-8)

TABLE B-4.1 INTEGRAL CONTRIBUTIONS TO THE MEAN SQUARE RESPONSE

(PROGRESSIVE WAVE — CLOSED FORM RESULTS)

k ↓ / j →	SYSTEM: $m_j m_k \omega_j^2 \omega_k^2 H_j(\omega) H_k^*(\omega)$,				$\mu = 1$, $\zeta_j = 0.025$	$\int_0^\infty R_{jk}^{(2)}(\beta)\, J_{jk}(\beta)\, d\beta$			
	1	2	3	4	5	6	7	8	9
1	8.326	0	0.1216	0	4.012(-2)	0	2.004(-2)	0	1.202(-2)
2	0	1.076	0	-0.3041	0	1.136(-4)	0	1.722(-4)	0
3		0	0.6826	0	-6.814(-4)	0	-1.892(-3)	0	-9.048(-2)
4	0		0	0.5889	0	-1.794(-4)	0	-2.614(-4)	0
5		0		0	0.5519	0	-6.721(-5)	0	-9.621(-5)
6	0		0		0	0.5338	0	-2.750(-5)	0
7		0		0		0	0.5237	0	-1.098(-5)
8	0		0		0		0	0.5175	0
9		0		0		0		0	0.5135

TABLE B-4.2 INTEGRAL CONTRIBUTIONS TO THE MEAN SQUARE RESPONSE

(PROGRESSIVE WAVE — CLOSED FORM RESULTS)

APPENDIX C

Shown are numerical values of the integral

$$\int_{0}^{\infty} R_{jk}^{(n)}(\beta)\, J_{jk}(\beta)\, d\beta$$

where the indices vary as $j = 1, 2, 3, \ldots 9$ and $k = 1, 2, 3, \ldots 9$; the superscript n varies as $n = 1, 2, 3$. The excitations are those for the reverberant field and turbulence only. For all cases, the system parameters $\mu = 1$ and $\zeta = 0.025$.

k ↓ / j →	SYSTEM: $H_j^*(\omega)\,H_k(\omega)$,	$\mu = 1$, $\zeta_j = 0.025$			$\int_0^\infty R^{(1)}_{jk}(\beta)\,J_{jk}(\beta)\,d\beta$				
	1	2	3	4	5	6	7	8	9
1	8.9581	0	1.111(-3)	0	9.314(-5)	0	1.874(-5)	0	5.482(-6)
2	0	6.094(-2)	0	1.756(-5)	0	2.595(-6)	0	6.563(-7)	0
3		0	2.423(-3)	0	1.312(-6)	0	2.723(-7)	0	8.297(-8)
4	0		0	2.506(-4)	0	1.439(-7)	0	3.679(-8)	0
5		0		0	4.192(-5)	0	2.915(-8)	0	9.090(-9)
6	0		0		0	9.891(-6)	0	6.642(-9)	0
7		0		0		0	2.860(-6)	0	2.088(-9)
8	0		0		0		0	9.834(-7)	0
9		0		0		0		0	3.808(-7)

TABLE C-1.1 INTEGRAL CONTRIBUTIONS TO THE MEAN SQUARE RESPONSE

(REVERBERANT FIELD — NUMERICAL INTEGRATION OF INTEGRAND)

k ↓ / j →	SYSTEM: $m_j m_k \omega_j^2 \omega_k^2 H_j^*(\omega) H_k(\omega)$, $\mu = 1$, $\zeta_j = 0.025$				$\int_0^\infty R_{jk}^{(2)}(\beta)\, J_{jk}(\beta)\, d\beta$				
	1	2	3	4	5	6	7	8	9
1	8.9581	0	8.094(-2)	0	6.003(-2)	0	4.497(-2)	0	3.598(-2)
2	0	15.606	0	7.192(-2)	0	5.380(-2)	0	4.301(-2)	0
3		0	16.020	0	6.642(-2)	0	5.296(-2)	0	1.137(-2)
4	0		0	16.423	0	4.778(-2)	0	3.937(-2)	0
5		0		0	16.376	0	4.384(-2)	0	3.727(-2)
6	0		0		0	16.613	0	3.426(-2)	0
7		0		0		0	16.493	0	3.289(-2)
8	0		0		0		0	16.499	0
9		0		0		0		0	16.394

TABLE C-1.2 INTEGRAL CONTRIBUTIONS TO THE MEAN SQUARE RESPONSE

(REVERBERANT FIELD — NUMERICAL INTEGRATION OF INTEGRAND)

k ↓ / j →	SYSTEM: $m_j m_k \omega^4 H_j^*(\omega) H_k(\omega)$, $\mu = 1$, $\zeta_j = 0.025$				$\int_0^\infty R_{jk}^{(3)}(\beta)\, J_{jk}(\beta)\, d\beta$				
	1	2	3	4	5	6	7	8	9
1	13.128	0	-5.640(-4)	0	-3.124(-4)	0	-3.001(-4)	0	-2.845(-4)
2	0	16.959	0	-6.420(-4)	0	-6.254(-4)	0	-4.877(-4)	0
3		0	16.697	0	-3.727(-4)	0	-6.768(-4)	0	-7.010(-4)
4	0		0	16.591	0	-6.843(-4)	0	-7.607(-4)	0
5		0		0	16.251	0	-6.943(-4)	0	-9.204(-4)
6	0		0		0	16.056	0	-6.290(-4)	0
7		0		0		0	15.675	0	-9.464(-4)
8	0		0		0		0	15.371	0
9		0		0		0		0	14.831

TABLE C-1.3 INTEGRAL CONTRIBUTIONS TO THE MEAN SQUARE RESPONSE

(REVERBERANT FIELD – NUMERICAL INTEGRATION OF INTEGRAND)

k ↓ / j →	SYSTEM: $H_j^*(\omega)\,H_k(\omega)$, $\mu = 1$, $\zeta_j = 0.025$				$\int_0^\infty R^{(1)}_{jk}(\beta)\,J_{jk}(\beta)\,d\beta$; $J_{jk} = J_I(\beta)$ for j odd, $J_{jk} = J_{II}(\beta)$ for j even				
	1	2	3	4	5	6	7	8	9
1	12.642	0	3.862(-4)	0	7.911(-5)	0	3.331(-5)	0	8.762(-6)
2	0	7.774(-2)	0	1.258(-7)	0	2.731(-6)	0	1.240(-6)	0
3		0	1.058(-2)	0	4.501(-5)	0	1.288(-5)	0	4.843(-6)
4	0		0	7.302(-4)	0	5.260(-6)	0	1.814(-6)	0
5		0		0	1.482(-4)	0	3.754(-6)	0	1.383(-6)
6	0		0		0	2.371(-5)	0	6.946(-7)	0
7		0		0		0	6.465(-6)	0	4.335(-7)
8	0		0		0		0	1.636(-6)	0
9		0		0		0		0	5.603(-7)

TABLE C-2.1 INTEGRAL CONTRIBUTIONS TO THE MEAN SQUARE RESPONSE

(REVERBERANT FIELD – NUMERICAL INTEGRATION OF FILTER APPROXIMATION)

k ↓ / j →	1	2	3	4	5	6	7	8	9
	SYSTEM: $m_j m_k \omega_j^2 \omega_k^2 H_j^*(\omega) H_k(\omega)$,	$\mu = 1$ $\zeta_j = 0.025$				$\int_0^\infty R_{jk}^{(2)}(\beta)\, J_{jk}(\beta)\, d\beta$;	$J_{jk} = J_I(\beta)$ for j odd $J_{jk} = J_{II}(\beta)$ for j even		
1	12.642	0	3.131(-2)	0	4.938(-2)	0	5.591(-2)	0	5.742(-2)
2	0	19.201	0	7.191 (-4)	0	5.647 (-2)	0	8.124(-2)	0
3		0	69.704	0	2.282	0	2.506	0	2.574
4	0		0	47.955	0	1.744	0	1.902	0
5		0		0	59.601	0	5.631	0	5.666
6	0		0		0	39.913	0	3.687	0
7		0		0		0	37.273	0	6.825
8	0		0		0		0	27.449	0
9		0		0		0		0	25.927

TABLE C-2.2 INTEGRAL CONTRIBUTIONS TO THE MEAN SQUARE RESPONSE

(REVERBERANT FIELD – NUMERICAL INTEGRATION OF FILTER APPROXIMATION)

k ↓ / j →	SYSTEM: $m_j m_k \omega^4 H_j^*(\omega) H_k(\omega)$, $\mu = 1$, $\zeta_j = 0.025$					$\int_0^\infty R_{jk}^{(3)}(\beta) J_{jk}(\beta) d\beta$; $J_{jk} = J_I(\beta)$ for j odd, $J_{jk} = J_{II}(\beta)$ for j even			
	1	2	3	4	5	6	7	8	9
1	26.096	0	3.858	0	0.7699	0	-0.2229	0	-0.5654
2	0	23.739	0	1.865	0	0.2264	0	-0.3048	0
3		0	70.966	0	0.4269	0	9.183 (-2)	0	-0.6132
4	0		0	47.801	0	1.260 (-2)	0	-0.4106	0
5		0		0	52.910	0	-0.3649	0	-0.6611
6	0		0		0	36.448	0	-0.3417	0
7		0		0		0	30.260	0	-0.5374
8	0		0		0		0	22.847	0
9		0		0		0		0	18.199

TABLE C-2.3 INTEGRAL CONTRIBUTIONS TO THE MEAN SQUARE RESPONSE

(REVERBERANT FIELD – NUMERICAL INTEGRATION OF FILTER APPROXIMATION)

k ↓ / j →	SYSTEM: $H_j^*(\omega)\, H_k(\omega)$, $\mu = 1$, $\zeta_j = 0.025$				$\int_0^\infty R^{(1)}_{jk}(\beta)\, J_{jk}(\beta)\, d\beta$; $J_{jk} = J_I(\beta)$ for j odd, $J_{jk} = J_{II}(\beta)$ for j even				
	1	2	3	4	5	6	7	8	9
1	12.361	0	3.474(-4)	0	7.495(-5)	0	2.181(-5)		
2	0	7.758(-2)	0	1.857(-7)	0	2.891(-6)	0	1.272(-6)	0
3		0	1.061(-2)	0	4.640(-5)	0	1.322(-5)	0	4.958(-6)
4	0		0	7.197(-4)	0	5.115(-6)	0	1.755(-6)	0
5		0		0	1.474(-4)	0	3.775(-6)	0	1.387(-6)
6	0		0		0	2.344(-5)	0	6.642(-7)	0
7		0		0		0	6.434(-6)	0	4.265(-7)
8	0		0		0		0	1.636(-6)	0
9		0		0		0		0	6.034(-7)

TABLE C-3.1 INTEGRAL CONTRIBUTIONS TO THE MEAN SQUARE RESPONSE (REVERBERANT FIELD - FILTER APPROXIMATION IN CLOSED FORM)

k ↓ / j →	SYSTEM: $m_j m_k \omega_j^2 \omega_k^2 H_j(\omega) H_k^*(\omega)$, $\mu = 1$, $\zeta_j = 0.025$				$\int_0^\infty R_{jk}^{(2)}(\beta) J_{jk}(\beta) d\beta$; $J_{jk} = J_I(\beta)$ for j odd, $J_{jk} = J_{II}(\beta)$ for j even			
	1	2	3	4	5	6	7	8	9
1	12.361	0	2.814(-2)	0	4.684(-2)	0	5.237(-2)	0	5.378(-2)
2	0	19.860	0	7.605(-4)	0	5.996(-2)	0	8.336(-2)	0
3		0	69.616	0	2.349	0	2.570	0	2.635
4	0		0	47.168	0	1.697	0	1.840	0
5		0		0	87.564	0	5.665	0	5.687
6	0		0		0	39.373	0	3.526	0
7		0		0		0	37.077	0	6.718
8	0		0		0		0	27.450	0
9		0		0		0		0	25.913

TABLE C-3.2 INTEGRAL CONTRIBUTIONS TO THE MEAN SQUARE RESPONSE

(REVERBERANT FIELD – FILTER APPROXIMATION IN CLOSED FORM)

SYSTEM: $m_j m_k \omega^4 H_j^*(\omega) H_k(\omega)$, $\mu = 1$, $\zeta_j = 0.025$

$\int_0^\infty R_{jk}^{(3)}(\beta)\, J_{jk}(\beta)\, d\beta$; $J_{jk} = J_I(\beta)$ for j odd, $J_{jk} = J_{II}(\beta)$ for j even

k ↓ / j →	1	2	3	4	5	6	7	8	9
1	19.247	0	0.5789	0	0.1214	0	3.406(-2)	0	1.270(-2)
2	0	24.106	0	0.2143	0	5.053(-2)	0	1.694(-2)	0
3		0	71.126	0	5.626(-2)	0	1.561(-2)	0	5.817(-3)
4	0		0	47.832	0	1.497(-2)	0	4.588(-3)	0
5		0		0	52.998	0	6.082(-3)	0	1.872(-3)
6	0		0		0	36.594	0	4.025(-3)	0
7		0		0		0	30.821	0	3.488(-3)
8	0		0		0		0	23.568	0
9		0		0		0		0	19.253

TABLE C-3.3 INTEGRAL CONTRIBUTIONS TO THE MEAN SQUARE RESPONSE (REVERBERANT FIELD — FILTER APPROXIMATION IN CLOSED FORM)

SYSTEM: $H_j^*(\omega)\,H_k(\omega)$, $\mu = 1.$, $\zeta_j = 0.025$, $\ell/\delta_b = 30$ $\int_0^\infty R^{(1)}_{jk}(\beta)\, J_{jk}(\beta)\, d\beta$

k ↓ / j →	1	2	3	4	5	6	7	8	9
1	3.037	0	7.432(-5)	0	7.052(-6)	0	1.362(-6)	0	3.895(-7)
2	0	2.329(-2)	0	2.044(-6)	0	6.264(-7)	0	1.984(-7)	0
3		0	7.038(-4)	0	-1.197(-7)	0	-4.558(-8)	0	-1.122(-8)
4	0		0	5.917(-5)	0	-1.115(-8)	0	2.920(-9)	0
5		0		0	7.066(-6)	0	7.670(-10)	0	1.414(-10)
6	0		0		0	1.391(-6)	0	2.060(-11)	0
7		0		0		0	3.653(-7)	0	7.539(-11)
8	0		0		0		0	1.170(-7)	0
9		0		0		0		0	4.310(-8)

TABLE C-4.1 INTEGRAL CONTRIBUTIONS TO THE MEAN SQUARE RESPONSE

(TURBULENCE – NUMERICAL INTEGRATION OF INTEGRAND)

k ↓ / j →	SYSTEM : $m_j m_k \omega_j^2 \omega_k^2 H_j^*(\omega) H_k(\omega)$, $\mu = 1$, $\zeta_j = 0.025$, $\ell/\delta_b = 30$					$\int_0^\infty R^{(2)}_{jk}(\beta)\, J_{jk}(\beta)\, d\beta$			
	1	2	3	4	5	6	7	8	9
1	3.037	0	6.034(-3)	0	4.409(-3)	0	5.074(-3)	0	2.562(-3)
2	0	5.961	0	8.374(-3)	0	12.991(-3)	0	12.994(-3)	0
3		0	4.607	0	-7.071(-3)	0	-8.859(-3)	0	-5.959(-3)
4	0		0	3.878	0	-1.772(-3)	0	-3.050(-3)	0
5		0		0	2.788	0	-2.141(-3)	0	-0.580(-3)
6	0		0		0	2.337	0	0.111(-3)	0
7		0		0		0	2.106	0	1.187(-3)
8	0		0		0		0	1.962	0
9		0		0		0		0	1.856

TABLE C-4.2 INTEGRAL CONTRIBUTIONS TO THE MEAN SQUARE RESPONSE

(TURBULENCE – NUMERICAL INTEGRATION OF INTEGRAND)

SYSTEM: $m_j m_k \omega^4 H_j^*(\omega) H_k(\omega)$, $\mu = 1, \zeta_j = 0.025$, $\ell/\delta_b = 30$ $\int_0^\infty R_{jk}^{(3)}(\beta)\, J_{jk}(\beta)\, d\beta$

k ↓ / j →	1	2	3	4	5	6	7	8	9
1	3.459	0	1.280(-3)	0	1.246(-4)	0	2.660(-5)	0	8.219(-6)
2	0	6.028	0	8.693(-4)	0	2.355(-4)	0	7.505(-5)	0
3		0	4.283	0	-6.227(-4)	0	-4.800(-4)	0	-7.853(-5)
4	0		0	3.502	0	-2.516(-4)	0	-1.273(-4)	0
5		0		0	2.243	0	-8.651(-5)	0	-5.614(-5)
6	0		0		0	1.807	0	-3.222(-5)	0
7		0		0		0	1.561	0	-1.594(-5)
8	0		0		0		0	1.399	0
9		0		0		0		0	1.264

TABLE C-4.3 INTEGRAL CONTRIBUTIONS TO THE MEAN SQUARE RESPONSE

(TURBULENCE – NUMERICAL INTEGRATION OF INTEGRAND)

k ↓ / j →	SYSTEM:	$H_j^*(\omega)\,H_k(\omega)$,	$\mu=1$, $\zeta_j = 0.025$, $\ell/\delta_b = 30$			$\int_0^\infty R_{jk}^{(1)}(\beta)\,J_I(\beta)\,d\beta$			
	1	2	3	4	5	6	7	8	9
1	3.692	0	2.239(-4)	0	3.891(-5)	0	1.072(-5)	0	3.951(-6)
2	0	4.427(-2)	0	5.887(-5)	0	1.328(-5)	0	4.310(-6)	0
3		0	2.151(-3)	0	1.412(-5)	0	3.326(-6)	0	1.425(-6)
4	0		0	1.822(-4)	0	3.318(-6)	0	1.063(-6)	0
5		0		0	2.296(-5)	0	8.300(-7)	0	3.039(-7)
6	0		0		0	4.245(-6)	0	2.566(-7)	0
7		0		0		0	9.831(-7)	0	8.783(-8)
8	0		0		0		0	2.825(-7)	0
9		0		0		0		0	9.322(-8)

TABLE C-5.1 INTEGRAL CONTRIBUTIONS TO THE MEAN SQUARE RESPONSE

(TURBULENCE — NUMERICAL INTEGRATION OF FILTER APPROXIMATION)

SYSTEM: $m_j m_k \omega_j^2 \omega_k^2 H_j^*(\omega) H_k(\omega)$, $\mu=1$, $\zeta_j = 0.025$, $\ell/\delta_b = 30$

$\int_0^\infty R_{jk}^{(2)}(\beta)\, J_1(\beta)\, d\beta$

k ↓ / j →	1	2	3	4	5	6	7	8	9
1	3.592	0	1.815(-2)	0	2.430(-2)	0	2.583(-2)	0	2.593(-2)
2	0	11.238	0	0.2416	0	0.2755	0	0.2825	0
3		0	14.194	0	0.7158	0	0.7482	0	0.6970
4	0		0	12.039	0	1.102	0	1.115	0
5		0		0	9.107	0	1.246	0	1.246
6	0		0		0	7.130	0	1.362	0
7		0		0		0	5.667	0	1.383
8	0		0		0		0	4.705	0
9		0		0		0		0	4.031

TABLE C-5.2 INTEGRAL CONTRIBUTIONS TO THE MEAN SQUARE RESPONSE

(TURBULENCE – NUMERICAL INTEGRATION OF FILTER APPROXIMATION)

k ↓ / j →	SYSTEM: $m_j m_k \omega^4 H_j^*(\omega) H_k(\omega)$, $\mu=1$, $\zeta_j = 0.025$, $\ell/\delta_b = 30$				$\int_0^\infty R_{jk}^{(3)}(\beta) J_I(\beta) d\beta$				
	1	2	3	4	5	6	7	8	9
1	4.772	0	0.5389	0	6.579(-2)	0	-4.487(-2)	0	-8.319(-2)
2	0	12.073	0	0.1458	0	-3.363(-2)	0	-6.624(-2)	0
3		0	13.977	0	0.1079	0	-6.111(-2)	0	-8.958(-2)
4	0		0	11.109	0	4.812(-2)	0	-7.401(-2)	0
5		0		0	7.922	0	-5.431(-2)	0	-9.258(-2)
6	0		0		0	5.760	0	-5.023(-2)	0
7		0		0		0	4.250	0	-7.386(-2)
8	0		0		0		0	3.249	0
9		0		0		0		0	2.514

TABLE C-5.3 INTEGRAL CONTRIBUTIONS TO THE MEAN SQUARE RESPONSE

(TURBULENCE – NUMERICAL INTEGRATION OF FILTER APPROXIMATION)

k ↓ / j →	SYSTEM: $H_j^*(\omega)\,H_k(\omega)$, $\mu = 1$, $\zeta_j = 0.025$, $\ell/\delta_b = 30$				$\int_0^\infty R^{(1)}_{jk}(\beta)\, J_z(\beta)\, d\bar{\beta}$				
	1	2	3	4	5	6	7	8	9
1	3.483	0	1.767(-4)	0	3.280(-5)	0	9.035(-6)	0	3.347(-6)
2	0	4.410(-2)	0	5.828(-5)	0	1.310(-5)	0	4.247(-6)	0
3		0	2.160(-3)	0	1.432(-5)	0	3.895(-6)	0	1.442(-6)
4	0		0	1.807(-4)	0	3.247(-6)	0	1.039(-6)	0
5		0		0	2.317(-5)	0	8.302(-7)	0	3.030(-7)
6	0		0		0	4.177(-6)	0	2.494(-7)	0
7		0		0		0	9.773(-7)	0	8.647(-8)
8	0		0		0		0	2.792(-7)	0
9		0		0		0		0	9.323(-8)

TABLE C-6.1 INTEGRAL CONTRIBUTIONS TO THE MEAN SQUARE RESPONSE

(TURBULENCE - FILTER APPROXIMATION IN CLOSED FORM)

k ↓ / j →	SYSTEM: $m_j m_k \omega_j^2 \omega_k^2 H_j^*(\omega) H_k(\omega)$, $\mu = 1, \zeta_j = 0.025$, $\ell/\delta_b = 30$					$\int_0^\infty R_{jk}^{(2)}(\beta) J_I(\beta) d\beta$			
	1	2	3	4	5	6	7	8	9
1	3.483	0	1.431(-2)	0	2.050(-2)	0	2.169(-2)	0	2.196(-2)
2	0	11.289	0	0.2347	0	0.2715	0	0.2783	0
3		0	14.175	0	0.7250	0	0.7576	0	0.7661
4	0		0	11.842	0	1.077	0	1.089	0
5		0		0	9.051	0	1.246	0	1.242
6	0		0		0	7.016	0	1.324	0
7		0		0		0	5.634	0	1.362
8	0		0		0		0	4.684	0
9		0		0		0		0	4.013

TABLE C-6.2 INTEGRAL CONTRIBUTIONS TO THE MEAN SQUARE RESPONSE

(TURBULENCE – FILTER APPROXIMATION IN CLOSED FORM)

$k \downarrow$ / $j \rightarrow$	SYSTEM: $m_j m_k \omega^4 H_j^*(\omega) H_k(\omega)$, $\mu = 1$, $\ell/\delta_b = 30$				$\int_0^\infty R_{jk}(\beta)\, J_I(\beta)\, d\beta$				
	1	2	3	4	5	6	7	8	9
1	4.821	0	4.187	0	1.167	0	0.3502	0	0.1329
2	0	12.080	0	2.379	0	0.8334	0	0.3049	0
3		0	13.987	0	0.7456	0	0.2225	0	8.438(-2)
4	0		0	11.024	0	0.6140	0	0.2050	0
5		0		0	7.982	0	7.937(-2)	0	2.716(-2)
6	0		0		0	5.777	0	0.2684	0
7		0		0		0	4.333	0	2.954(-2)
8	0		0		0		0	3.352	0
9		0		0		0		0	2.663

TABLE C-6.3 INTEGRAL CONTRIBUTIONS TO THE MEAN SQUARE RESPONSE

(TURBULENCE — FILTER APPROXIMATION IN CLOSED FORM)

APPENDIX D

TABLE OF SELECTED INTEGRALS

This table of integrals is a partial list of integrals encountered in using a frequency domain approach to determine the mean square response of single degree of freedom systems to random excitation. In most instances, the integrand is written in terms of a basic system frequency response function, $H(\omega)$, and a spectral density function, $S(\omega)$, both defined as follows:

$H(\omega)$ = basic system frequency response function

$$H(\omega) = \frac{1}{(\omega_o^2 - \omega^2) + i2\zeta\omega_o\omega}$$

$$H(\omega) = -\frac{1}{(\omega - s_1)(\omega - s_2)}$$

$$s_1 = a + ib = -s_2^*$$

$$a = \omega_o\sqrt{1 - \zeta^2}$$

$$b = \omega_o\zeta$$

$$\omega_o^2 = a^2 + b^2$$

$H^*(\omega)$ = conjugate of $H(\omega)$

$$\left|H(\omega)\right|^2 = H(\omega)\ H^*(\omega) = \frac{1}{(\omega^2 - s_1^2)\ (\omega^2 - s_2^2)}$$

$H_j(\omega)$ = system frequency response function at the modal frequency ω_j

$$H_j(\omega) = \frac{1}{(\omega_j^2 - \omega^2) + i\ 2\ \zeta_j\ \omega_j\ \omega}$$

$$H_j(\omega) = - \frac{1}{(\omega - s_{j1})\ (\omega - s_{j2})}$$

$$s_{j1} = a_j + i\ b_j = - s_{j2}^*$$

$$a_j = \omega_j \sqrt{1 - \zeta_j^2}$$

$$b_j = \omega_j\ \zeta_j$$

$$\omega_j^2 = a_j^2 + b_j^2$$

$S(\omega)$ = spectral density function

$$S(\omega) = \frac{\alpha\,(\rho^2 + \alpha^2 + \omega^2)}{\pi\,(\omega^2 - s_3^2)\,(\omega^2 - s_4^3)}$$

$$s_3 = \rho + i\alpha = -s_4^*$$

Note: $$S(\omega) = \frac{1}{2\pi}\int_{-\infty}^{\infty}\left(e^{-\alpha|\tau|}\cos\rho\tau\right)e^{i\omega\tau}\,d\tau$$

$U(t)$ = unit step function

$$U(t) = \begin{cases} 0 & t < 0 \\ 1/2 & t = 0 \\ 1 & t > 0 \end{cases}$$

$\delta(t)$ = unit impulse function, defined by the integral

$$\int_{-\infty}^{\infty} \delta(t - t_o)\, f(t)dt = f(t_o)$$

TABLE OF INTEGRALS

$$(1)\quad \int_{-\infty}^{\infty} \frac{e^{i\omega t}}{\omega - s_1}\, d\omega = 2\pi i \; e^{is_1 t}\, U(t)$$

$$= 2\pi i \; e^{-bt}(\cos at + \sin at)U(t)$$

$$(2)\quad \int_{-\infty}^{\infty} \left[\frac{1}{(\omega - s_1)(\omega' - s_2)} - \frac{1}{(\omega - s_2)(\omega' - s_1)} \right] e^{i\omega' t}\, d\omega' = -2\pi i H(\omega)\, e^{-bt}\left(\cos\, at + \frac{b+i\omega}{a} \sin\, at\right) U(t)$$

$$(3)\quad \int_{-\infty}^{\infty} \left[\pi\delta(\omega' - \omega) + \frac{1}{i(\omega' - \omega)} \right] e^{i\omega' t}\, d\omega' = 2\pi\, e^{i\omega t}\, U(t)$$

$$(4)\quad \int_{-\infty}^{\infty} H(\omega)\, e^{i\omega t}\, d\omega = \frac{2\pi}{a}\, e^{-bt} \sin\, at\, U(t)$$

$$(5)\quad \int_{-\infty}^{\infty} H(\omega') \left[\pi\delta(\omega' - \omega) + \frac{1}{i(\omega' - \omega)} \right] e^{i\omega' t}\, d\omega' = 2\pi H(\omega) \left[e^{i\omega t} - e^{-bt}\left(\cos\, at + \frac{b+i\omega}{a} \sin\, at\right) \right] U(t)$$

$$(6)\quad \int_{-\infty}^{\infty} \left|H(\omega)\right|^2 d\omega = \frac{\pi}{2b\omega_o^2}$$

$$(7)\quad \int_{-\infty}^{\infty} \omega^2 \left|H(\omega)\right|^2 d\omega = \frac{\pi}{2b}$$

$$(8)\quad \int_{-\infty}^{\infty} (b^2 - a^2 + \omega^2) \left|H(\omega)\right|^2 d\omega = \frac{\pi b}{\omega_o^2}$$

$$(9)\quad \int_{-\infty}^{\infty} \omega^4 \left|H(\omega)\right|^2 d\omega = \frac{\pi}{2b} (a^2 - 3b^2)$$

$$(10)\quad \int_{-\infty}^{\infty} \left(C \cos \omega t + \frac{\omega}{a} D \sin \omega t\right) \left|H(\omega)\right|^2 d\omega = \frac{\pi}{2ab\omega_o^2} e^{-bt} \left[a C \cos at + \left(bC + \frac{\omega_o^2}{a^2} D\right) \sin at\right] U(t)$$

$$(11)\quad \int_{-\infty}^{\infty} H(\omega + \omega_e) H^*(\omega - \omega_e)\, d\omega = \frac{\pi}{2(b + i\omega_e)(\omega_o^2 - \omega_e^2 + i2b\omega_e)}$$

$$(12)\quad \int_{-\infty}^{\infty} \frac{b^2 - a^2 - \omega_e^2 + \omega^2}{a^2}\, H(\omega + \omega_e)\, H^*(\omega - \omega_e)\, d\omega = \frac{\pi\,(b^2 - \omega_e^2 + i2b\omega_e)}{a^2\,(b + i\omega_e)\,(\omega_o^2 - \omega_e^2 + i2b\omega_e)}$$

$$(13)\quad \int_{-\infty}^{\infty} \left(C \cos \omega t + \frac{\omega}{a} D \sin \omega t\right) H(\omega + \omega_e)\, H^*(\omega - \omega_e)\, d\omega$$

$$= \frac{\pi}{2a(b + i\omega_e)}\, e^{-(b + i\omega_e)t} \left[\frac{D}{a} \sin a t + C\, \frac{a \cos a t + (b + i\omega_e) \sin a t}{\omega_o^2 - \omega_e^2 + i2b\omega_e}\right]$$

$$(14)\quad \int_{-\infty}^{\infty} \left| H(\omega + i\alpha) \right| d\omega = \begin{cases} \dfrac{\pi}{2\,(b - \alpha)\left[a^2 + (b - \alpha)^2\right]} & \alpha < b \\ \infty & \alpha = b \\ \dfrac{\pi}{2\,(\alpha - b)\left[a^2 + (\alpha - b)^2\right]} & \alpha > b \end{cases}$$

$$(15)\quad \int_{-\infty}^{\infty} \frac{b^2 - a^2 + \alpha^2 + \omega^2}{a^2} \left| H(\omega + i\alpha) \right|^2 d\omega = \begin{cases} \dfrac{\pi}{a^2(b - \alpha)} \left[\dfrac{b^2 + \alpha^2 - b\alpha}{a^2 + (b - \alpha)^2}\right] & \alpha < b \\ \infty & \alpha = b \\ \dfrac{\pi}{a^2\,(\alpha - b)} \left[\dfrac{b^2 + \alpha^2 - b\alpha}{a^2 + (\alpha - b)^2}\right] & \alpha > b \end{cases}$$

(16) $$\int_{-\infty}^{\infty} \left(C \cos \omega t + \frac{\omega}{a} D \sin \omega t\right) \left|H(\omega + i\alpha)\right|^{2} d\omega$$

$$= \begin{cases} \dfrac{\pi e^{-(b-\alpha)t}}{2(b-\alpha)\left[a^{2} + (b-\alpha)^{2}\right]} \left[C\left(\cos at + \dfrac{b-\alpha}{a} \sin at\right) + D \dfrac{a^{2} + (b-\alpha)^{2}}{a^{2}} \sin at\right] & \alpha < b \\ \infty & \alpha = b \\ \dfrac{\pi e^{(b-\alpha)t}}{2(\alpha-b)\left[a^{2} + (\alpha-b)^{2}\right]} \left[C\left(\cos at + \dfrac{\alpha-b}{a} \sin at\right) + D \dfrac{a^{2} + (\alpha-b)^{2}}{a^{2}} \sin at\right] & \alpha > b \end{cases}$$

(17) $$\int_{-\infty}^{\infty} S(\omega) \left|H(\omega)\right|^{2} d\omega = \frac{a}{2b} R_1 + R_3 \quad \text{for } s_1 \neq s_3$$

where: $$R_1 = \operatorname{Re} \left\{ \frac{\alpha (s_1^2 + \alpha^2 + \rho^2)}{a^2 s_1 (s_1^2 - s_3^2)(s_1^2 - s_4^2)} \right\}$$

$$R_3 = \operatorname{Re} \left\{ \frac{1}{(s_3^2 - s_1^2)(s_3^2 - s_2^2)} \right\}$$

$$(18) \qquad \int_{\infty}^{\infty} \frac{b^2 - a^2 + \omega^2}{a^2} S(\omega) \left| H(\omega) \right|^2 d\omega = -X_1 + \frac{b^2 - a^2 + \rho^2 - \alpha^2}{a^2} R_3 - \frac{2\rho\alpha}{a^2} X_3 \qquad \text{for } s_1 \neq s_3$$

$$\text{where:} \quad X_1 = \text{Im} \left\{ \frac{\alpha(s_1^2 + \alpha^2 + \rho^2)}{a^2 s_1 (s_1^2 - s_3^2)(s_1^2 - s_4^2)} \right\}$$

$$X_3 = \text{Im} \left\{ \frac{1}{(s_3^2 - s_1^2)(s_3^2 - s_2^2)} \right\} \qquad \left[\text{See (17) for } R_3\right]$$

$$(19) \qquad \int_{\infty}^{\infty} (C \cos \omega t + \frac{\omega}{a} D \sin \omega t) S(\omega) \left| H(\omega) \right|^2 d\omega = \frac{a}{2b} e^{-bt} \left\{ R_1 \left[(C + \frac{b}{a} D) \cos at + D \sin at \right] \right.$$

$$\left. + X_1 \left[D \cos at - (C + \frac{b}{a} D) \sin at \right] \right\} + e^{-\alpha t} \left\{ R_3 \left[(C + \frac{\alpha}{a} D) \cos \rho t + \frac{\rho}{a} D \sin \rho t \right] \right.$$

$$\left. + X_3 \left[\frac{\rho}{a} D \cos \rho t - (C + \frac{\alpha}{a} D) \sin \rho t \right] \right\} \qquad \text{for } s_1 \neq s_3$$

$$\left[\text{See (17), (18) for } R_1, R_3, X_1, X_3\right]$$

For $s_1 = s_3$ ($a = \rho$ and $\alpha = b$) the integrals (17), (18) and (19) reduce to equations (20), (21) and (22) respectively.

$$\int_{-\infty}^{\infty} \frac{b(\omega^2 + \omega_o^2)}{\pi} \left|H(\omega)\right|^4 d\omega = \frac{a^2 + 3b^2}{8b^2\omega_o^4} \tag{20}$$

$$\int_{-\infty}^{\infty} \frac{b(b^2 - a^2 + \omega^2)}{\pi a^2} (\omega^2 + \omega_o^2) \left|H(\omega)\right|^4 d\omega = \frac{b^2}{2a^2\omega_o^4} \tag{21}$$

$$\frac{b}{\pi}\int_{-\infty}^{\infty} \left(C\cos\omega t + \frac{\omega}{a} D \sin\omega t\right)(\omega^2 + \omega_o^2) \left|H(\omega)\right|^4 d\omega = \frac{1}{2\omega_o^2} e^{-bt} \left[\frac{C}{b^2}\left(\frac{a^2 + 3b^2}{\omega_o^2} + bt\right)\cos at + \frac{C}{ab}\left(\frac{2b^2}{\omega_o^2} + bt\right)\sin at + \frac{\omega_o^2}{a^2b^2} D(1 + bt)\sin at\right] \tag{22}$$

$$\int_{-\infty}^{\infty} H_j(\omega) H_k^*(\omega)\, d\omega = \frac{4\pi(b_j + b_k)}{(a_j^2 - a_k^2)^2 + 2(a_j^2 + a_k^2)(b_j + b_k)^2 + (b_j + b_k)^4} \tag{23}$$

(24)
$$\int_{-\infty}^{\infty} \frac{1}{\omega^2 + q^2} \, H_j(\omega) \, H_k^*(\omega) \, d\omega$$

$$= \frac{4\pi}{\omega_j^2 - 2b_j q + q^2} \left\{ \frac{b_j \left[a_j^2 - a_k^2 - (b_j + b_k)^2 \right] + (b_j + b_k)(a_j^2 - b_j^2 + q^2)}{(\omega_j^2 + 2b_j q + q^2) \left[(a_j^2 - a_k^2)^2 + 2(a_j^2 + a_k^2)(b_j + b_k)^2 + (b_j + b_k)^4 \right]} \right.$$

$$+ \frac{1}{4q(\omega_k^2 + 2b_k q + q^2)}$$

(25)
$$\int_{-\infty}^{\infty} \frac{1}{\omega^2 + q^2} \left| H(\omega) \right|^2 d\omega = \frac{\pi}{2b\omega_o^2 q} \left[\frac{q(a^2 - 3b^2 + q^2) + 2b\omega_o^2}{\omega_o^4 + 2(a^2 - b^2)q^2 + q^4} \right]$$

(26)
$$\int_{-\infty}^{\infty} \omega^2 \, H_j(\omega) H_k^*(\omega) \, d\omega = 4\pi \left[\frac{b_j a_k^2 + b_k a_j^2 + b_j b_k (b_j + b_k)}{(a_j^2 - a_k^2)^2 + 2(a_j^2 + a_k^2)(b_j + b_k)^2 + (b_j + b_k)^4} \right]$$

(27)
$$\int_{-\infty}^{\infty} \omega^4 H_j(\omega) \, H_k^*(\omega) d\omega = 4\pi \left[\frac{2a_k^2 b_j (a_j^2 - b_j^2) + a_j^4 (b_k - b_j) - 2a_j^2 \, b_j (b_j^2 + b_j b_k - b_k^2) - b_j^3 \, (b_j + b_k)(b_j + 2b_k)}{(a_j^2 - a_k^2)^2 + 2(a_j^2 + a_k^2)(b_j + b_k)^2 + (b_j + b_k)^4} \right]$$

(28) $$\int_{-\infty}^{\infty} \frac{\omega^2}{\omega^4 + 2\rho^2 q^2 + q^4}\, H_j(\omega)\, H_k^*(\omega)\, d\omega$$

$$= \frac{4\pi}{c_j}\left[\frac{b_j(\omega_j^4 - q^4)\left[a_j^2 - a_k^2 - (b_j+b_k)^2\right] + (b_j+b_k)\ (a_j^2 - b_j^2)(\omega_j^4+q^4)+2\,\omega_j^4 p^2}{(a_j^2 - a_k^2)^2 + 2(a_j^2 + a_k^2)(b_j + b_k)^2 + (b_j + b_k)^4}\right]$$

$$+ \frac{\pi(c+d)}{2cd\left[a_j^2 + (b_j - c - d)^2 \quad a_k^2 + (b_k + c + d)^2\right]}$$

$$= \frac{\pi(c-d)}{2cd\left[a_j^2 + (b_j - c + d)^2 \quad a_k^2 + (b_k + c - d)^2\right]}$$

where:

$$c = 1/2\ (p^2 + q^2)$$

$$d = 1/2\ (p^2 - q^2)$$

$$c_j = \left[(a_j^2 - b_j^2)(a_j^2 - b_j^2 + 2\ {}^2) - 4a_j^2 b_j^2 + q^4\right]^2 + 16\, a_j^2 b_j^2 (a_j^2 - b_j^2 + \rho^2)^2$$

(29)
$$\int_{-\infty}^{\infty} \frac{\omega^2}{\omega^4 + 2\ {}^{2}\omega^2 + q^4} \left|H(\omega)\right|^2 d\omega = \frac{\pi}{2b\omega_o^2} \frac{(a^2-3b^2+2\rho^2)\,\omega_o^4 + (a^2-b^2)\,q^4}{\left[(a^2-b^2)(a^2-b^2+2\rho^2)-4a^2b^2+q^4\right]^2 + 16\,a^2b^2(a^2-b^2+\rho^2)^2}$$

$$+ \frac{\pi(c+d)}{4\,cd\left[\omega_o^4 + 2(a^2-b^2)(c+d)^2 + (c+d)^4\right]} - \frac{\pi(c-d)}{4\,cd\left[\omega_o^4 + 2(a^2-b^2)(c-d)^2 + (c-d)^4\right]}$$

[For c and d see (28)]

(30)
$$\int_{-\infty}^{\infty} \frac{\omega^4}{\omega^2+q^2} H_j(\omega)\, H_k^*(\omega)\, d\omega = 4\pi \left\{ \frac{b_j\left[\omega_j^4+2(a_j^2-b_j^2)q^2\right]\omega_k^2 + b_k\left[\omega_j^4+(a_j^2-3b_j^2)q^2\right]\omega_j^2 - b_j\omega_j^4 q^2}{\left[(a_j^2-a_k^2)^2+2(a_j^2+a_k^2)(b_j+b_k)^2+(b_j+b_k)^4\right]\left[\omega_j^4+2(a_j^2-b_j^2)q^2+q^4\right]} \right\}$$

$$+ \frac{\pi q^3}{\left[a_j^2 + (b_j-q)^2\right]\left[a_k^2 + (b_k+q)^2\right]}$$

(31)
$$\int_{-\infty}^{\infty} \frac{\omega^4}{\omega^2+q^2} \left|H(\omega)\right|^2 d\omega = \frac{\pi}{2b}\left[\frac{\omega_o^4 + (a^2-3b^2)\,q^2 + 2bq}{\omega_o^4 + 2(a^2-b^2)\,q^2 + q^4}\right]$$

(32)

$$\int_{-\infty}^{\infty} \frac{\omega^6}{\omega^4 + 2\rho^2\omega + q^4}\, H_j(\omega)\, H_k^*(\omega)\, d\omega$$

$$= \frac{4\pi}{b_{jk} c_j} \left\{ \left[\omega_j^8 + 2\omega_j^4 (a_j^2 - b_j^2)\rho^2 + (a_j^4 - 10\, a_j^2\, b_j^2 + 5 b_j^4) q^4\right] b_k \omega_j^2 + \left[\omega_j^8 + 4\omega_j^4 (a_j^2 - b_j^2)\rho^2 + (3a_j^2 - b_j^2)(a_j^2 - 3b_j^2) q^4\right] b_j \omega_k^2 - 2 b_j \omega_j^4 \left[\omega_j^4 \rho^2 + (a_j^2 - b_j^2) q^4\right] \right\}$$

$$+ \frac{\pi (c+d)^5}{4cd \left[a_j^2 + (b_j - c - d)^2\right]\left[a_k^2 + (b_k + c + d)^2\right]} - \frac{\pi (c-d)^5}{4cd \left[a_j^2 + (b_j - c + d)^2\right]\left[a_k^2 + (b_k + c - d)^2\right]}$$

where:

$$B_{jk} = (a_j^2 - a_k^2)^2 + 2(a_j^2 + a_k^2)(b_j + b_k)^2 + (b_j + b_k)^4$$

[For c, d and c_j see (28)]

$$(33) \qquad \int_{-\infty}^{\infty} \frac{\omega^6}{\omega^4 + 2\rho^2\omega^2 + q^4} \left|H(\omega)\right|^2 d\omega = \frac{\pi}{2b}\left[\frac{\omega_o^8 + 2\omega_o^4 (a^2-2b^2)\rho^2 + (a^4-10a^2b^2+5b^4)q^4}{\left[(a^2-b^2)(a^2-b^2+2\rho^2)-4a^2b^2+q^4\right]^2 + 16a^2b^2(a^2-b^2+\rho^2)^2}\right]$$

$$+ \frac{\pi(c+d)^5}{4cd\left[a^2+(b-c-d)^2\right]\left[a^2+(b+c+d)^2\right]} - \frac{\pi(c-d)^5}{4cd\left[a^2+(b-c+d)^2\right]\left[a^2+(b+c-d)^2\right]}$$